

**PLANT VIRUSES:
THE MANY ASPECTS OF A FASCINATING
NANO-BIOTECHNOLOGICAL TOOL**



Roberta Zampieri

Cover picture courtesy of Valentina Rigo

UNIVERSITY OF VERONA

DEPARTMENT OF BIOTECHNOLOGY

GRADUATE SCHOOL OF NATURAL SCIENCES AND ENGINEERING

DOCTORAL PROGRAM IN BIOTECHNOLOGY

XXIX cycle

Plant viruses: the many aspects of a fascinating nano-biotechnological tool

S.S.D. AGR/07

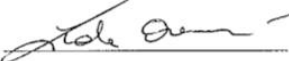
Coordinator: Prof. Massimo Delledonne

Signature 

Tutor: Prof. Mario Pezzotti

Signature 

Co-tutor: Dr. Linda Avesani

Signature 

Doctoral Student: Roberta Zampieri

Signature 

***Think, believe,
dream, and dare***

***Pensa, credi,
sogna, e osa***

Walt Disney

TABLE OF CONTENTS

ABSTRACT	1
INTRODUCTION	3
1. Plants as biofactories	3
2. Plant viruses	8
3. The use of plant viruses for functional peptide display	13
4. Plant viruses as biotechnology tools: the protagonist	15
4.1. Cowpea Mosaic Virus (CPMV)	15
4.2. Potato Virus X (PVX)	18
4.3. Tomato Bushy Stunt Virus (TBSV)	20
4.4. Turnip Mosaic Virus (TuMV)	21
AIM OF THE PROJECT	23
TARGET AUTOIMMUNE DISEASES	25
1. Type 1 Diabetes (T1D)	25
2. Rheumatoid Arthritis (RA)	27
3. Sjögren's Syndrome (SjS)	28
MATERIALS AND METHODS	31
1. Materials and methods for microbiology	31
1.1. Bacterial strains	31
1.1.1. <i>Escherichia coli</i> strains	31

1.1.2. <i>Agrobacterium tumefaciens</i> strains	31
1.2. Culture media	31
1.3. Competent cell preparation	32
1.3.1. <i>E. coli</i> competent cells	32
1.3.2. <i>A. tumefaciens</i> competent cells	32
1.4. Bacterial transformation	32
1.4.1. Heat-shock	32
1.4.2. Electroporation	33
1.4.3. Plasmid DNA extraction	33
2. Materials and methods for molecular biology	33
2.1. Nucleic acid agar gel electrophoresis	33
2.2. RNA extraction and reverse transcription	34
2.3. Polymerase chain reaction (PCR)	34
2.4. Vectors and cloning procedure	36
2.4.1. PVX CVPs peptide display system	36
2.4.2. CPMV eVLPs peptide display system	39
2.4.3. TBSV CVPs peptide display system	42
2.4.4. TuMV CVPs peptide display system	43
3. Plant materials and methods	44
3.1. Plant material	44
3.2. Expression of PVX CVPs in <i>N. benthamiana</i>	44
3.3. Expression of CPMV eVLPs in <i>N. benthamiana</i>	44
3.4. Expression of TBSV CVPs in <i>N. benthamiana</i>	45
3.5. Expression of TuMV CVPs in <i>N. benthamiana</i>	45
4. Biochemical materials and methods	45
4.1. Protein extraction from leaf material	45
4.2. SDS-PAGE	46
4.2.1. Gel Coomassie staining	46

4.2.2. Gel Silver staining	47
4.3. Western blot analysis	47
4.4. CVPs and eVLPs purification	48
4.4.1. PVX CVPs purification from leaf material	48
4.4.2. CPMV eVLPs purification from leaf material	49
4.4.2.1. PEG 6000 precipitation	49
4.4.2.2. Protocol based in anion-exchange and size exclusion chromatography	49
4.4.2.3. Protocol based on double sucrose cushion and Nycodenz gradient	50
4.5. CVPs and eVLPs characterization	50
4.5.1. Dynamic Light Scattering	50
4.5.2. Limulus Amebocyte Lysate-test (LAL-test)	50
4.6. ELISA test	50
5. Human Cell Culture	50
5.1. SH-SY5Y neuroblastoma cells	50
6. Animal models	51
6.1. NOD mice	51
6.2. DBA-1/CIA mice	51
7. T1D cytokines analysis	52
8. RA cytokines analysis	52

CHAPTER 1: THERAPY

INTRODUCTION	53
1. Immunological tolerance and autoimmune disease	53

2. Current strategies and ongoing studies for the treatment of autoimmune diseases	54
3. Antigen-specific immunotherapy (ASI)	57
RESULTS AND DISCUSSION	59
<i>TYPE 1 DIABETES PREVENTION</i>	59
1. Experimental design	59
2. Cloning of GAD65 derived peptide p524	63
3. Analysis of the expression in plant of CPMV eVLPs displaying p524	65
4. Purification of CPMV eVLPs.p524 and unmodified CPMV eVLPs for T1D peptide display	67
4.1. CPMV eVLPs.p524	67
4.2. Unmodified CPMV eVLPs	72
5. Characterization of purified CPMV eVLPs.p524 and unmodified CPMV eVLPs	74
5.1. Quantification and yields	74
5.2. Structural particles evaluation	74
5.3. Qualitative analysis	77
6. Pre-clinical trials in T1D animal models	77
6.1. Histopathological analysis of the pancreatic Langerhans islets	79
6.2. Cytokines analysis in serum	81
6.3. Analysis of Treg cell	86
<i>EXPRESSION OF CPMV eVLPs.p524 IN EDIBLE PLANTS</i>	88
1. Experimental design	88

2. Analysis of the expression in Spinach and Red beet of CPMV eVLPs displaying p524	88
<i>RHEUMATOID ARTHRITIS TREATMENT</i>	91
1. Experimental design	91
2. Cloning of LIP₁ and FADK₂	93
3. Analysis of the expression in plant of TBSV CVPs.FADK₂ and TBSV CVPs.LIP₁	95
4. Purification of TBSV CVPs.FADK₂, TBSV CVPs.LIP₁ and unmodified TBSV CVPs	98
4.1. TBSV CVPs.LIP ₁ and TBSV CVPs.FADK ₂	98
4.2. Unmodified TBSV CVPs	99
5. Characterization of purified TBSV CVPs.FADK₂, TBSV CVPs.LIP₁ and unmodified TBSV CVPs	99
5.1. Quantification of purified TBSV CVPs.LIP ₁ , TBSV CVPs.FADK ₂ and unmodified TBSV CVPs	100
5.2. Limulus Amebocyte Lysate-test (LAL-test)	100
6. Pre-clinical trials in AR animal models	101
6.1. Induction of autoimmune arthritis in mice with type II collagen (CII)	101
6.2. Injection of LIP ₁ and FADK ₂ synthetic peptides, TBSV CVPs.LIP ₁ , TBSV CVPs.FADK ₂ and unmodified TBSV CVPs in mice	102
6.3. Treg determination in lymph nodes	105
6.4. Cytokines analysis in different sites	106

CHAPTER 2: DIAGNOSIS

INTRODUCTION	109
1. Autoimmune disease diagnosis	109
2. Sjögren’s Syndrome diagnosis	110
3. Rheumatoid arthritis diagnosis	111
RESULTS AND DISCUSSION	113
<i>SJÖGREN’S SYNDROME DIAGNOSIS</i>	113
1. Experimental design	113
2. Production of PVX CVPs.lipo, CPMV eVLPs.lipo and TBSV CVPs.lipo	114
2.1. PVX CVPs.lipo expression in plant and purification	114
2.2. CPMV eVLPs.lipo expression in plant and purification	115
2.3. TBSV CVPs.lipo expression in plant and purification	117
3. Development of an indirect ELISA using PVX CVPs.lipo, CPMV eVLPs.lipo and TBSV CVPs.lipo	117
4. Stability of ELISA test over time	121
<i>RHEUMATOID ARTHRITIS DIAGNOSIS</i>	123
1. PVX CVPs expression system	123
1.1. Experimental design	123
1.2. Cloning of LIP ₁ , FADK ₂ and BANK ₁ with the PVX CVPs expression system	124
1.3. Analysis of the expression and genetic stability of PVX CVPs.LIP ₁ , PVX CVPs.FADK ₂ and PVX BANK ₁	126

1.4. Purification of PVX CVPs.LIP ₁ and PVX CVPs.BANK ₂	128
1.4.1. PVX CVPs.LIP ₁ purification yield	130
2. TuMV CVPs expression system	130
2.1. Cloning of LIP ₁ and FADK ₂ with the TuMV CVPs expression system	130
2.2. Expression of TuMV CVPs.LIP ₁ and TuMV CVPs.FADK ₂ In <i>Brassica juncea</i>	131
2.3. TuMV CVPs.LIP ₁ and TuMV CVPs.FADK ₂ purification	132
CHAPTER 3: OTHER APPLICATIONS	
INTRODUCTION	135
1. eVLPs internalization	135
1.1. Tat peptide	135
2. Antimicrobial Peptides (AMPs)	135
2.1. BP100 peptide	136
RESULTS AND DISCUSSION	139
<i>DEVELOPMENT OF A SYSTEM FOR CELLULAR PEPTIDE INTERNALIZATION</i>	139
1. Experimental design	139
2. Unmodified CPMV eVLPs internalisation experiments in Neuroblastoma SH-SY5Y cells	140
3. Design of new insertion site in the pEAQ-HT-VP60 vector And development of newpEAQ-HT-VP60/Tat	142
4. CPMV eVLPs.Tat expression in <i>N. benthamiana</i> plants	144
5. CPMV eVLPs.Tat purification	145

5.1. Chromatography based protocol	145
5.2. Double sucrose cushion and Nycodenz gradient	147
<i>DEVELOPMENT OF AN ECO-PESTICIDE</i>	151
1. Experimental design	151
2. Cloning of BP100 peptide for the expression of CPMV eVLPs.BP100	151
3. Analysis of the expression in plant of CPMV eVLPs displaying BP100	154
4. Purification of CPMV eVLPs.BP100	155
4.1 PEG 6000 precipitation based protocol	155
4.2 CPMV eVLPs precipitation experiments	157
4.3 Double sucrose cushion and Nycodenz gradient	159
CONCLUSION REMARKS	161
REFERENCES	165

ABSTRACT

The capsids of most plant viruses are simple and robust structures consisting of multiple copies of one or few types of protein subunits arranged with either icosahedral or helical ordered symmetry. In many cases, capsids can be produced in large quantities either by the infection of plants or by the expression of the subunits. In view of their relative simplicity, stability and easy production, plant chimeric virus particles (CVPs) or empty virus-like particles (eVLPs) have attracted attention as potential reagents for applications in bionanotechnology.

In this work CVPs and eVLPs have been exploited for the expression of functional peptides, in order to stabilize them and avoid peptide low intrinsic stability and susceptibility to degradation.

In particular, the viral expression platforms chosen for the expression of target peptides are based on four plant viruses widely used as scaffold for peptide display: Potato Virus X (PVX), Cowpea Mosaic Virus (CPMV), Tomato Bushy Stunt Virus (TBSV) and Turnip Mosaic Virus (TuMV).

The first application explored in this work regards the therapy of Type 1 diabetes (T1D) and Rheumatoid arthritis (RA), two autoimmune diseases that share a strong social impact. Currently, there are treatments able to manage and/or stem the effects of these disorders.

In particular, plant viruses displaying peptides associated to T1D and RA have been used respectively for the development of a preventive and therapeutic drug.

Virus particles displaying autoantigenic peptide specific for these diseases have been expressed and used for pre-clinical studies in T1D and RA animal models.

The results observed suggest that the use of viral structure for peptide display works as an adjuvant by increasing peptide modulation capability.

The second part of this work regards the use of plant viruses displaying peptide as reagents for the development of innovative kit for the Sjögren's Syndrome (SjS) and RA diagnosis. These two autoimmune diseases are difficult to be diagnosed and either for SjS or RA there are subgroups of patient seronegative to the main diagnostic serological markers. In this work, the use of filamentous particles for the display of specific SjS peptide allowed to increase the diagnostic performances of an ELISA kit in comparison to the use of the

peptide alone. Moreover, autoantigenic peptides associated to RA were successfully expressed in plants on the surface of viral particles that will be exploited in the future for the development of a kit for seronegative RA diagnosis.

A third part of this PhD thesis regards another possible application of plant viruses as tools for peptide display. In particular, viral particles have been used for the expression of an antimicrobial peptide (AMP) that could be exploited as eco-friendly pesticide and for “nanoagriculture” application. Finally, the possibility of developing a biotechnological tool for peptide internalisation into the cells has been exploited by fusing on the surface of an icosahedral plant virus a cell-penetrating peptide (CPP) derive from HIV. Regarding this third part, CVPs and eVLPs displaying the selected peptides have been successfully expressed in plants; however, several drawbacks have been encountered in the purification process.

INTRODUCTION

1. Plants as biofactories

Throughout human evolution, plants have provided us with food, fiber to produce clothes and medicine to treat many diseases. Examples of important therapeutic molecules historically obtained from plants are morphine, atropine and codeine (Farnsworth *et al.*, 1985). At the beginning of 2000s, about 40% of drugs prescribed in the USA and Europe came from active compounds found in plants (Rates, 2001; Sivakumar, 2006).

The chemical synthesis of these plant-derived compounds has led to the production of pharmaceuticals at industrial levels. These active compounds from plants are basically small molecules, such as aspirin which was developed as an analogue of salicylic acid extracted from willow bark in the 19th century (Knäblein, 2005).

Moreover, the development of more sophisticated extraction and purification procedures has allowed the production of alkaloids, such as morphine, from plants and mammals (Liénard *et al.*, 2007).

Although the chemical synthesis of these plant-derived compounds has led to the production of pharmaceuticals at an industrial level, this method has some significant limitations when producing complex molecules such as antibodies. For this reason, many therapeutic molecules have to be isolated and purified from living material, notable blood plasma, which involves a high risk of pathogen contamination in the final product (Engelhard, 2007).

The emergence of genetic engineering in the early 1970s has paved the way to the production of pharmaceuticals outside their natural host. Genetic transformation techniques have allowed the transformation of bacteria, yeasts, animal cells and plants into production “biofactories” (Rai *et Padh*, 2001). In particular, in the 1980s genetic engineering in plants was finally proven and thereafter plants began to be used to produce high-value recombinant proteins.

The first example goes back to 1986, when the chimeric human growth hormone was expressed in transgenic tobacco and sunflowers, using the *Agrobacterium tumefaciens* Ti plasmid for the first time (Barta *et al.*, 1986).

Since the 1970s it is known that *A. tumefaciens* is a gram-negative bacterium able to transfer the T-DNA region of its tumor-inducing (Ti) plasmid into plants, leading to its expression in plant cells (Chilton *et al.*, 1977). Using this evidence, the gene coding for a protein of interest can be cloned into T-DNA between the natural borders of the *A. tumefaciens* Ti-plasmid and the resulting vector can be used to transform plants.

Transformed plants can correctly produce antibodies and other complex recombinant proteins (Hiatt *et al.*, 1989; Sijmons *et al.*, 1990).

In the 21st century, the definitive term “Plant Molecular farming” was coined, which refers to a new branch of plant biotechnology mainly focused on exploiting plants as factories for biomolecule heterologous production (Lico *et al.*, 2005). Since then, transgenic plants have become one of the most interesting and promising pharmaceutical expression platforms as they offer many advantages over traditional fermentative systems (such as bacteria, yeasts and mammalian cell cultures).

There are two methods of protein production in plants: stable and transient expression transformations.

Stable transformation has the advantage of allowing production scalability, low-cost biomass production and the potential for crossing transgenic lines to obtain complex proteins in plant (Taket *et al.*, 1998).

Transient expression is achieved using *A. tumefaciens* to deliver foreign nucleotidic sequences to plants allowing their expression in plant cells without transgene integration into the plant genome. This advanced technology is flexible and quickly produces high yields of recombinant proteins unmatched by the production technologies based on traditional fermentative expression systems (Qiang *et al.*, 2016). Indeed, transient expression avoids the position effects occurring in stable transformation that may suppress transgene expression by surrounding genomic DNA following integration (Komorova *et al.*, 2010).

Transient expression allows significant reduction of production time as heterologous protein expression can be achieved 3 to 14 days post-infection, depending on the system used (Santi *et al.*, 2006). This enables quick and easy testing of a wide variety of different constructs in order to optimize protein production. Moreover, transient expression allows

a prompt response to emerging epidemics (Kusnadi *et al.*, 1997) by producing high levels of therapeutics and vaccines in little time.

Plant systems to produce therapeutics are scalable and cost-effective. In table 1 production costs of therapeutic antibodies are compared (including both upstream and downstream processes) and reported in different expression systems.

Table 1 Therapeutic antibodies production costs in different systems (Hood *et al.*, 2002).

Production system	\$/g
Chinese Hamster Ovary Cells (CHO)	300
Transgenic chickens/Eggs	1-2
Transgenic goats/milk	1-2
Microbial fermentation	1.00
Plants	0.10

Furthermore, being eukaryotic organisms, plants are able to correctly fold and assemble proteins as well as perform post-translation modifications when necessary for protein activity and stability (Kamenarova *et al.*, 2005). Finally, plants ensure a safe final product, avoiding contamination with human pathogens or prions, oncogenic DNA sequences or endotoxins.

As a consequence, some companies currently produce human pharmaceuticals using plant molecular farming (Table 2). Many studies have been published in the last fifteen years, starting from the production of human lysozyme and lactoferrin in rice (Hennegan *et al.*, 2005; Yang *et al.*, 2002) to the use of tobacco for the expression of human type I collagen (Shoseyov *et al.*, 2014). The definitive breakthrough to commercial success was in 2012, with the approval from the United States Food and Drug Administration (FDA) of taliglucerase alfa (table 2), a recombinant form of human glucocerebrosidase developed by Protalix Biotherapeutics for the treatment of Gaucher's disease (Tschofen *et al.*, 2016).

Table 2 Companies focused on plant molecular farming for the production of human pharmaceuticals (adapted from Yao *et al.*, 2015).

Company	Plant host	Lead Product	Status
Mapp Biopharmaceutical/ LeafBio, USA	Tobacco leaves	ZMapp™ for Ebola crisis	Phase 1 and 2 (2016)
Protalix Biotherapeutics, Israel	Carrot or tobacco cell culture	ELELYSO™ (taliglucerase alfa) Enzyme replacement	Phase 3 completed and FDA approved (2012)
Icon Genetics, Germany	<i>Nicotiana benthamiana</i> leaves	Vaccine for non-Hodgkin's Lymphoma	Phase 1 completed (2014)
Ventria Bioscience, USA	Rice seeds	VEN150 for HIV-associated chronic inflammation	Phase 2 (2016)
Greenovation Biotech GmbH, Germany	Moss	Moss-GBA for Gaucher's Disease Moss-AGAL for Fabry Disease	Preclinical test (2016) Phase 1 completed (2015)
Kentucky BioProcessing, USA	<i>Nicotiana benthamiana</i> leaves	Protein expression service	-
PhycoBiologics Inc. Bloomington, USA	Algae	Vaccine Growth Factor and enzyme	Phase 2 (2016)
Medicago, Canada	<i>Nicotiana benthamiana</i> Alfalfa	Vaccine for influenza, Pandemic market, Rabies and Rotavirus	Phase 2 completed
Synthon, Netherlands	Duckweed LeafyBiomass	Antibody for non-Hodgkin's Lymphoma	-
Fraunhofer IME, Germany	Tobacco leaves	HIV Antibody	Phase 1 completed (2011)
Fraunhofer CMB, USA	<i>Nicotiana benthamiana</i> leaves	Influenza vaccine	Phase 1
PlanetBiotechnology, USA	Tobacco leaves	CaroRx for dental caries; PBI-220 antibody for anthrax; DPPA-Fc for MERS coronavirus infection	Preclinical test and searching for investor

Another important economical application of plant molecular farming concerns the recombinant production of non-pharmaceutical protein, such as technical enzymes, research reagents, cosmetics and veterinary products. In comparison with pharmaceutical, non-pharmaceuticals product can reach the market more quickly because of the much

lower regulatory burden. Table 3 shows the plant-derived non-pharmaceutical products already on the market.

Table 3 Commercial development of nonpharmaceutical proteins produced in plants (Adapted from Tschofen *et al.*, 2016).

Company	Plant host	Lead Product	Application	Status
ProdiGene/Sigma-Aldrich, USA	Maize seeds	Trypsin, avidin, endo-1, 4- β -D-glucanase	Technical reagents	Commercialized
Infinite Enzymes/ Sigma Aldrich, USA	Maize seeds	Cellobiohydrolase I	Technical reagents	Commercialized
Agrenvec, Spain	Tobacco leaves, transient expression	Growth factor, cytokines, thioredoxin, TIMP-2	Research reagents	Commercialized
ORF Genetics, Iceland	Barley seeds	Growth factor, cytokines	Research reagents	Commercialized
Sif Cosmetics, Iceland	Barley seeds	Epithelial growth factor	Cosmetics	Commercialized
Ventria Bioscience/Invitria, USA	Rice seeds	Albumin, lactoferrin, lysozyme, transferrin, insulin	Research reagents	Commercialized
Kentucky Bio-Processing, USA	Tobacco leaves, transient expression	Aprotinin	Research reagents	Commercialized
CollPlant Israel	Transgenic tobacco	Collagen	Research reagents, tissue culture, health applications	Commercialized
Natural Bio-Materials, South Korea	Rice cell suspension	Trypsin, enterokinase, growth factor, cytokines	Research reagents, cosmetics ingredients	Commercialized
Center of Genetic Engineering and Biotechnology, Cuba	Transgenic tobacco	Antibody	Purification of a Hepatitis B vaccine	Commercial application

Syngenta, USA	Maize seeds	α -Amylase	Bioethanol production	Commercialized
Origin Agritech, China	Maize seeds	Phytase	Feed	Commercial pending
NexGen, South Korea	Tobacco leaves, transient expression	Growth factor	Tissue culture reagent	Commercialized

This evidence confirms the versatility of plants as expression platforms and one can thus predict their valuable potential from an industrial point of view.

2. Plant viruses

Several works describe how plants can be exploited for human virus production (whole particles or part of them) as a safe and fast vaccine production system (McGarvey *et al.*, 1995; Kong *et al.*, 2001; Thanavala *et al.*, 2005; Peyret *et al.*, 2015; Natsumi *et al.*, 2015). On the other hand, another facet of plant molecular farming regards plant viruses as a tool for recombinant protein expression in plants.

Recent developments in molecular biology technology have led to new systems for transient expression using viral vectors or parts of them (e.g. magnICON, geminiviral and pEAQ) (Circelli *et al.*, 2010; Boivin *et al.*, 2010).

The first viruses transformed into gene vectors were with DNA genomes. This choice was done because DNA viruses were easily manipulated genetically for transgene insertion in their genome (Porta *et Lomonossoff*, 2002) but, the complex replication cycle of these viruses made them inadequate for expression of heterologous proteins. The majority of plant virus genomes are made of one or more molecules of positive-sense RNA and have the advantage of directly translating RNA positive-sense molecules entering the plant cell. Several plants support the replication of these viruses and can reach high titres of virions. All these characteristics make positive-sense RNAs excellent candidates for transient expression of foreign protein.

There are four main strategies for *in planta* expression of heterologous proteins exploiting plant viruses:

- Gene replacement;
- Gene insertion;
- Virus deconstruction;
- pEAQ vector series.

The gene replacement strategy uses viral genomes to express recombinant protein, using specific vectors in which either the viral genome sequence or the gene coding the protein of interest are present. Initially, the development of viral vectors was done by replacing the gene sequence coding the protein of interest into viral genome (Figure 1).

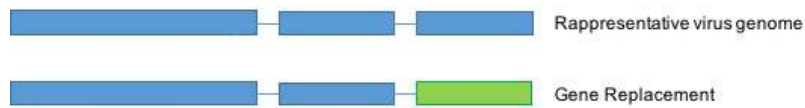


Figure 1 The gene replacement strategy for the transient expression of foreign genes using plant viruses.

The gene replacement strategy was drawn-up in order to avoid possible negative effects of increasing viral genome size by introducing a foreign gene. The replaced viral genes should not be essential for viral amplification and replication in plant cells. However, the replacement strategy has limitations due to the deletions of a viral gene that, even if nonessential, is likely to contribute to overall virus fitness (Scholthof *et al.*, 1996).

A more successful approach is the gene insertion strategy which is shown in figure 2.

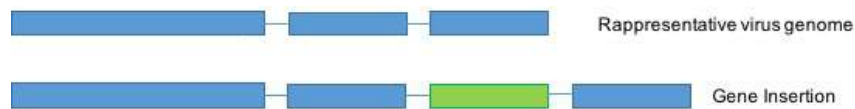


Figure 2 The gene insertion strategy for the transient expression of foreign gene using plant viruses.

The insertion of an added exogenous gene, avoiding the deletion of any viral genes, prevents potential negative effects of the gene replacement strategy, leaving the viral genome unharmed.

The deconstructed virus strategy is a new generation strategy, inspired to replace approaches for heterologous protein expression in plants.

This method is based on evidence that the viral genome can be deconstructed in many expression plasmids and deconstructed viral vectors can be assembled *in planta* from pro-vectors delivered by *Agrobacterium*. Indeed, T-DNAs can be delivered to the same cell from different *Agrobacteria* and can recombine efficiently in plant cells. The most commonly used vector so far is that based on Tobacco Mosaic Virus (TMV).

This vector has been engineered to split the TMV genome into two cDNA modules: the 5'-module harbouring the RNA dependent RNA polymerase (RdRP) and the viral movement protein (MP). The second module is 3', containing the sequence code for the protein of interest and the viral 3'-untranslated region (UTR) needed for replication and amplification of the vector. These modules are delivered to the plant cell by two independent *A. tumefaciens* transformed cell lines, that are assembled together *in vivo* by a site specific recombinase delivered by a third *Agrobacterium* cell line.

After recombination, the DNA is transcribed and spliced, thus undesired elements are removed and a fully infective replicon carrying the sequence of interest is assembled (Marillonet *et al.*, 2004).

In this method, bacteria and viruses work together to ensure the best performance, in particular *A. tumefaciens* assumes the functions of primary infection, while the viral vector provides cell-to-cell spread, amplification and high levels of expression.

A schematic representation of magniffection system is reported in figure 3.

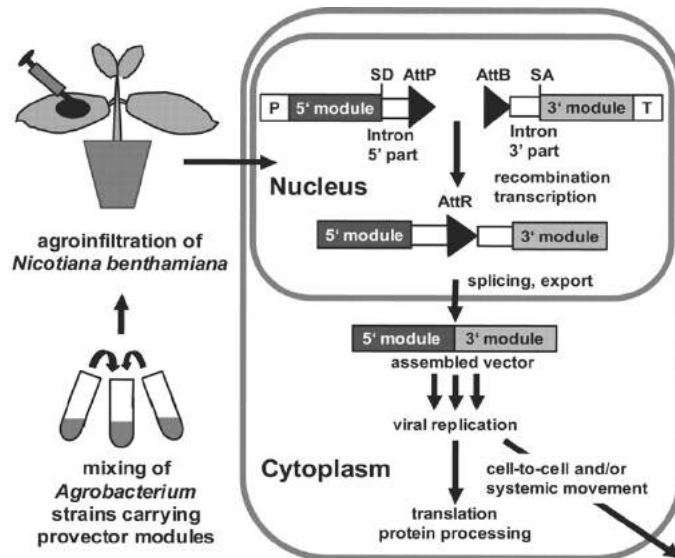


Figure 3 Schematic overview of magnification system shows in planta assembly of 5'-module and 3'-module. SD, splice donor site; SA, splice acceptor site. (Marillonnet et al., 2004).

In summary, this technology combines the advantages of two biological systems: vector efficiency and systemic delivery capabilities of *Agrobacterium*, speed and expression level/yield of a plant virus (Gleba *et al.*, 2005).

Finally, regarding the pEAQ vector series, these vectors were developed in the attempt to exploit the viral CPMV genome to set up a novel expression system.

The CPMV genome is composed of two separately-encapsidated RNAs: RNA-1 (6.0 kb) and RNA-2 (3.5 kb). The latter encodes for a polyprotein and is entirely dependent on RNA-1 for its replication. It has been demonstrated that RNA-2 polyprotein can be partially deleted and replaced with a foreign gene without interfering with replication of the molecule driven by RNA-1 (Cañizares *et al.*, 2006; Rohll *et al.*, 1993). It has been previously demonstrated that the sequences essential for delRNA-2 to be replicated by RNA-1 were the entire 3'-UTR and the first 512 nucleotides at 5', including two in-frame AUGs at position 161 and 512 (Rohll *et al.*, 1993).

This evidence has led to the development of a replication-competent deleted RNA-2 (delRNA-2) plasmid. In comparison with the system based on the use of native RNA-2, delRNA-2 has some advantages mainly in terms of biocontainment. On the other hand,

lacking the movement protein means it is unable to spread from cell to cell and for the absence of the small CP, which acts as native suppressor of gene silencing (Liu *et al.*, 2004), delRNA2 has to be agroinfiltrated in the presence of RNA-1 and of a heterologous suppressor (Cañizares *et al.*, 2006).

Subsequently, it was found that the removal of AUG 161 together with another out-of-frame AUG 115 caused a marked increase in the translational efficiency of the mRNA transcribed from the T-DNA of the foreign gene inserted into delRNA-2 (Sainsbury *et Lomonossoff*, 2008). This evidence leads to the set up of a new expression system based on a 5'UTR mutated version of delRNA-2 that, being characterised on an enhanced translation rather than replication, was called CPMV-*hypertrans* (or CPMV-*HT*). This system allows the expression of multiple foreign genes in the same tissue.

Despite several advantages, cloning a gene into the CPMV-*HT* system required a two-step procedure, described in van Engelen *et al.* (1995). Furthermore, optimal transgene expression required co-infiltration with the suppressor of silencing p19. To overcome these drawbacks, a series of binary vectors that make cloning and transformation with the CPMV-*HT* system much easier and quicker were developed. These plasmids, called pEAQ vectors are modular, allowing the insertion of multiple CPMV-*HT* cassettes on the same T-DNA.

Once a gene or many genes have been inserted into a pEAQ vector, the DNA is transferred into *A. tumefaciens* that are used for *N. benthamiana* inoculation.

In conclusion, this system allows for cloning and expression of the protein of interest to take place within 2-3 weeks (Peyret *et al.*, 2013).

3. The use of plant viruses for functional peptide display

One of the most interesting applications that exploits plant viruses for heterologous expression in plant, is peptide displaying on the capsid (figure 4).

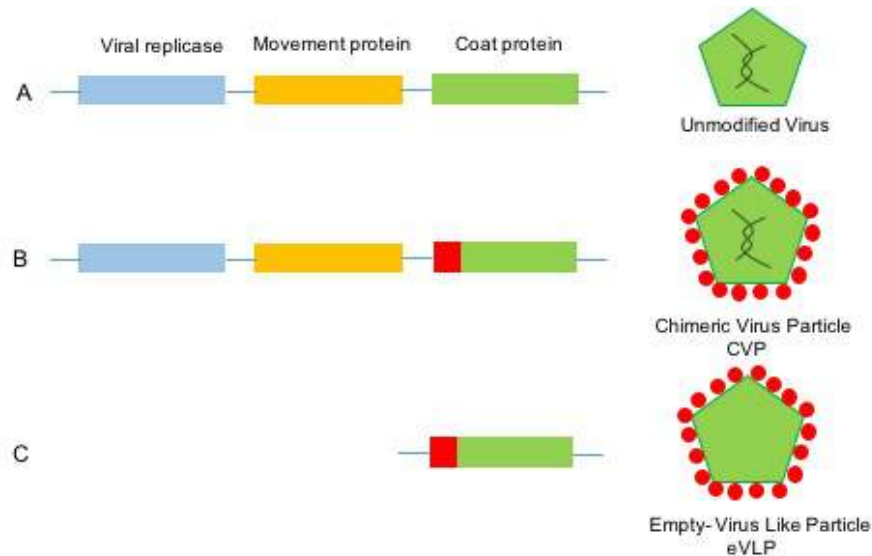


Figura 4 Plant viruses modified for in planta peptide expression; A: schematic representation of the genome of a representative plant virus: the replicase (in light blue), the movement protein (in yellow) and the coat protein (in green), with the corresponding unmodified viral particles; B: the sequence coding the peptide of interest (in red) genetically fused to the coat protein gene resulting in a Chimeric Virus Particle (CVP) bearing the viral genome (in dark green); C: Virus Like Particle (eVLP) resulted from the expression in plant of sequence coding the peptide of interest (in red) genetically fused to the coat protein gene without the rest of viral genome.

This approach makes peptides easier to produce, cutting the cost associated with their production in comparison with traditional methods mainly based on chemical synthesis. Indeed, peptides have unique interesting characteristics in terms of efficacy, selectivity and low toxicity that makes them particularly suitable as therapeutic, diagnostic and industrial reagents. Unfortunately, the main problems of peptides, besides the high costs of production, are their metabolic instability and short half-life. Furthermore, in the bloodstream they have a low immunogenicity which makes the use of an adjuvant necessary (Lico *et al.*, 2012). These issues often make the use of peptides unaffordable.

Plant viruses can be used as a strategic tool to overcome these drawbacks; virus capsids provide nanoscale particles with interesting sizes and shapes that make them useful for a number of chemical and biological applications (Sainsbury *et al.*, 2010). Specifically, the sequence coding for a peptide of interest can be inserted into a specific viral vector fused to the coat protein gene to the 5' or 3' terminus or in a region known to be exposed on the viral surface. The result is the assembly in plants of chimeric virus particles (CVPs) with the same shape of the original virus, but displaying multiple copies of peptide on its surface (Lico *et al.*, 2009). CVPs, maintaining the viral genome, are able to replicate themselves and spread into the host plant. In this way, high yields of the peptide of interest are achieved, reducing the production costs associated with their chemical synthesis.

The viral structural coat protein stabilizes the peptide on the surface and acts as a carrier. Furthermore, there is some evidence demonstrating that when CVPs are used for vaccine development, the viral structure works as an adjuvant, because of the particulate and repetitive nature of virion particles (Jegerlehner *et al.*, 2002).

The coat proteins of some plant viruses can auto-assemble without needing a viral genome, leading to the formation of eVLPs which are structurally identical to the plant virus from which they are derived but completely lacking the viral genes. VLPs, maintaining all the advantages of CVPs but being devoid of viral genome, are non-replicative particles. This is a benefit in terms of safety because any possibility of the modified virus to infect other plants is avoided. On the other hand, the eVLP expression occurs only in the cells reached by the viral vector that might be infiltrated using *A. tumefaciens* as a delivery vector.

4. Plant viruses as biotechnology tools: the protagonists

Several plant viruses have been developed as a peptide presentation system, among them the most commonly used are listed below:

- PPV: Plum Pox Virus;
- TMV: Tobacco Mosaic Virus;
- PVX: Potato Virus X;
- CMV: Cucumber Mosaic Virus;
- AIMV: Alfalfa Mosaic Virus;
- CPMV: Cowpea Mosaic Virus;
- TBSV: Tomato Bushy Stunt Virus;
- TuMV: Turnip Mosaic Virus.

This list is in constant expansion as structural information about more viruses is available. The viral systems described below were used in this work.

4.1. Cowpea mosaic virus (CPMV)

Cowpea mosaic virus (CPMV) is the first virus exploited in biotechnology as a peptide display system, thanks to its growth at high titres in plants, its particles are robust and it cannot infect mammalian cells.

CPMV belongs to the genus *Comovirus* of the *Secoviridae* family; it is a bipartite RNA plant virus whose particles are made up of 60 copies each of large (L) and small (S) coat protein (CP) arranged in an icosahedral symmetry with a diameter of 28 nm (Sainsbury *et al.*, 2010). The particle structure is known at an atomic resolution level (Lin *et al.*, 2003), thus allowing the identification of possible superficial sites for peptide insertion.

The CPMV genome structure is reported in figure 5 (A) and is composed of 2 separately encapsidated positive-strand RNA molecules of 5889 (RNA-1) and 3481 (RNA-2) nucleosides.

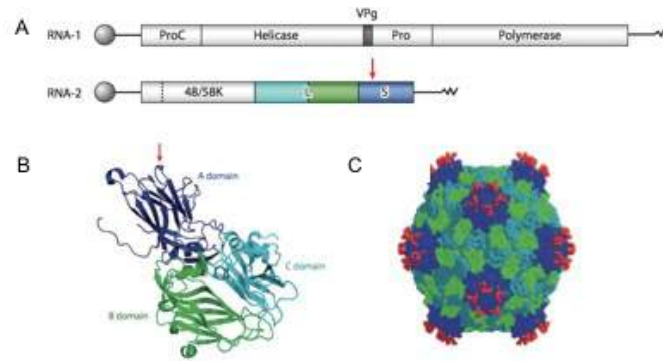


Figure 5 Peptide presentation system based on CPMV. The red arrow indicates the position of βB - βC loop of S CP corresponding to the most common site used for peptide expression; A: genome organization of CPMV RNAs; B: ribbon diagram of the icosahedral asymmetric unit, consisting of the two domains of the large (L) coat protein (cyan and green) and the S coat protein (dark blue); C: tridimensional CPMV representation displayed a peptide of interest (in red); ProC, proteinase cofactor; VPg, genome-linked protein; Pro, 24K proteinase; 48/58K, movement protein; L, large coat protein; S, small coat protein. (Sainsbury *et al.*, 2010).

As shown in figure 5, RNA-1 includes all sequences coding for proteins responsible for the replication of viral RNA and polyprotein processing such as the RNA-dependent RNA polymerase, a helicase, the 24K proteinase and a proteinase cofactor. RNA-2 encodes for proteins required for viral movement (48/58K) and for polyprotein VP60, the precursor of the two coat proteins.

The atomic resolution of CPMV 3-D structure can identify the most exposed external sites suitable for peptide display (Lomonosoff *et al.*, 1995). In literature, most cases using the CPMV-based system report the display of target peptides into the most exposed loop on the virus surface which is the βB - βC loop of S CP (red arrow in figure 5-A, B) (Porta *et al.*, 1994). However, other loops have also been used successfully, for example the $\beta\text{C}'$ - $\beta\text{C}''$ loop of the S CP and the βE - αB loop of the L CP (Brennan *et al.*, 1999; Taylor *et al.*, 2000).

The genome of CPMV has been genetically manipulated at different degrees in order to set up vectors for the expression in plants of either CVPs or eVLPs.

For *in planta* expression of CPMV-based CVPs, the systems developed so far are based on the modification of the sequence of RNA-2 and its co-inoculation with unmodified RNA-1 to provide polyprotein processing and viral replication functions.

Even if the potential of CVPs in several fields are up to now demonstrated, in some cases they could show some limitations as described below.

For their expression, CVPs must retain cell-to-cell movement capability in plant, thus placing limitations on the sequences that can be expressed on the particle surface. Furthermore, to maintain their movement ability, particles must encapsidate the RNA genomes, remaining infective and thus raising biosafety issues. Finally, considering the presence of the 2 genomic RNAs inside the particles they can not be loaded with heterologous material.

The most recent development of the CPMV-based expression system allows assembly of viral capsids in plants without needing viral RNAs. The result are eVLPs self-assembled structures that mimic the viral structure but are not infective because they are devoid of viral genome. To achieve CPMV eVLPs in plant, the sequence of the coat protein (S and L) precursor VP60 was cloned into the pEAQ-*HT* expression vector; to process the precursor in order to obtain the two coat proteins, the expression construct harbouring the VP60 sequence was coinfiltrated in *N. benthamiana* plants with a second pEAQ-*HT* expression vector in which the sequence of proteinase 24K was cloned (Sainsbury *et al.*, 2010) (figure 6).

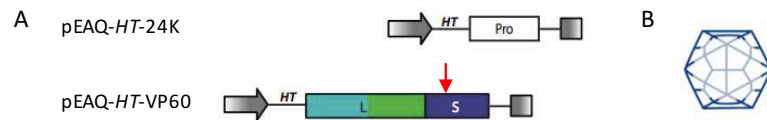


Figure 6 Production of CPMV eVLPs. A. Schematic representation of the plasmid used to express eVLPs; gray arrow indicates CaMV 35S promoter; gray box indicates the nos terminator. B. Schematic representation of CPMV eVLPs without any genetic material inside.

In literature, there are some technical indications about the characteristics that peptides should have for an optimal expression with the CPMV-based systems indicating that peptide should be less than 40 amino acids and have an isoelectric point below 9.0 (Porta *et al.*, 2003).

Finally, another interesting face of CPMV based expression system is that it can be adopted to load a cargo inside its eVLPs (Hesketh *et al.*, 2015).

4.2. Potato Virus X (PVX)

Potato Virus X (PVX) belongs to the genus *Potexvirus* of the *Flexiviridae* family. PVX has been shown to be an ideal, high ordered and multivalent scaffold to be exploited for peptide display (Brennan *et al.*, 1999; Marusic *et al.*, 2001).

The PVX structure is simple, filamentous and flexible. The virion is 500 nm in length, 15 nm in diameter and it has helical symmetry. The viral capsid is made up of up to 1300 of a single CP that wrap the genome of virus, with 8.9 CP per helix turn (Kendall *et al.*, 2008). PVX genome is approximately 6.4 Kb (figure 7) and is made of a single-stranded positive RNA. The genome contains 3 open reading frames (ORFs) coding for 5 proteins: the RNA-dependent RNA Polymerase (RdRP), the CP and 3 movement proteins encoded by 3 overlapping ORFs that form the Triple Gene Block module (TGBp1, TGBp2 and TGBp3) (Sonnenbeng *et al.*, 1978).

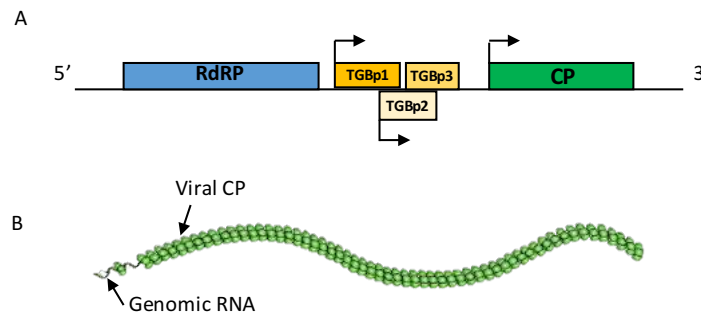


Figure 7 Schematic representation of PVX features. A. Diagram of PVX genome; B. Three-dimensional representation of PVX particle. RdRP: RNA-dependent RNA Polymerase; TGBp1/p2/p3: Triple Gene Block proteins; CP: Coat Protein. Arrows represent the subgenomic promoters (Lico *et al.*, 2015).

Although the structural organization and CP folding are not known because no atomic-resolution data is available, it is assumed that the viral CPs are arranged in a helical structure with the CP N-terminus exposed on the viral surface (Parker *et al.*, 2002). Given this assumption, the use of PVX as a scaffold for peptide display requires the fusion of peptide sequence at the 5' terminus of CP gene. For the production of PVX-based CVP expression vectors such as pPVX201, a vector has been developed that harbours cDNA which encodes the whole PVX genome (Baulcombe *et al.*, 1995; Chapman *et al.*, 1992).

In Lico *et al.* 2006, a spontaneous PVX mutant was isolated and characterized by a 21 aminoacid deletion at the 5' terminus of the CP gene. This mutant was exploited for the generation of a vector that allows the fusion and display of longer peptides.

With the PVX expression system, CVP production is firstly obtained by direct infection of *N. benthamiana* leaves with plasmid carrying the modified PVX genome, and subsequently, infection can be propagated using sap from primary infected leaves.

The peptide selected for the expression on PVX surface should fit a list of parameters in order to avoid interference with the viral structural stability and infectivity. According to published (Lico *et al.*, 2006) and unpublished data (Dr. Lico, personal communication), the target peptide should meet the following criteria:

- the peptide isoelectric point should be in the range of 5.24 – 9.18. If the isoelectric point of the target peptide does not fit this range, it is possible to modify it by the addition of basic or acid aminoacids at the ends of its sequence;
- up to now the length of peptides expressed with this system range between 10 – 24 aminoacids. This range results optimal although there is no evidence that longer or shorter peptides can negatively influence viral assembly and movement;
- the presence of tryptophan (W) residues in the peptide should be avoided because this aminoacid critically affects cell-to-cell and phloem movement of the virus. However, it has been demonstrated that PVX particles carrying a peptide with a 3.7% W content, were correctly assembled in plant and were able to move properly while a peptide of 6.2 % W content has not made the PVX CVPs infective;
- it would be desirable to display a peptide containing serine (S) and/or threonine (T) because these phosphorylated residues promote virus disassembling and viral RNA replication;
- Finally, to develop a CVP-based vaccine, it is suggested the presence of a spacer aminoacid at the peptide N-terminal, because the CP is often acetylated and this could interfere with the displayed peptide's immunological effects.

4.3. Tomato Bushy Stunt Virus (TBSV)

Tomato Bushy Stunt Virus (TBSV) is a prototype member of the *Tombusviridae* family and it belongs to the genus *Tombusvirus*.

TBSV has a single-stranded positive RNA genome of about 4.8 kb that contains 5 ORFs. The capsid is made up of 180 copies of the unique 41 KDa CP that assembles into particles of 30 nm in diameter characterized by an icosahedral symmetry.

The TBSV CP has a ternary structure defined by 3 separate domains: at the CP N-terminal the RNA binding (R), the shell (S) and the C-protruding (P). The CP R domain is placed within the virus particles while the C-terminal P domain is exposed on the external surface (Harrison *et al.*, 1978; Olson *et al.*, 1983).

Different vectors were constructed which allow the genetic fusion of the foreign peptide at the C-terminal protruding domain of the TBSV CP, resulting in the display of the peptide on the surface of the viral capsid. The resulting particles, maintaining their viral genome retain infectivity. In literature, it is possible to find several examples of different peptides expressed with the TBSV-based system, thus demonstrating the correct assembly in plant of TBSV CVPs carrying peptides up to 56 aminoacids in length.

The expression of TBSV CVPs in plants was achieved by the genetic engineering of the TBSV-P plasmid. This vector carries the whole cDNA of TBSV genome (Szittyá *et al.*, 2000) and a multi-cloning site (MCS) was inserted by transforming the CP stop codon. The resulting pTBSV-vector (figure 8), harbouring the promoter for T7 RNA polymerase, is essential for *in vitro* cDNA transcription in order to obtain infectious RNA. Accordingly, the production of TBSV CVPs is firstly obtained by direct infection of *N. benthamiana* leaves with infectious transcribed RNA and subsequent infection can be propagated using sap from primary infected leaves (Grasso *et al.*, 2013).

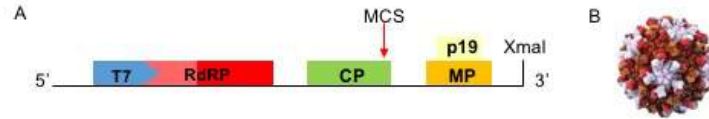


Figure 8 Schematic representation of TBSV features. A. Diagram of TBSV genome; B. Tridimensional representation of TBSV particle. T7: T7 viral promoter; RdRP: RNA-dependent RNA Polymerase; CP: Coat Protein; MP: movement protein; p19: silencing inhibitor. Red arrows indicate the multi-cloning site within the CP gene in which the foreign peptide sequence is cloned. (Adapted from Grasso *et al.*, 2013).

In order to avoid the critical step of *in vitro* retro-transcription, some other vectors were developed by the replacement of T7 promoter with the *Cauliflower mosaic virus* (CaMV) 35S promoter (Odell *et al.*, 1985). Finally, the *A. tumefaciens* nopaline synthase (NOS) termination sequence (Depicker *et al.*, 1982) was introduced downstream of the 3' viral end. For plant infection, these vectors harbouring the TBSV cDNA fused to the foreign peptide sequence, are directly inoculated on *N. benthamiana* leaves. Re-infections were performed using saps from infected leaves as well.

Finally, another interesting facet of TBSV is that it can be adopted to load cargo inside its CVPs. The inner TBSV CVP core can be easily reached by switchable pH-dependent gating (Aramayo *et al.*, 2005; Kruse *et al.*, 1982).

4.4. Turnip Mosaic Virus (TuMV)

Turnip Mosaic Virus (TuMV) belongs to the genus of *Potyvirus* of the family *Potyviridae*. TuMV is a positive-single strand RNA virus (approximately 10 kb long) forming flexuous and filamentous particles with an average length of 720 nm and a diameter of 12-15 nm (Sánchez *et al.*, 1998). TuMV virions are characterized by 2000 copies of the same CP that has a molecular weight of approximately 32-33 kDa.

The viral genome encodes for a single polyprotein that is processed into at least eight mature proteins by three viral proteinases (Richmann *et al.*, 1992; Verchot *et al.*, 1992).

TuMV was an attractive candidate as expression vector because it infects most of the species in the family *Brassicaceae*, including some of the largest plants in terms of biomass.

A biosafe viral vector was developed from the original TuMV infectious cDNA clone (p35Tunos), modified by introducing a restriction site by substitution of third-base nucleotides in the codons of the first two amino acids of the CP (Ala e Gly). The resulting plasmid was named p35Tunos-vec01 (Tourinho *et al.*,2008). Moreover, the non-aphid-trasmissible (NAT) mutation was introduced in a particular motif located at residues 6-8 of the CP which was mutated by PCR site-directed mutagenesis. The resulting p35-Tunos-vec01-NAT1 is not transmitted through seeds or by contact between plants.

With this system up to 2000 peptide copies can be expressed on the TuMV particles' surface.

The sequence encoding the foreign peptide of interest is cloned into the p35-Tunos-vec01-NAT that is then used for *N. benthamiana* inoculation. The presence and integrity of the exogenous sequence is analysed by immunocapture-RT-PCR (IC-RT-PCR) from extracts of infected plants (Nolasco *et al.*, 1993) using a monoclonal antibody antiPoty to capture the virus. Extracts of infected *N. benthamiana* leaf are used to inoculate *Brassica juncea* plants and TuMV CVPs particles are then purified from the subsequent infected leaves.

A new expression system has been developed to produce TuMV eVLPs in *N. benthamiana* (personal communication of Fernando Ponz). This virus system lacks the RNA inner skeleton, consequently the CPs to form TuMV eVLPs are assembled randomly, and particles are expressed at different lengths.

AIM OF THE PROJECT

The advantages of the expression of proteins in plants combined with the high yield and the short production time achieved with the expression platforms based on plant viruses, allow to consider this approach interesting for several applications.

This project is focused on the exploitation of plant virus nanoparticles, either CVPs or eVLPs, for different applications.

First of all, for therapy and diagnosis our approach was focused on autoimmune diseases; the target diseases are Type 1 Diabetes (T1D), Rheumatoid Arthritis (RA) and Sjögren's Syndrome (SjS).

The therapeutic application, in the first part of this PhD thesis, is focused on the prevention of T1D and on the treatment of RA;

In the second chapter, the diagnostic application has been explored for SjS and RA.

Finally, the last part of this project regards other applications of eVLPs; these uses include the set up of system for internalization of peptide inside the cell and the development of eco-pesticides.

TARGET AUTOIMMUNE DISEASES

1. Type 1 Diabetes (T1D)

Type 1 Diabetes (T1D) is a chronic autoimmune disease characterised by the loss of self-tolerance to insulin-producing β -cells in the islets of Langerhans within the pancreas. The destruction of these pancreatic cells engaged to the insulin production results in plasma glucose deregulation leading to a chronic hyperglycemia.

The incidence peak is in children aged less than 15 years; after the pubertal years, the incidence rate significantly drops in young women, but remains relatively high in young adult males up to the age of 29-35 (Soltesz *et al.*, 2007).

According to the latest edition of Diabetes Atlas (7th edition, 2015) 542 000 children around the world have T1D and there is an increase of around 86 000 new cases per year. Europe has the higher (140 000) number of children with T1D.

Up to now there are not therapies able to prevent or revert the onset of T1D and people affected by this disorder need daily insulin injection in order to control blood glucose level. Without insulin, a person affected by T1D will die.

Despite the insulin replacement therapies, long-term complications affecting eye, cardiovascular system, foot, oral cavity, kidney and nervous system can appear.

T1D develops as a consequence of a combination of genetic predisposition, environmental factor and stochastic events (Bluestone *et al.*, 2010).

Considering that human pancreas it is not easily accessible, most of the knowledge about the T1D pathogenesis comes from studies done in the last 30 years in animal model, first of all non-obese diabetic (NOD) mice. T1D developed in this animal share with human many aspects including the disease pathogenesis.

The studies in NOD-mice have demonstrated that the T1D occurs as a consequence of a breakdown in the immune regulation, resulting in the destruction of insulin producing β -cells through the expansion of autoreactive $CD4^+$ and $CD8^+$ T cells, autoantibody-producing B lymphocytes and the activation of the innate immune system.

Although, the presence of autoantibodies in sera from T1D patients is the first diagnostic evidence of autoimmunity, autoreactive T cells play a dominant role in disease initiation and progression. T cells $CD4^+ CD8^+$ are present in the surrounding area of the β -cells islets in 3-4 weeks old NOD mice (Anderson *et al.*, 2005) together with dendritic cells and

macrophages. These cells are the first infiltrates and have been shown to recognize islet autoantigens similar to those binded by autoantibodies (e.g. Insulin B chain, Glutamic acid decarboxylase (GAD) and zinc transporter 8 (ZnT8)) presumably resulting from the β -cells turnover (Turley *et al.*, 2003; Nakayama *et al.*, 2005). These effector T cells generally exhibit a type 1 phenotype characterized by the secretion of pro-inflammatory cytokines such as IFN γ and TNF α (Wang et Tisch, 2008). Although the molecular events that initiate the loss of tolerance in this setting are still speculative, several studies suggest that a limited number of primary islet autoantigens recognized by these infiltrating cells may be responsible for disease initiation (Lennon *et al.*, 2009), that can be explained with a defect in thymic T-cell negative selection.

To corroborate this hypothesis, 20% of individuals with spontaneous mutations of the autoimmune regulator gene AIRE developed T1D; indeed, insulin is an AIRE-regulated islet protein expressed in thymic medullary epithelial cells where autoreactive T-cells can come into contact for the first time with the autoantigen (Gardner *et al.*, 2009).

This is not the only genetic variation linked to the development of T1D, indeed the most important genetic association in T1D is found within HLA-DR class II genes, encoding major histocompatibility complex (MHC) class II molecules (Erlich *et al.*, 2008). Other established common variants include Insulin, CTLA-4, PTPN22 and CD25 genes (Sgouroudis et Ciriaco, 2009).

Moreover, number of reports demonstrate that the frequency and/or function of various immunoregulatory effectors such as FoxP3-expressing CD4⁺CD25⁺ Tregs and IL-4 secreting Th2 cells are reduced in NOD mice and diabetic patients (Wang *et Tisch*, 2008).

Finally, the environment is likely to have a strong effect on the development and progression of T1D. In NOD mice the incidence of T1D decreases dramatically when they are exposed to microbial stimuli (Qin *et al.*, 1997; Wen *et al.*, 2008). Similar observation has been noted in humans as the incidence of T1D is higher in the industrialized societies with reduced exposure to parasites (Weintrob *et al.*, 2001). The influence of other environmental factors has been demonstrated ranging from cows' milk/bovine serum albumin, meat preservatives/N-nitroso compounds, vitamin D and analogues, omega-3 fatty acids, environmental stress and toxins (Virtanen *et al.*, 2006; Akerblom *et al.*, 2005; Norris *et al.*, 2007; Jun *et al.*, 2004). Finally, recent evidences suggested a potential role for viruses in T1D pathogenesis (Richardson *et al.*, 2009; Nejentsev *et al.*, 2009).

2. Rheumatoid Arthritis (RA)

Rheumatoid Arthritis (RA) is a common chronic, inflammatory autoimmune disease affecting approximately 1% of the world population, increasing with age and peaking between the ages of 35 and 50 years. The annual incidence of RA is approximately 3 cases per 10,000 individuals in the general population (<http://emedicine.medscape.com>).

This disease is characterized by synovial inflammation and hyperplasia, rheumatoid factor (RF) and anti-citrullinated protein antibody production (ACPA), cartilage and bone destruction and systemic feature, including cardiovascular, pulmonary, psychological and skeletal disorders.

The quality of life of RA patients is reduced by pain, fatigue and loss of body function. Moreover, a number of extra-articular manifestation and comorbidities are present in RA patients, resulting in increased mortality (Gonzalez *et al.*, 2008). Even if the cause of RA is unknown, it is demonstrated that this disease involves a complex interplay among genotype, environmental factor and chance.

Citrullination is a normal process in which dying cells, that normally do not come in contact with the immune system, incur. The interaction between environmental factor (e.g. smoking, bronchial stress as exposure to silica) and genetic susceptibility (e.g. HLA-DR4 alleles) (Symmons *et al.*, 1997) lead to altered post-transcriptional regulation and self-protein citrullination. In particular, peptidylarginine deiminase (PAD) enzyme and citrullinated protein leak out of the dying cells and contact the immune system. PAD citrullinate extracellular protein containing arginine, generating citrullinate antigens that are not recognized as self and consequently develop ACPA and the loss of tolerance. Also the presence of RF is indicative of autoantibody production.

The production of ACPA and RF usually precedes inflammation and adhesion molecule formation in the synovium and the clinical RA (Van de Sande *et al.*, 2011).

The relationship between the loss of tolerance and the synovitis is unclear, but synovial involvement occurs when various inflammatory cell types infiltrate the synovium and ultimately work together to cause joint destruction. In particular, dendritic cells express cytokines, HLA class II molecules and costimulatory molecules and are involved in antigen-presentation and T-cell activation. The latter causes recruiting of T helper cells such as Th17 cell that, with the collaboration of dendritic cells and macrophages, created an inflammatory

environment. Th17 also triggers humoral adaptive immunity mediated by synovial B-cells that secrete antibodies, present antigen to T-cell and secrete cytokines stimulating synovial fibroblasts (Isaacs *et al.*, 2010).

Also cells of the innate immune system (e.g. macrophages and neutrophils) are involved in the pathophysiology of synovial inflammation in RA.

Finally, intracellular signal transduction pathway may be also involved, since cytokines release reflects the way cells respond to environmental stress (Rasheed *et al.*, 2008).

This complex pathophysiology leads to synovial hyperplasia that results in the loss of normally protective effects of synovium and cartilage damage (Rhee *et al.*, 2005); bone erosion occurs rapidly affecting 80% of the patients within 1 year after diagnosis (van der Heijde *et al.*, 1995).

Despite RF and ACPA are crucial in RA pathophysiology, the presence of these two autoantibodies is no longer considered necessary for the diagnosis; indeed, when RF and ACPA are negative, but there are symptoms similar to those of RA, seronegative RA can be diagnosed.

In particular, 38 % of RA patient are diagnosed with seronegative RA (De Winter *et al.*, 2016). However, often within the first two years of diagnosis around 80% of seronegative RA cases could become seropositive or develop into other autoimmune disease as well (<http://www.everydayhealth.com>).

In a study done by Nordberg *et al.* (2016) on a total of 234 European patients it has been demonstrated that patients with seronegative RA have more inflammatory activity compared with those with RA seropositive.

3. Sjögren's Syndrome (SjS)

Sjögren's Syndrome (SjS) is a chronic autoimmune systemic disease, characterized by a lymphoplasmocytic infiltration and a progressive salivary and lachrymal glands destruction, leading to ocular and mouth dryness.

Beyond these first sicca symptoms manifestations, half of SjS patients develop extraglandular complications, including lung interstitial disease, nervous system involvement and tubular nephropathy (Cornec *et al.*, 2012).

There are two forms of SjS: 1. primary SjS occurs without other autoimmune and rheumatic disorders; 2. secondary SjS is associated with another rheumatic disease such as systemic lupus erythematosus (SLE), RA or scleroderma.

The geo-epidemiological distribution of SjS in the global population is extremely variable according to study design and geographic area.

A meta-analysis of studies, published between 1993 and 2013, allows to evaluate the SjS incidence and prevalence. The data, emerged comparing six studies reporting heterogeneous data, estimates 6.92 cases per 100 000 person-years with an incidence ratio between female and males of 9.29. On the other hand, prevalence data coming from a meta-analysis of 18 studies elaborated a prevalence of 60.82 cases per 100 000 inhabitants and an incidence ratio between females and males of 10.72 (Qin *et al.*, 2015).

Regarding SjS pathogenesis, both genetic and non-genetic factors are involved in disease susceptibility and initiation of disease process.

Regarding the genetic factor, some HLA class II loci have been demonstrated to be associated to SjS (Huang *et al.*, 2015); moreover, Markeljevic *et al.* (2015) reported an association between low platelet serotonin level in SjS patients and polymorphism in the serotonin transporter gene (5-HTT).

Also the epigenetic alterations, in particular those related to DNA methylation mainly present in B cells, have been shown to play a central role in the pathogenesis of SjS (Miceli-Richard *et al.*, 2016).

Beyond genetics and epigenetics, alteration in the cytokines networks seem to be crucial in the onset of SjS. In particular, it as been demonstrated that an up-regulation of IFN activity in labial salivary gland is associated with a more severe disease phenotype (Hall *et al.*, 2015). An important point in the role of cytokines in SjS are the over-expression of IL-18 (that induce and aberrant expression of IL-22 receptor) (Ciccia *et al.*, 2015) and/or IL-33 (Jung *et al.*, 2015).

Another two important protagonists in the pathogenesis of SjS are B-cell Activation Factor (BAFF) which rescue B cells from apoptosis, and APRIL (proliferation-inducing ligand) which participate in B-cell activation (Mackay *et al.*, 2003). Deregulation in this pathway could be involved in the onset of SjS.

Another aspect that need to be considered is the role of salivary gland epithelium; in particular, the loss of apical-basolateral acinar-cell polarity could lead to the presence of

salivary mucins in the extracellular matrix of salivary gland resulting in the expression of proinflammatory cytokines (Barrera *et al.*, 2015).

Finally, the acquired immunity plays a central role in the SjS pathogenesis. The main player in this contest results to be the thymic selection of T_{reg} cells (Yaciuk *et al.*, 2015), a different distribution of lymphocytes in the peripheral blood (PB) in comparison to healthy individuals (Sudzius *et al.*, 2015), the number of Th17 cells that seems to be a central role as initiators of the inflammatory process in SjS (Lin *et al.*, 2015) and the activation of various Signal Transducer and Activator of transcription (STAT) proteins in PB mononuclear cells that have a role in signal transduction induced by inflammatory cytokines (Pertovaara *et al.*, 2015).

MATERIALS AND METHODS

1. Materials and methods for microbiology

1.1. Bacterial strains

1.1.1. *Escherichia coli* strains

- DH5 α

The *Escherichia coli* DH5 α strain carries the mutations recA1, endA1, the gene *lacZ* Δ M15, and shows high transformation efficiency. Moreover, it carries no antibiotic resistance genes.

- TOP10

Competent One Shot® TOP10 *E. coli* provided by Invitrogen (C4040-03) were used. Strain features are reported in the product information provided by the manufacturer.

- XL1-blue

The *E. coli* XL1-blue derived from the *E. coli* K12 strain and carries the mutations recA1, endA1, gyrA96, thi-1, hsdR17, supE44, relA1, *lacZ* Δ M15. Moreover, it carries antibiotic resistance to tetracycline.

1.1.2. *Agrobacterium tumefaciens* strains

- LBA4404

This is an octopine strain with a disarmed octopine vir plasmid. Cells are selected on medium containing 50 mg/l of rifampicin and 100 mg/l of streptomycin.

1.2. Culture media

- LB (Luria-Bertani) broth, pH 7.5.
- SOC (Super Optimal broth with Catabolite repression) broth, pH 7.0: it is obtained by the addition of 20 mM glucose and 10 mM MgCl₂ to the SOB broth.

For solid medium preparation, 15 g/l of bacteriological agar were added.

1.3. Competent cell preparation

1.3.1. *E. coli* competent cells

Competent cells were prepared using the simple and efficient method (SEM), as described in Inoue *et al.* (1990).

1.3.2. *A. tumefaciens* competent cells

In order to obtain electro-competent cells of EHA105 and LBA4404 strains, a single colony was inoculated in 5 ml of rifampicin-containing LB broth (50 mg/l). After 24 hours, an aliquot of 1.5 ml of culture was centrifuged at 14000 rpm for 1 minute at room temperature (RT). In order to completely eliminate antibiotic, pellet was washed three times in 500 μ l of cold and sterile glycerol 10% (v/v) and finally resuspended in 40 μ l of glycerol 10% (v/v).

To obtain electro-competent cells of GV3101, the same procedure was followed but each final aliquot was derived from 20 ml of saturated o/n culture, instead of 1.5 ml.

1.4. Bacterial transformation

1.4.1. Heat-shock

Plasmid DNA or ligation reaction product were added to a vial of *E. coli* competent cells. The vial(s) was incubated on ice for 15-30 minutes, then heat-shocked at 42°C for 30 seconds and placed on ice for 1-2 additional minute(s). 250 μ l of pre-warmed SOC medium were added and the vial was shaken at 37°C for 1 hour at 200 rpm. After incubation different amounts of cell suspension were spread on LB agar plates containing antibiotics for the selection. For *E. coli* transformation with plasmid containing the *lazZ* gene α fragment 100 μ l of 100 mM IPTG and 20 μ l of 50 mg/ml X-Gal were spread on the plate surface approximately 30 minutes before *bacteria* spreading. Plates were incubating at 37°C overnight (o/n).

1.4.2. Electroporation

This protocol was used for transformation of electro-competent *A. tumefaciens* cells. Bacterial transformation was performed using Bio-Rad electroporation instrument, at 25 μ F, 200 Ω and 2.5 kV. 10-20 ng of DNA plasmid for EHA105 and LBA4404 strains and 600-900 ng for GV3101 strain in a maximum volume of 5 μ l of a low ionic buffer (such as TE or water) were added to 40 μ l aliquots of electro-competent cells. The solution was subjected to the electric pulse and then rapidly 1 ml of LB broth without antibiotics was added. After 30-60 minutes of growth at 28°C by vigorous shaking, different amounts of cell culture were spread on selective medium. Plates were incubated at 28°C for 2-3 days.

1.4.3. Plasmid DNA extraction

For mini- and maxi preparation of plasmid DNA “QIAprep Spin Miniprep kit” (QIAGEN, 27106) and “HiSpeed Plasmid Maxi kit” (QIAGEN, 12663) were used respectively. Extraction was performed by following the procedure described in the Handbook provided by the company.

2. Materials and methods for molecular biology

2.1. Nucleic acid agar gel electrophoresis

The gel was obtained by boiling a solution of agar (a purified polysaccharidic linear polymer) and TAE buffer 1X (40 mM Tris-acetate, 1 mM EDTA, pH 8.0). Gels of 1% w/v agar were usually employed as they allow separating neatly fragments between 0.5 and 10 kbp; 0.7% w/v agar gels were used to improve the separation of longer fragments; for DNA molecules of length inferior to 1.5 kbp, gels with 2% w/v agar were employed. Before the gel became solid and while its temperature was higher than 50° C, the intercalator “SYBR® safe DNA gel stain” (Invitrogen) was added to the solution, at a final concentration 10 000 times lower than the stock solution. One volume of the solution “6X Blue/orange loading dye” (Promega) was added to each sample prior to the loading, to reach a final concentration of 1X. The electrophoresis was performed at room temperature,

applying a constant voltage of 80-100V to the gel for 15-30 minutes, depending on the desired degree of separation between DNA bands.

2.2. RNA extraction and reverse transcription

Total RNA extraction was performed by using TRIzol® Reagent (Invitrogen), according to the procedure provided by the company. RNA samples were quantified with the NanoDrop spectrophotometer (NanoDrop Thermo Scientific Technologies). 1 µg of RNA was treated with 1 unit (U) of DNase (Promega) for 30 min at 37°C in 1X DNase Buffer. DNase-treated RNA was used for cDNA synthesis using the enzyme SuperScriptIII (Promega) through a reaction protocol provided by the producing company. In order to assess if the cDNA was produced properly, an amplification step using primers (Act1 - Act2) designed on the 3'-UTR of the gene transcript which codify for a member of the *Nicotiana* actin family was performed.

2.3. Polymerase chain reaction (PCR)

PCR analyses were performed by using the GoTaq®DNA polymerase (Promega) and the 5X buffer provided with the enzyme. Reaction mix and cycle were set-up following the protocol of the producing company. Extension time was calculated on the basis of the length of each target amplicon, considering an amplification rate of 1000 bp/min for the enzyme used. The annealing temperature (T_a) was calculated as the mean T_a of the two primers used for each reaction. For the amplification of gene that had to be cloned, the enzyme AccuPrime™ *Pfx* DNA Polymerase (Invitrogen) was used; reaction mix was assembled as described in the product information, using the buffer provided with the enzyme. Reaction cycle was set-up following Invitrogen indications, considering that the enzyme has an extension temperature of 68°C and an amplification rate of 1000 bp/min. Also in this case the T_a was calculated as the mean T_a of the two primers used for each reaction. The complete list of primers used is reported in the table 1, where T_m is referred as the melting temperature of each primer.

Table 1 List of primers used in PCR.

Primer name	Sequence	T _m °C
ACT1	TCTCGAGTTCCTGTTTCATAGTC	64
ACT2	GGCCCGCCATACTGGTGTGAT	68
pCP for	AGGTCAGCACCAGCTAGC	58
CP rev	AGTTCATACCACTGGAGC	58
RT-PCR1for	TGACATTTTCGTGCAACTTGG	58
TBSV-2Back	AAGATCCAAGGACTCTGTGC	56
CPMV Seq for	TCTAATCCGGGTATTGATGG	56
CPMV Seq rev	CAGATTTCCAAGCAGCAGTA	56

Different quantities of different DNA templates were employed, considering a volume of 50 µl for each reaction tube: 1-10 ng for plasmid DNA, 1 µl for cDNA or genomic DNA obtained as described above.

To detect *E. coli* recombinant clones carrying a vector with a fragment of interest, bacterial colonies were directly screened by PCR: a sterile tip was used to sample colony from the plate and dissolve it in the reaction mix. For *A. tumefaciens* transformed cells, the colony was previously dissolved in 5 µl of sterile water and warmed at 95°C for 10 minutes; this product was then used as template for PCR in a reaction volume of 50 µl.

2.4. Vectors and cloning procedure

2.4.1. PVX CVPs peptide display system

- pPVX201

This vector contains the cDNA encoding the complete Potato Virus X (PVX) genome (Chapman *et al.*, 1992). A schematic representation of the vector is reported in figure 9. Viral genome transcription is controlled by CaMV 35S promoter and *nos* terminator. 8k-, 12k- and 25k-protein are viral movement proteins. Viral genome replication is conducted by RNA-dependent RNA polymerase (RdRp). Coat protein CP gene is preceded by a sub-genomic (sg) promoter. At 5'- and 3'-ends of the viral genome cDNA, PVX 5'- and 3'-untranslated region (UTR) are present. B-lactamase gene allows the selection of transformed cloned on ampicillin-containing medium (100 mg/l).

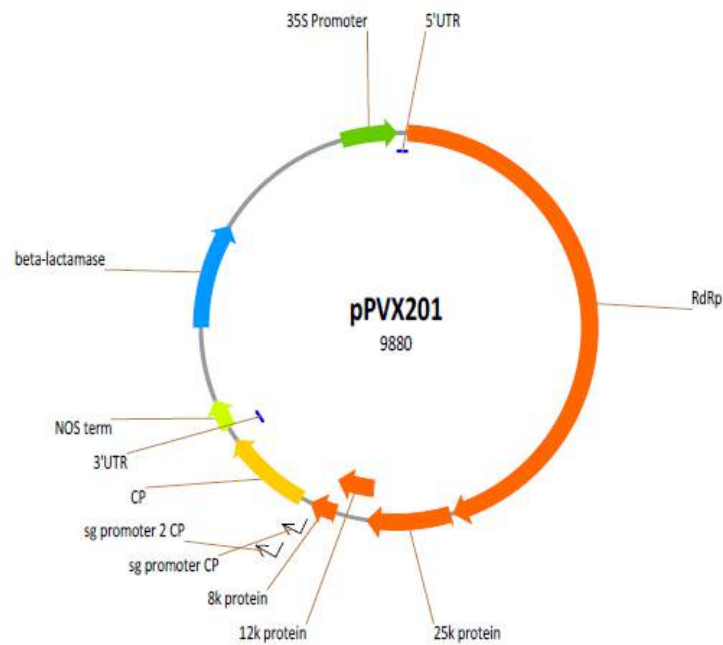


Figure 1 Schematic representation of pPVX201 vector.

- pPVXSma

This vector (Lico *et al.*, 2006) has the same features of pPVX201 vector, but it encodes for a 21 aminoacids (aa) N-terminal truncated version of the CP. Its map is reported in figure 2.

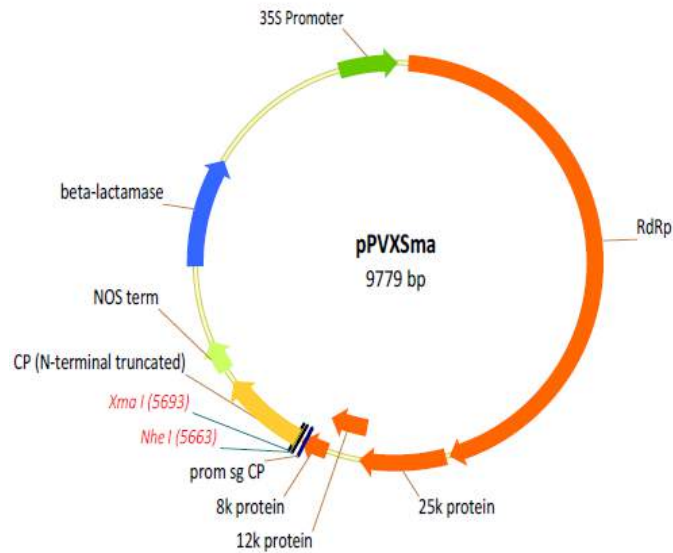


Figure 2 Schematic representation of pPVXSma vector.

To insert the sequences encoding the heterologous peptides as fusions with the CP gene into pPVXSma, oligonucleotide pairs were designed to obtain *NheI*-compatible 5'- and *XmaI*-compatible 3'-end DNA fragments, that were ligated into the *NheI*-*XmaI*-digested vector. Sequences encoding the peptides were preceded by an ATG codon. The complete list of oligonucleotide (oligo) sequences used with the PVX CVPs peptide display system is reported in the table 2. The autoantigen protein from which the peptide sequences derive are also reported.

Table 2 Oligonucleotids cloned with the PVX CVPs peptide display system.

Autoantigen	Oligo	Sequence
Lipocalin	Lipo for	CTAGCCTCGAGATGTCTTTTGAAAA GGCTGCTGGTGCTAGAGGTTTGTCT ACT
Lipocalin	Lipo rev	CCGGGAGTAGACAAACCTCTAGCA CCAGCAGCCTTTTCAAAGACATCTC GAGG
Liprin	LIP1 for	CTAGCCTCGAGATGGCTTCTGTTCT TGCTAATGTTGCTCAAGCTTTTGAA AAGTCTACTC
Liprin	LIP1 rev	CCGGGAGTAGACTTTTCAAAGCTT GAGCAACATTAGCAAGAACAGAAG CCATCTCGAGG
FADK ₂	FADK ₂ for	CTAGCCTCGAGATGTCTGAAGCT AAGGTTCTTGCTAATCTTGCTCAT CCTCCTGCTACTC
FADK ₂	FADK ₂ rev	CCGGGAGTAGCAGGAGGATGAGC AAGATTAGCAAGAACCTTAGCTTC AGACATCTCGAGG
BANK ₁	BANK ₁ for	CTAGCCTCGAGATGTCTGATATG ATTCTTGCTAATCTTTCTATTAAG AAGAAAACCTGAAC
BANK ₁	BANK ₁ rev	CCGGGTTTCAGTTTTCTTCTTAAT AGAAAGATTAGCAAGAATCATATC AGACATCTCGAGG

2.4.2. CPMV eVLPs peptide display system

This system is based on the use of two vectors, sharing a common backbone: pEAQ-*HT*-24K and pEAQ-*HT*-VP60 (Sainsbury *et Lomonossoff*, 2008; Sainsbury *et al.*, 2009; Saunders *et al.*, 2009). The two vectors were kindly provided by professor Lomonossoff (John Innes Centre, Norwich, UK). Target gene transcription is regulated by CaMV 35S promoter and terminator. *Cowpea mosaic virus* (CPMV) 5'-UTR and 3'-UTR function as translation enhancer; P19 gene encodes for a viral suppressor of silencing. Transformed clones are selected on kanamycin-containing medium (50 mg/l).

- pEAQ-*HT*-24K

In this vector the gene encoding CPMV 24K proteinase was cloned (Saunders *et al.*, 2009). A schematic representation of the vector map is reported in figure 3.

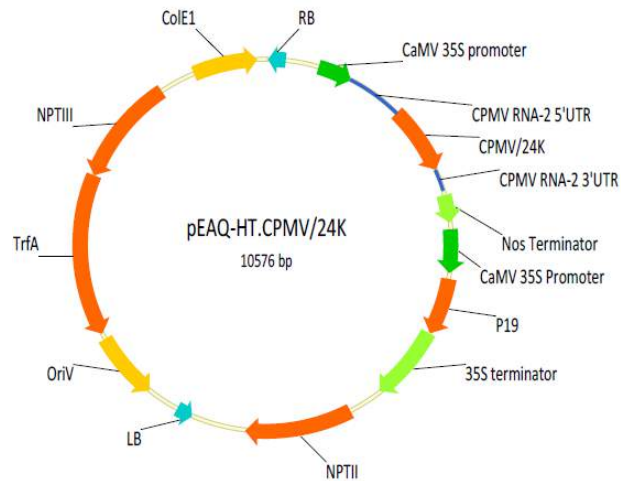


Figure 3 Schematic representation of pEAQ-HT.CPMV/24K vector.

- pEAQ-*HT*-VP60

In this vector the gene encoding CPMV VP60 (precursor of viral small and large coat protein) was cloned (Saunders *et al.*, 2009). A schematic representation of the vector map is reported in figure 4.

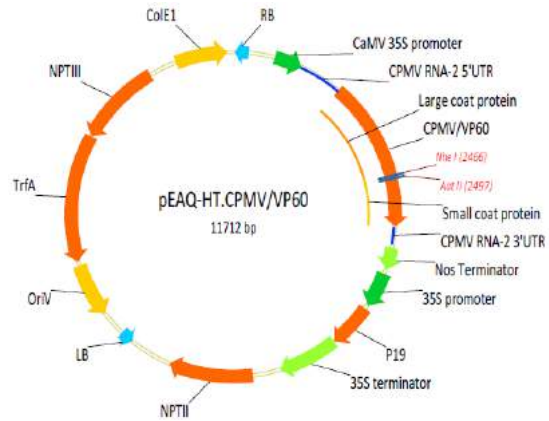


Figure 4 Schematic representation of pEAQ-*HT*-VP60 vector.

To insert the sequences encoding the heterologous peptides as fusions with the small CP gene, oligonucleotide pairs were designed to obtain *NheI*-compatible 5'- and *AatII*-compatible 3'-end DNA fragments that were ligated into the *NheI*-*AatII*-digested vector. The complete list of oligonucleotide (oligo) sequences used with the CPMV eVLPs peptide display system is reported in the table 3.

Table 3 Oligonucleotids cloned with the CPMV eVLPs peptide display system. Bold letters correspond to the nucleotids added in order to restor the pEAQ-*HT*-VP60 vector.

Autoantigen	Oligo	Sequence
Lipocalin	Lipo for	CTAGCACTCCTCCTGCTTTTGAAAAGGCTGCTGGT GCTAGAGGTTTGTCTACTCCATTTTCAGACGT
Lipocalin	Lipo rev	CTGAAAATGGAGTAGACAAACCTCTAGCACCAGC AGCCTTTTCAAAGCAGGAGGAGTG
GAD65	p524 for	CTAGCACTCCTCCTGCTGATTCTCGTCTTTCTAAG GTTGCTCCTGTTATTAAGGCTAGAATGATGGAAGA TCCATTTTCAGACGT
GAD65	p524 rev	CTGAAAATGGATCTTCCATCATTCTAGCCTTAATA ACAGGAGCAACCTTAGAAAGACGAGAATCAGCAG GAGGAGTG
Protein	Oligo	Sequence
BP100	BP100 for	CTAGCACTCCTGCTGATAAGAACTTTTAAAGAA AATTCTTAAGTATCTTGAAGATCCATTTTCAGACG T
BP100	BP100 rev	CTTGAAAATGGATCTTCAAGATACTTAAGAATTTT CTTAAAAAGTTTCTTATCAGCAGGAGGAGTG

2.4.3. TBSV CVPs peptide display system

The cloning steps in the pTBSV vector have been conducted by the research group of the professor Luca Santi at the Department of Agriculture and Forestry Science (DAFNE) of the University of Tuscia following the procedures reported in Grasso *et al.* 2013.

A schematic representation of the pTBSV vector map is reported in figure 5.

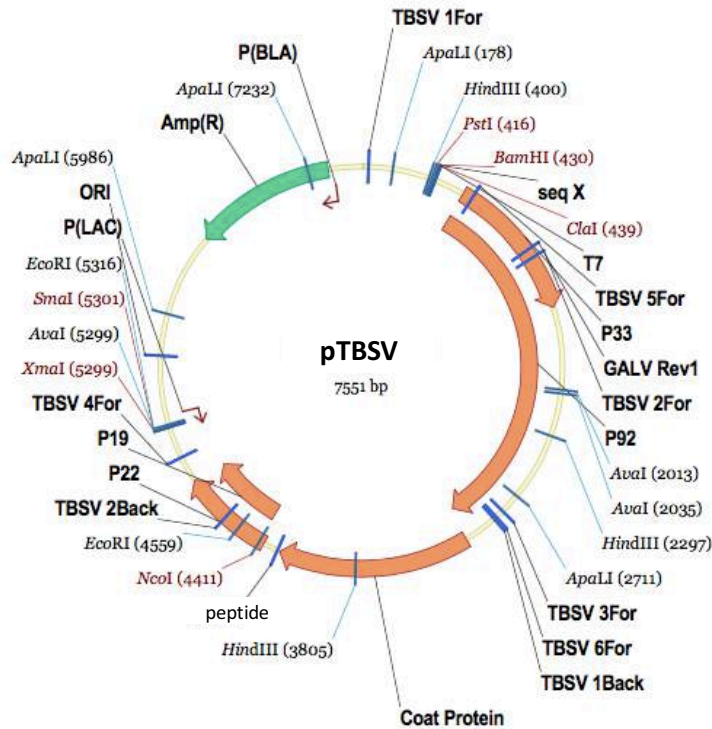


Figure 5 Schematic representation of pTBSV vector.

The complete list of oligonucleotide (oligo) sequences used with the TBSV CVPs peptide display system is reported in the table 4.

3. Plant materials and methods

3.1. Plant material

Nicotiana benthamiana plants were grown from seeds in heat-sterilized soil and cultivated in a growth chamber at 25°C with a light/dark cycle of 16 h/8 h and a relative humidity 20-40%.

Brassica juncea plants were grown from seeds in heat-sterilized soil and cultivated in a greenhouse with temperature between 30°C and 21°C, relative humidity of approximately 32-50% and a 15 h/9 h light/dark cycle.

3.2. Expression of PVX CVPs in *N. benthamiana*

N. benthamiana plants were inoculated with the different pPVXSma constructs or with pPVX201 as described previously (Marusic *et al.*, 2001). To verify the genomic stability and infectivity of virus particles that cause systemic infection, repeated cycles of re-infection were performed using leaf sap, prepared by homogenizing infected tissue in 1X PBS pH 7.2 (3 g/l Na₂HPO₄·12H₂O, 0.256 g/l NaH₂PO₄·H₂O, 8.8 g/l NaCl) and centrifuging the sample for 3 min at 20 000 g and 4°C. The supernatant was used directly to infect the plants. Briefly, sap obtained from symptomatic systemic leaves of the plants inoculated with the construct of interest (#1) was used to inoculate a second group of plants (#2). Afterwards, a third group of plants (#3) was infected by using the sap of the symptomatic systemic leaves from #2 plants.

3.3. Expression of CPMV eVLPs in *N. benthamiana*

For CPMV eVLPs expression, pEAQ-*HT*-24K and pEAQ-*HT*-VP60 vectors were transformed into *A. tumefaciens* LBA4404 strain. Bacterial cultures carrying the two vectors were grown separately to stable phase in LB medium supplemented with the appropriate antibiotics and then pelleted by centrifugation at 4 000 g and resuspended in MMA (10 mM MES, pH 5.6, 10 mM MgCl₂, 100 mM acetosyringone) to an OD₆₀₀ of 0.8. After 1- to 4-h incubation at room temperature, equal volumes of the two bacterial suspensions were mixed and used for syringe infiltration of 4-5 weeks-old *N. benthamiana*

leaves; 4 expanded leaves were infiltrated in each plant. Infiltrated leaves were sampled 6 days post infection (dpi).

3.4. Expression of TBSV CVPs in *N. benthamiana*

The expression of TBSV CVPs in *N. benthamiana* has been conducted as reported in Grasso *et al.* 2013.

3.5. Expression of TuMV in *N. benthamiana* and *B. juncea*

The expression of TuMV CVPs in *N. benthamiana* and the following propagation of them in *B. juncea* have been conducted as reported in Sánchez *et al.* (2013).

4. Biochemical materials and methods

4.1. Protein extraction from leaf material

Leaf samples were ground to fine powder with liquid nitrogen, homogenized in extraction buffer supplemented with Protease Inhibitor Cocktail (cOmplete™ EDTA-free Protease Inhibitor-Roche) and then centrifuged at 13 000 g for 20 minutes at 4°C. The selected ratio between plant tissue weight (g) and buffer volume (ml) was 1:3. Supernatant was collected and conserved at -80°C for further analyses. Buffers used for protein extraction are listed below.

- Sodium phosphate buffer 0.1 M pH 7.0
 - Solution A: 0.1 M NaH₂PO₄
 - Solution B: 0.1 M di Na₂HPO₄.

Final solution at pH 7.0 was obtained by mixing 39 ml of solution A and 61 ml of solution B. This buffer was used for protein extraction from *N. benthamiana* leaves expressing CPMV eVLPs.

- Boric acid 0.5 M pH 7.8.

This buffer was used for protein extraction from *N. benthamiana* leaves expressing PVX CVPs.

4.2. SDS-PAGE

For SDS-PAGE, protein samples were supplemented with 0.5 volume of R buffer (0.1 M Tris-HCl, 3% SDS, 1% w/v Bromophenol blue, 15% glycerol, pH 6.8) and boiled for 10 minutes. Samples were loaded on gel with different percentage of polyacrylamide:

- 12% for protein extracts of plant leaves expressing CPMV eVLPs;
- 14% for protein extracts of plant leaves expressing PVX CVPs and TuMV CVPs.

For the TBSV CVPs samples were supplemented with 0.5 volume of R buffer (for 10 ml: 3 ml 0.1 M Tris-HCl 0.5 M pH 6.8, 2.4 ml glycerol 100%, 1.6 ml SDS 10%, 1 ml Bromophenol blue in TE, 300 µl EDTA, 1.7 ml H₂O; every 160 µl add 10 µl of 2-mercaptoethanol). The sample were treated as follow: 3 minutes room temperature, mixed with vortex, 1 minute at 60 °C, mixed with vortex, 1 minute room temperature and stored in ice.

Running buffer used for electrophoresis was Tris-glycine 1X pH 8.3 (3 g/l Tris-base, 18.8 g/l glycine) supplemented with 0.1% SDS. The electrophoresis was performed at room temperature, applying a constant voltage of 150V to the gel for approximately 1 hour.

4.2.1. Gel Coomassie staining

After electrophoresis, gel was washed with water and stained by heating it in the presence of Coomassie staining solution A in a microwave oven for about two minutes, until boiling point. After that, it was cooled down at room temperature and gentle shaken. Solution A was discarded and gel was destained by subsequent heating and cooling in the presence of solution B, C and D, following the same protocol described for staining solution A. The compositions of the solutions are following described.

- Staining solution A

Component	Concentration
Coomassie R-250	0.05%
Isopropanol	25%
Acid acid	10%

- Distaining solution B

Component	Concentration
Coomassie R-250	0.05%
Isopropanol	25%

- Distaining solution C

Component	Concentration
Coomassie R-250	0.002%
Acetic acid	10%

- Distaining solution D: acetic acid 10%

4.2.2. Gel Silver staining

For silver staining of gels, after electrophoresis the procedure described in Mortz *et al.* (2001) was applied.

4.3. Western blot analysis

- **Tris-glycine 5X pH 8.3:** 15.1 g/l Tris-base, 94 g/l glycine.
- **Blotting buffer:** 1X Tris-glycine pH 8.3, 20% methanol.

- **PBS 10X pH 7.4:** 80 g/l NaCl, 2 g/l KCl, 14.4 g/l Na₂HPO₄, 2.4 g/l KH₂PO₄.
- **Blocking solution:** 1X PBS pH 7.4, 4% powder milk, 0.05% Tween-20.
- **Washing solution:** 1X PBS pH 7.4, 0.1% Tween-20.

After electrophoresis, proteins were transferred to a nitrocellulose membrane by electroblotting in the presence of blotting buffer. To decrease non specific antibody binding, membrane was incubated in blocking solution for 1 hour at room temperature.

Different detection antibodies and protocol were employed for the different kinds of sample analyzed, as following described.

- For the detection of CPMV coat proteins, the same protocol described for GAD65-containing samples was used, but membrane was probed with a primary polyclonal antibody (G49) specific to CPMV particles (Saunders *et al.*, 2009) used at a concentration of 1:2 000.
- For the detection of PVX coat protein, an alkaline phosphatase conjugated anti-PVX antibody (Agdia, PSA10000/0288) was used. It was diluted 1:200 in 1X PBS and the membrane was incubated for 2 hours at room temperature. The detection was performed with the NBT/BCIP System. NBT (Sigma-Aldrich, N6659) and BCIP (Sigma-Aldrich, B1026) were prepared according to manufacturer's information and the procedure provided by the company was used for signal detection.

4.4. CVPs and eVLPs purification

4.4.1. PVX CVPs purification from leaf material

For large scale purification of PVX particles, approximately 50 g of symptomatic *N. benthamiana* leaves were used. The process was carried out as described in Uhde *et al.* (2004).

4.4.2. CPMV eVLPs purification from leaf material

4.4.2.1. PEG 6000 precipitation

Large scale CPMV eVLPs purification was carried out starting from 15-20 g of *N. benthamiana* infiltrated leaf material. Leaf tissue was homogenized with 3 volumes (*i.e.* 3 ml of buffer for 1 g of tissue) of 0.1 M Sodium phosphate buffer, pH 7.0 using a blender. Polyvinyl-pyrrolidone (PVPP) was added to the buffer to a final concentration of 2%. Homogenate was squeezed through three layers of muslin cloth and spin at 30 000 g for 60 minutes at 4 °C to remove cell debris. To the supernatant, polyethylene glycol 6 000 (PEG 6000) to a final concentration of 4% and NaCl to 0.2 M were added. Sample was stirred o/n at 4 °C to precipitate the virus particles. Then it was spun at 13 000 g for 20 minutes at 4 °C to pellet the PEG precipitate. The pellet was dissolved in 0.01 M sodium phosphate buffer, pH 7 (0.5 ml/g leaf tissue) and resuspended thoroughly by vortexing. Sample was spun at 27 000 g for 20 minutes at 4 °C. The supernatant was transferred to ultracentrifuge tubes and spin at 118 700 g for 150 minutes at 4 °C in an ultracentrifuge. The pellet was resuspended in 200 µl of 0.01 M phosphate buffer o/n at 4°C. The day after, the sample was spun again at 10 000 g for 15 minutes on a bench-top centrifuge to remove aggregates and remaining plant contaminants. The supernatant containing purified CPMV eVLPs was conserved at 4°C.

4.4.2.2. Protocol based on anion-exchange and size exclusion chromatography

Large scale CPMV eVLPs purification was carried out starting from 15-20 g of *N. benthamiana* infiltrated leaf material. Leaf tissue was homogenized with 3 volumes (*i.e.* 3 ml of buffer for 1 g of tissue) of 0.1 M Sodium phosphate buffer, pH 7.0 using a blender. Polyvinyl-pyrrolidone (PVPP) was added to the buffer to a final concentration of 2%. Homogenate was squeezed through three layers of muslin cloth and spin at 30 000 g for 60 minutes at 4 °C to remove cell debris. The DEAE SephadexTM A-50 (GE Healthcare) (regenerated in sodium phosphate buffer 0.1 M pH 7, 0.02% Tween 20) were used in sample:resin ratio 1:4, the flow through was concentrated to 4-5 ml and loaded of size exclusion chromatography. For the size exclusion chromatography HiPrepTM 16/60

Sephacryl S-500 HR was used with a flow rate of 0.9 ml/min. This column has a resolution of 4×10^4 - 2×10^7 .

4.4.2.3. Protocol based of double sucrose cushion and Nycodenz gradient

Large scale CPMV eVLPs purification was carried out starting from 15-20 g of *N. benthamiana* infiltrated leaf material following the procedure reported in Peyret *et al.* (2015).

4.5. CVPs and eVLPs characterization

4.5.1. Dynamic Light Scattering (DLS)

The DLS analyzing the Brownian motion of the particles present in solution, allows to analyze the CPMV eVLPs conformation to gain their diameter.

The sample was centrifuged at 10 000 rcf for 10 minutes in order to eliminate aggregated particles. The sample must to be at the concentration 0.4-0.5 mg/ml. 3 measurements was done and each measurement was the results of the mean of 12 repetitions.

4.5.2. Limulus Amebocyte Lysate-test (LAL-test)

LAL-test was conducted following the product sheet instruction (International Pbi s.p.a.). the acceptable limits of endotoxins for injectable is 0.25 UE/ml.

4.6. ELISA test

Indirect ELISA for the set up of diagnostic kits were done following the procedure reported in Tinazzi *et al.* (2015).

5. Human Cell Culture

5.1. SH-SY5Y neuroblastoma cells

SH-SY5Y (ATCC® CRL-2266TM) were propagated and subculture as reported in the product sheet and the Cell culture guideline (abcam ®).

The compositions of the DMEM culture medium are following described.

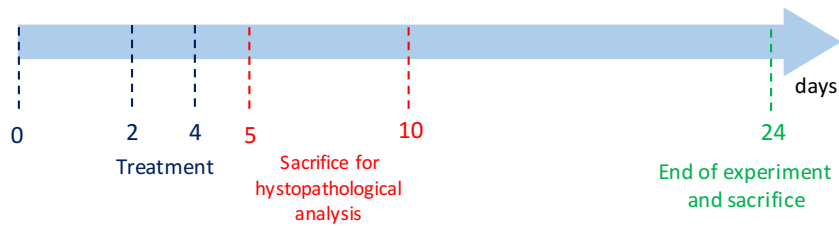
Component	Concentration
Non essential aminoacids	1%
Glu-T	1%
Penicillin-streptomycin	1%
FBS	15%

6. Animal models

6.1. NOD mice

NOD mice are the animal model of T1D. The characteristics of this animal models are reported in Kachapati *et al.*, 2012.

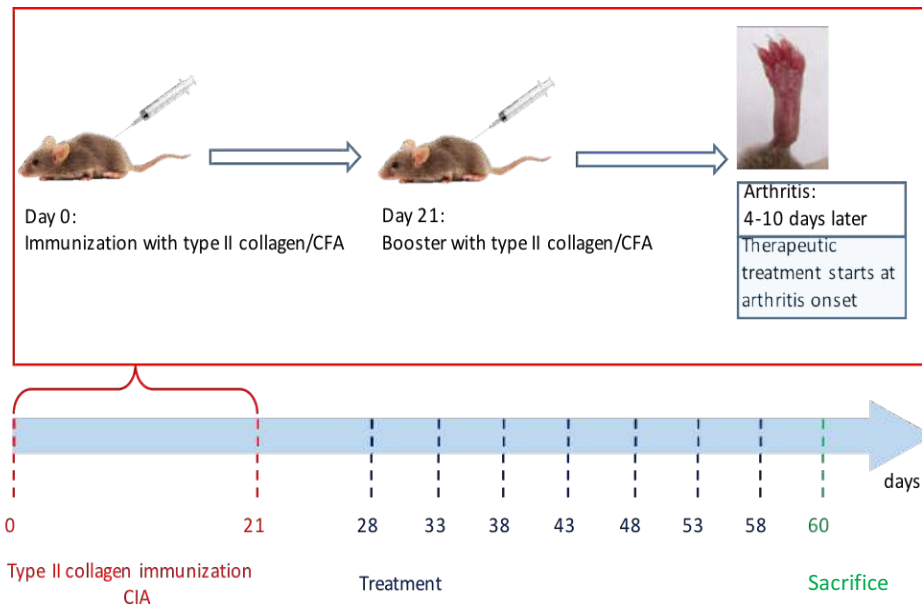
The treatments were done as reported in the following scheme.



6.2. DBA-1/CIA mice

DBA-1 (Dilute Brown Non-Agouti) mice are immunized with type II collagen (CII) as reported in Bran *et al.* 2007 in order to obtained CIA (collagen-induced arthritis) mice, the animal model of RA.

CII immunization and treatment were done as reported in the following schema.



7. T1D cytokines analysis

The cytokines analysis was conducted using the Luminex xMAP technology Bio-Plex Pro™ Mouse Cytokine 23-plex following the product sheet instruction.

8. RA cytokines analysis

To quantify cytokines from mouse joints, tissues were pulverized, resuspended in 1 ml of lysis medium/100 mg of joint weight for 60 min at 37°C, and centrifuged. To assess cytokine production from lymph nodes, these were removed, homogenized, and centrifuged. Supernatant fluids from joints and lymph nodes were sterilized through a Millipore filter (0.45 µm pore size) and stored at -80°C until analysis. TNF- α , IL-17A, IL-1 β , IFN- γ , TGF- β 1, and IL-10 concentrations were determined in serum and supernatant fluids from joints and lymph nodes by using commercial ELISA kits (eBioscience) according to manufacturer's recommended.

CHAPTER 1: THERAPY**INTRODUCTION****1. Immunological tolerance and autoimmune disease**

The immune system is a network of cellular, chemical, and soluble protein components that interact with each other in a sequential and regulated manner and are charged with protecting the body against foreign substances. Foreign or self-molecules that evoke a specific immune response are referred as antigens. The immune system components are located throughout the body, either inside specific organs (e.g. spleen and thymus) or as accumulations of lymphoid and myeloid cells placed in strategic sites (e.g. associated with the skin and gut) to monitor the entry of foreign substances.

The distinction between self and non-self occurs through complex mechanisms depending either on non-specific effectors that act as first line of defence against pathogens (e.g. macrophages, natural killer cells and polymorphonuclear leukocytes and cytokines) or on specific recognition molecules present on the surface of T and B lymphocytes (Smith *et* Germolec, 1999).

Despite the fact that lymphocytes with the ability to recognise self antigens are constantly being generated during the normal process of lymphocyte maturation, there are a complex series of mechanisms, generally referred as immunological tolerance, that impair the immune system to mount responses against self antigens.

In particular, immunological tolerance is the failure of a lymphocyte clone to respond to an antigen, due to a prior exposure to the same antigen.

Tolerance can occur by two main mechanisms named central or peripheral tolerance. central tolerance occurs when immature lymphocytes encounter the antigen in the primary lymphocytes organ, and consequently they die or become unreactive.

The peripheral tolerance occurs when mature lymphocytes, escape from negative selection during ontogeny, encounter the antigen in peripheral or secondary lymphoid tissues and undergo to one of the following mechanism to prevent self-response:

- 1) clonal deletion, which requires the physical elimination of autoreactive lymphocytes;
- 2) clonal anergy, which requires the functional elimination of autoreactive lymphocytes via downregulation of responsiveness;
- 3) suppression or inhibition of autoreactive lymphocyte via interaction with other cell type or cytotoxic T lymphocytes of Natural Killer cells.

Finally, a heterogeneous family of T regulatory cells (Tregs) have been discovered to play an important role in suppressing immune responses against self.

The breakdown in the network of this mechanism results in an immune response against self-molecules leading to the establishment of an autoimmune disease (Romagnani, 2006). Autoimmune diseases (AD) are a spectrum of diseases ranging from organ specific to systemic. In organ specific, antibodies and T cells react to self-antigens in a define tissue (e.g. Hashimoto thyroiditis and type 1 diabetes), whereas systemic AD are characterized by reactivity against a specific antigen spread throughout various tissues in the body (e.g. systemic lupus erythematosus and rheumatoid arthritis).

The American Autoimmune Related Diseases Association reported the identification of 80-100 different autoimmune diseases with annual direct health care costs in the range of \$ 100 billion.

Direct costs are costs paid to health service by patients and insurance companies.

Epidemiological studies have indicated ADs to be the 10th most common cause of mortality in developing countries. The incidence is estimated to be around 10% (Cooper *et al.*, 2009).

2. Current strategies and ongoing studies for the treatment of autoimmune diseases

The current AD therapeutic approach can be categorized into two groups: the symptomatic or replacement therapy (conservative approach) and the immunosuppressive therapy (aggressive therapy).

T1D could be an example of disease managed by replacing the hormone insulin once pancreatic β -cells are damaged. However, this kind of therapy could only stem the disease effect without preventing the organ damage. Moreover, the replacement therapy must be adopted all life long with consequent side-effects and high-costs associated.

Furthermore, the symptomatic therapy is often associated to the immunosuppressive one. For example, in RA the symptoms are treated with non-steroidal anti-inflammatory drug (NSAIDS) associated with corticosteroid hormones (and other immunosuppressor).

The immunosuppressive therapy is used for dampen the immune response to prevent further organ damage and considering that is highly effective for many patients remain the current “gold standard” of care.

The response to immunosuppression in AD is initially in 60-70% of the cases, and subsequently the disease may progress or stop responding to the drug used.

On the other hand, the use of immunosuppressive agents causes several side-effects. Indeed, long-term treatments with high doses are often needed to maintain diseases control, leaving the patient susceptible to life-threatening opportunistic infections and long-term risk malignancy.

Considering that immunosuppressive drugs are non-specific, they interfere in non-target pathways and cells. Moreover, some of the ADs may go for clinical remission to relapse sometime (van der Kooij *et al.*, 2007).

In recent years, more experimental studies were focused on the development of new target-specific drugs that decrease the risk of systemic immune suppression and improve tolerability.

In particular, the optimal ADs therapy should fit these four goals:

- specifically target the pathogenic cells leaving the rest of the immune system unaltered;
- reestablished immune tolerance that is stable over time;
- have low toxicity and few side effects
- its associated costs low when compared to alternative approach.

In literature there are many examples of ongoing studies aimed to the development of biological molecules that could meet the abovementioned criteria.

One of the most promising one is the costimulatory blockade. This approach is based on the evidence that the achievement of a total T cells activation requires two signals: the first is the antigen recognized by T-cell receptor (TCR) and the second is a costimulatory signal provided by the cell presenting the antigen (APC); without the second signal the T cell become suboptimally stimulated, resulting unresponsive in a state of anergy (Mueller *et al.*, 2010). On the basis of this, the greatest success up to now is the development of a cytotoxic T lymphocyte-associated antigen 4 (CTLA-4)-immunoglobulin (Ig) which is able to prevent costimulation by interacting with the costimulatory receptor CD28 on T cells. Treatment with CTLA-4-Ig results to be effective in RA (Maxwell *et al.*, 2010; Mease *et al.*, 2011).

However, despite monthly administration of this drug over 24 months the beneficial effects were observed only within the first 6 months of therapy (Orban *et al.*, 2011). Moreover, blocking the costimulation may be unable to suppress the pathogenicity of T cells and for this reason this approach could be better exploited in the prevention of the disease. Furthermore, this approach is not target-specific for autoreactive T cells and can cause patient susceptibility to pathogens. Finally, this approach does not induce self-tolerance and needs continuous treatments.

Another strategy relies on the exploitation of the potential of regulatory T cell (T_{regs}).

T_{regs} are a subset of $CD4^+$ T cells that express high levels of the IL-2 receptor α chain CD25 and the transcription factor FoxP3. It has been broadly demonstrated that T_{regs} play a central role in suppressing auto-immunity (Sakaguchi *et al.*, 2010). The strategy consists in the isolation of Tregs cell, activation and expansion *ex-vivo* to high number, and adoptively transfer of them to AD patient in an attempt to suppress the ongoing autoimmune response. Unfortunately, this strategy is highly hampered by the inability to isolate an appropriate pure T_{regs} and the suppression function of this cell may not be stable over time (Roncarolo *et al.*, 2006).

Another approach that has been explored is the manipulation of the IL-2 pathway. This interleukin is a T cell growth factor with opposing role in the immune system. On one hand, IL-2 triggers the immune response by promoting the proliferation and generation of effector T cell. On the other hand, IL-2 can promote the survival and function of T_{reg} suppressing the immune response. It has been demonstrated that the use of a particular

cytokine/anti-cytokine complex built up by recombinant-IL-2 bound to anti-IL-2 antibody preferentially enhances T_{reg} numbers (Boyman *et al.*, 2006). A similar strategy with IL-2 noncomplex (without the anti-IL-2 antibody) has also been attempted and demonstrated to be successful (Koreth *et al.*, 2011). However, as the previous strategies described, also the manipulation of IL-2 pathway leads to a non-specific immune system suppression that results in important side effects.

3. Antigen-specific immunotherapy (ASI)

The antigen-specific immunotherapy (ASI) meets on the major goal for the treatment of autoimmune disease, which is acting upon the relevant autoimmune response without inducing a state of generalized immunosuppression.

ASI consists in the delivery of autoantigenic protein or specific immunodominant peptides derived from them, administered at different disease stages via a variety of routes (Peakman *et von Herrath*, 2010).

It was noted, several decades ago, that the administration of autoantigenic proteins or peptides derived from them could inhibit the subsequent immune response against the same antigen. The effect of the treatment with autoantigens has been widely explored in antigen-induced and spontaneous animal models and it has been demonstrated that this strategy resulted in protection from disease (Myers *et al.*, 1989; Gaur *et al.*, 1992; Mukasa *et al.*, 1992; Sasamoto *et al.*, 1992; Fuller *et al.*, 1993).

The immune response obtained with ASI strongly depends on the molecule chosen for immunization, the dose, the frequency, and route of administration but also on the precise context, in which the use of suitable adjuvants and inflammation can profoundly influence the resulting immune response (Peakman *et von Herrath*, 2010).

The administration of autoantigens seems to act through two different mechanisms; indeed, recent full genome transcriptional analysis of T cells exposed to a dose escalation of peptide suggests that ASI shifts T cells towards production of IL-10, a regulatory cytokine (Burton *et al.*, 2014); while a single dose of ASI can drive T cells to apoptosis (Konkel *et al.*, 2014).

As mentioned in the introduction, peptides derived from autoantigens have attracted attentions as potential ASI agents. Peptides offer several advantages over whole protein, being the smaller functional part of the protein, they ensure greater efficacy, selectivity and specificity than antigenic protein. Moreover, they minimized drug-drug interaction because peptide degradation products are aminoacids that are not toxic.

ASI can be applied at different disease stages:

- before the development of autoimmunity in at-risk subjects (primary prevention) or when autoimmunity is present but not disease (secondary prevention), to suppress the response and prevent the development of autoimmune disease blocking the organ damage;
- after diagnosis when the autoimmune disease is established (tertiary prevention or intervention) to prevent complications.

This thesis is focused on the development of immunodominant peptide-ASI for the therapy of T1D and RA.

In particular, in order to stabilize and cost-effectively produce the peptide of interest, expression systems based on plant viruses are exploited. Plant viruses are used for the display of several copies of selected immunodominant peptide associated either to T1D or RA. In this approach, the viral structure not only acts as scaffold in order to increase peptide stabilization but works as an adjuvant able to boost the regulative immune response enhanced by the peptide displayed on viral surface.

Finally, two different therapeutic approaches were chosen for T1D and RA. Regarding T1D pre-clinical studies treatments of NOD mice were done before the onset of the disease in order to find a preventive therapy.

On the other hand, for the RA pre-clinical studies, the disease was induced in DBA mice by two immunizations with type II collagens and 7 therapeutic treatments were started at the arthritis onset in order to find a potential RA cure.

RESULTS AND DISCUSSION

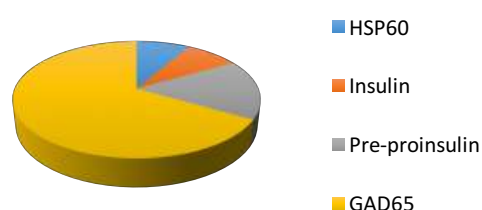
TYPE 1 DIABETES PREVENTION

1. Experimental design

Non-obese diabetic (NOD) mice spontaneously develop autoimmune diabetes with clinical manifestations and a disease pattern comparable with those of human T1D, including lymphocytic infiltration of the islet of Langerhans (insulinitis). Consequently, NOD mice became the elite animal model for studying human T1D (Saï *et al.*, 1996).

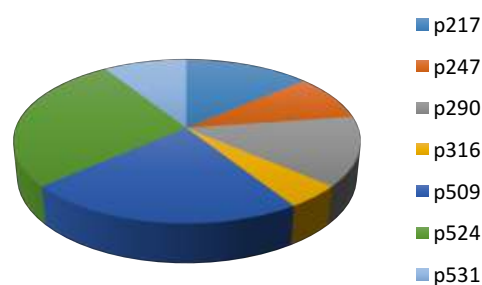
The major autoantigens associated to T1D are the 65 kDa human isoform of glutamate decarboxylase (GAD65), the heat shock protein 60 (HSP60), the zinc transporter 8 (ZnT8), the insulinoma associated antigen 2 (IA-2c) and insulin (Ins).

Graph 1 T1D autoantigens tested in pre-clinical studies



Studies over the past 35 years on NOD mice showed that a number of T1D autoantigen-derived peptides can prevent or even reverse T1D (Elias *et Cohen*, 1995; Tian *et al.*, 1996; Daniel *et Wegmann* 1996; Tisch *et al.*, 1999; Ogino *et al.*, 2000; Quinn *et al.*, 2001; Martinez *et al.*, 2003; Carter *et al.*, 2006; Lie *et al.*, 2009; Chen *et al.*, 2009; Gong *et*, 2010; Lianget *et al.*, 2010; Arai *et al.*, 2010) when are used alone or together with other peptides. Among the autoantigens associated to T1D, peptides derived from GAD65 are the most widely used in pre-clinical studies for immunological tolerance induction.

Graph 2 GAD65 derived immunodominant peptide



Dose and administration route are crucial parameters to be considered in the set up of a pre-clinical study in animal models. In table 1, the details of pre-clinical studies for prevention or suppression of T1D done with peptides derived from GAD65 showed in graph 2 are summarized.

In a previous PhD thesis (Merlin, 2013) the GAD65-derived peptides p217, p290 and p524, the insulin and pro-insulin derived peptides InsB9 and L7 and the HSP60 derived DiaPep277 were selected for their expression in *N. benthamiana* plants using the PVX CVPs system. None of them was successfully expressed either because of the incompatibility between the selected peptide and the PVX replication and/or assembly or the instability of the peptide sequence on the viral surface.

In order to avoid the abovementioned issues, the CPMV eVLP system was tested for the expression of p217, p290, InsB9, L7 and DiaPep277 peptides but even with this platform none of them was expressed.

Vectors used in this part of the work were kindly provided by Professor George P. Lomonosoff from the Department of Biological Chemistry of the John Innes Centre, (Norwich, UK).

None of the selected peptides was successfully express with the CPMV eVLPs based system. Different results were reached with the p524 peptide which was correctly express on the surface of CPMV eVLPs.

eVLPs are produced only in infiltrated tissues and cannot spread systemically because they lack viral genome. This can be considered an additional advantage in terms of bio-containment, because eVLPs preparation do not retain the ability to infect plants (Montague et al., 2011).

After cloning the p524 peptide sequence in the expression vector pEAQ-*HT*-VP60, a small scale agroinfection of 1-2 *N. benthamiana* plant (4 leaves/plants) was carried on to check the expression of CPMV eVLPs displaying p524 peptide (CPMV eVLPs.p524).

The unmodified CPMV eVLPs (i.e. lacking heterologous peptides on their surface) were expressed and purified following the same procedure of the CPMV eVLPs.p524, in order to be used as negative controls in animal model studies.

After purification and characterization to confirm the correct assembly and shape, the capability of the CPMV eVLPs.p524 (and the unmodified CPMV eVLPs) in induction of immunological tolerance in autoimmune diabetes was *in vivo* tested in NOD mice.

In particular, mice treatments were scheduled at 4 weeks of age in order to precede the onset of insulinitis and to assess the preventive effect of the CPMV eVLPs.p524 in the development of the disease.

Dose, administration route and timing are crucial parameters to be considered in the set up of a pre-clinical study in animal model. In table 1, the details of pre-clinical studies for the prevention or the suppression of T1D done with peptides derived from GAD65 showed in graph 2 are summarized.

The intra-peritoneal administration route was chosen and, on the basis of evidences present in literature and reported in table 1, a dose of 50 µg of CPMV eVLPs.p524 without any adjuvant was used per each injection. In the immunological tolerance induction study, the use of an adjuvant (e.g. Incomplete Freund Adjuvant, IFA) is usually adopted mixed to an immunodominant peptide in order to boost the immune response; it has been demonstrated that the use of a viral structure as a scaffold for peptide display can boost the immune system without the need of any other agents (Lico *et al.*, 2012).

Table 1: T1D studies done with GAD65 derived immunodominant peptides.

Peptide	Prevention (P)	Suppression (S)	Studies	Administration	Dose	Note	Ref
p217	Yes	Yes co-administered with p290	P (in vivo trials): 4 weeks old female NOD mice; S (in vivo trials): 12 weeks old female NOD mice.	Intra-peritoneal	P: 2 injection (2 weeks a part) of 50 µg of peptide mixed with 0.05 ml of IFA; S: 3 injection (every 7-10 days) of 200 µg of peptide mixed 0.10 ml of IFA	-	Tisch et al., 1999
	-	Yes	S (in vivo trials): 12 weeks old female NOD mice	Intravenous	1 injection a day for 3 days with 50 µg of p217-sMHCII-Ig (corresponding to ~1.1 µg of peptide) in 200 µl of PBS without IFA . After 3 weeks repetition of the same treatment.	Peptide fused to sMHCII-Ig	Li et al., 2009; Arnold et al., 2002
p247	Yes co-administered with p524	No co-administer with p524	P (in vivo trials): 4 weeks old female NOD mice; S (in vivo trials): 12 weeks old female NOD mice.	Intra-peritoneal	P: 2 injection (2 weeks a part) of 50 µg of peptide mixed with 0.05 ml of IFA; S: 3 injection (every 7-10 days) of 200 µg of peptide mixed 0.10 ml of IFA.	p247-265	Tisch et al., 1999
	Yes co-administered with p509 and p524	-	P (in vivo trials): 2-3 weeks old female NOD mice	Intranasal	Single dose of a mix of 50 µg of each peptide in 50 µl of PBS without IFA .	p247-266	Tian et al., 1996
p290	Yes	No administered alone; Yes co-administered with p217	P (in vivo trials): 4 weeks old female NOD mice; S (in vivo trials): 12 weeks old female NOD mice.	Intra-peritoneal	P: 2 injection (2 weeks a part) of 50 µg of peptide mixed with 0.05 ml of IFA ; S: 3 injection (every 7-10 days) of 200 µg of peptide mixed 0.10 ml of IFA.	Peptide fused to sMHCII-Ig	Tisch et al., 1999
	-	Yes	S (in vivo trials): 12 weeks old female NOD mice.	Intravenous	1 injection a day for 3 days with 50 µg of p290-sMHCII-Ig (corresponding to ~1.1 µg of peptide) in 200 µl of PBS without IFA . After 3 weeks repetition of the same treatment.	-	Li et al., 2009; Arnold et al., 2002
p316	Yes co-administered with p531	-	P (in vivo trials): 4 weeks old female NOD mice	Intravenous	1 injection with 50 µg of each peptide in RPMI 1640	-	Ogino et al., 2000
p509	Yes co-administered with p247 and p524	-	P (in vivo trials): 2-3 weeks old female NOD mice	Intranasal	Single dose of a mix of 50 µg of each peptide in 50 µl of PBS without IFA .	-	Tian et al., 1996
	Yes	No	P (in vitro trials): expansion of CD4+CD25+Foxp3+ T lymphocyte	Intra-peritoneal	P: 2 injection (2 weeks a part) of 50 µg of peptide mixed with 0.05 ml of IFA; S: 3 injection (every 7-10 days) of 200 µg of peptide mixed 0.10 ml of IFA.	-	Chen et al., 2009
	Yes	-	P (in vitro trials): proliferation test of T lymphocytes derived from rAAV/GAD500-585 treated mice	-	-	-	Han et al., 2005
p524	Yes	Yes	P (in vitro trials): expansion of CD4+CD25+Foxp3+ T lymphocyte; S (in vivo test): Adoptive transfer in 4-8 weeks old NOD.scid mice	Intra-peritoneal	P: 2 injection (2 weeks a part) of 50 µg of peptide mixed with 0.05 ml of IFA; S: 3 injection (every 7-10 days) of 200 µg of peptide mixed 0.10 ml of IFA	-	Chen et al., 2009
	Yes co-administered with p247 and p509	-	P (in vivo trials): 2-3 weeks old female NOD mice	Intranasal	Single dose of a mix of 50 µg of each peptide in 50 µl of PBS without IFA .	-	Tian et al., 1996
	Yes co-administered with p247	No co-administered with p247	P (in vivo trials): 4 weeks old female NOD mice; S (in vivo trials): 12 weeks old female NOD mice.	Intra-peritoneal	P: 2 injection (2 weeks a part) of 50 µg of peptide mixed with 0.05 ml of IFA; S: 3 injection (every 7-10 days) of 200 µg of peptide mixed 0.10 ml of IFA.	-	Tisch et al., 1999
p531	Yes	No	P (in vitro trials): expansion of CD4+CD25+Foxp3+ T lymphocyte	-	-	p530-543	Chen et al., 2009
	Yes co-administered with p316	-	P (in vivo trials): 4 weeks old female NOD mice	Intravenous	1 injection with 50 µg of each peptide in RPMI 1640	p532-543	Ogino et al., 2000
	Yes	-	P (in vivo trials): 5 weeks old female mice (peptide administration up to 10 or 35 weeks)	Direct administration into esophagus/gut	1 injection of 20 µg of recombinant protein every other day for 5 (insult analysis) or 30 (disease incidence study) weeks.	Fusion protein between cholera toxin B subunit and p531-545 peptide triple tandem (CTB-GAD(531-545)3); conjugated CTB works as carrier and adjuvant	Gong et al., 2009

2. Cloning of GAD65 derived peptide p524

As mentioned in the introduction, to be expressed with the system based on CPMV peptide should meet the criteria reported in the Cowpea Mosaic Virus (CPMV) section on page 15. Because of that, the p524 aminoacidic sequence was optimized (table 2) by the addition of one acid aminoacid at the peptide N-terminus and two at the C-terminus in order to decrease the peptide pI that is too high for the expression with this platform.

Table 2 Optimization of GAD65 p524 peptides for its expression with CPMV eVLPs system

Aminoacids sequence	SRLSKVAPVIKARMM
Nucleotidic sequence	TCT CGT CTT TCT AAG GTT GCT CCT GTT ATT AAG GCT AGA ATG ATG
Peptide length (aminoacids)	pI
15	12.02
Optimized aminoacids sequence	DSRLSKVAPVIKARMMED
Optimized nucleotidic sequence	GAT TCT CGT CTT TCT AAG GTT GCT CCT GTT ATT AAG GCT AGA ATG ATG GAA GAT
Peptide length (aminoacids)	pI
18	8.59

For the expression with the CPMV eVLPs system the nucleotidic optimized sequence encoding for the p524 peptide was cloned in the pEAQ-*HT*-VP60 vector within the sequence of the S CP located into the VP60 precursor sequence.

Oligonucleotide pairs were designed to obtain *NheI*-compatible 5'- and *AatII*-compatible 3'-end DNA fragments that were ligated into the *NheI*-*AatII*-digested vector.

After ligation of the DNA fragments encoding p524 peptide into pEAQ-*HT*-VP60 vector, the resulting pEAQ-*HT*-VP60.p524 plasmid was transformed in *E. coli* DH5 α strain competent cells by heat-shock. *E. coli* cells were plated on kanamycin containing medium (50 μ g/ml) and PCR selected using vector-specific primers CPMV Seq-for and CPMV Seq rev, annealing respectively upstream and downstream of the insertion site. The length of

the amplification fragments obtained is 200 bp plus the length of the p524 inserted sequence, making a total of 254 bp.

Results of the PCR analysis on the colonies growth on selection medium after transformation with pEAQ-*HT*-VP60.p524 vector are reported in figure 1.



Figure 1 PCR analysis of *E. coli* colonies transformed with pEAQ-*HT*-VP60 vector after ligation with p524 oligonucleotide. PCR amplification products obtained with two vector-specific primers (CPMV Seq for – CPMV Seq rev) were loaded on a 2% agarose gel. M: molecular marker (Benchtop 100bp DNA ladder - Promega); 1-7: number of *E. coli* DH5 α colonies tested; P: positive control (using pEAQ-*HT*-VP60 vector as template); N: negative control.

The PCR results showed that among the seven colonies tested six of them were presumably correctly transformed; indeed, the resulting bands correspond to an amplicon of approximately 254 bp as expected. As opposed, the colony number 4 shows a band corresponding to an amplicon of 200 bp comparable with that of positive control (P) obtained using as template the unmodified pEAQ-*HT*-VP60 vector. Positive bacterial colonies were propagated in selective broth and plasmids were extracted, PCR analysed and sequenced to assess that the insert was correct.

Selected pEAQ-*HT*-VP60.p524 resulting suitable from the PCR and sequencing analysis was transformed in competent cells of *A. tumefaciens* LBA4404 strain by electroporation and plated on kanamycin (50 μ g/ml), rifampicin (50 μ g/ml) and streptomycin (100 μ g/ml) containing medium. After three days at 28 °C incubation, colonies were PCR selected using vector-specific primers CPMV Seq-for and CPMV Seq rev to assess their effective transformation. Positive *A. tumefaciens* LBA4404 colonies were propagated in selective broth and used for the next expression step.

3. Analysis of the expression in plant of CPMV eVLPs displaying p524

For the assessment of the *in planta* expression of CPMV eVLPs.p524 a small scale first trial was carried out.

4 leaves of *N. benthamiana* were infiltrated with a mixed suspension of *A. tumefaciens* carrying pEAQ-HT-24K or pEAQ-HT-VP60.p524 plasmid.

At the same time, 4 leaves of *N. benthamiana* were infiltrated with a mixed suspension of *A. tumefaciens* carrying pEAQ-HT-24K or pEAQ-HT-VP60 plasmid in order to express in plant unmodified CPMV eVLPs to be used as positive control.

Finally, as negative control, 4 leaves of *N. benthamiana* were infiltrated with the infiltration buffer used for the resuspension of bacterial cells (MMA)

The agroinfiltrated leaves sampled at 6 days post infection (dpi) did not showed viral symptoms, as expected.

Indeed, CPMV eVLPs systems leads to the expression of empty viral particles that being deprived of the viral genome are not infective and therefore cannot cause viral symptoms as reported in figure 2.

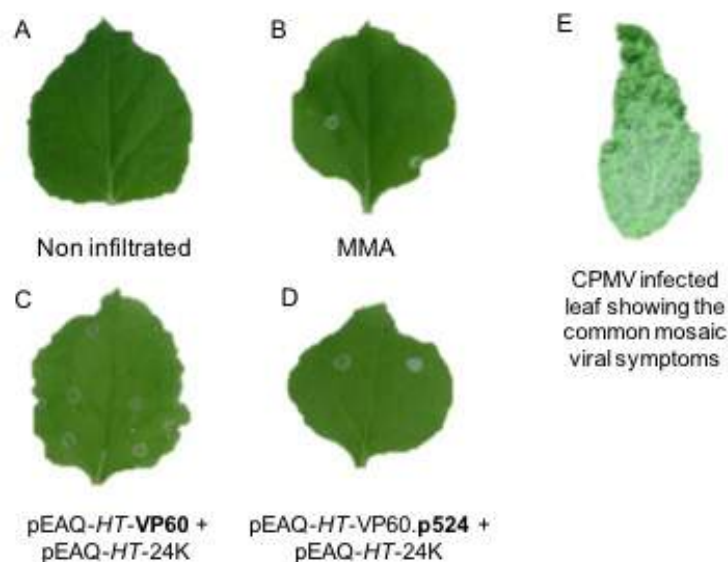


Figure 2 *N. benthamiana* leaf agroinfiltrated for the expression of CPMV eVLPs.p524 (D) and unmodified CPMV eVLPs (C) in comparison with a control leaf infiltrated only with infiltration buffer (B), *wild type* non infiltrated leaf (A) and *Vigna unguiculata* leaf with typical CPMV symptoms (E).

Total soluble proteins (TSP) were extracted from infiltrated leaves and analysed by western blot, using a polyclonal antibody (G49) specific to CPMV particles for the detection of specific signals. Results of this analysis are reported in figure 3.

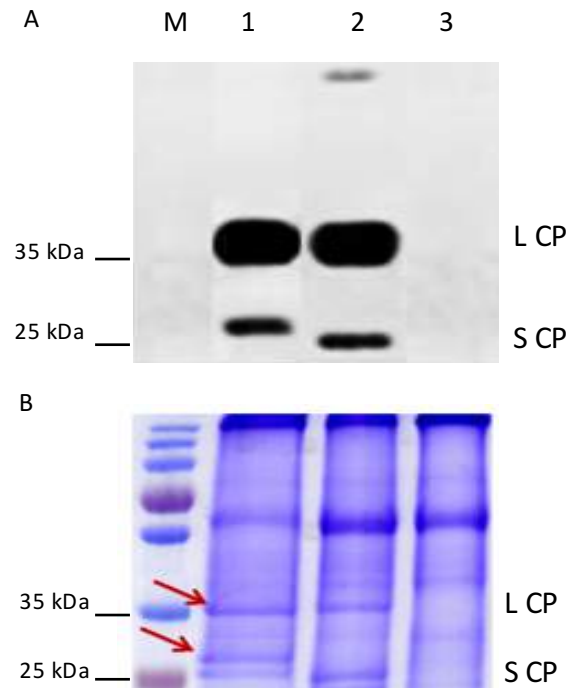


Figure 3. SDS-PAGE, western blot analysis (A) and Coomassie staining (B) of TSP extracted from agroinfiltrated leaves expressing CPMV eVLPs.p524 (1), unmodified CPMV eVLPs (2) and as a negative control protein extract from leaves infiltrated with infiltration buffer (3). Extracts were obtained using PBS buffer pH 7.2 and loaded on 12% polyacrylamide gels then blot was probed with a polyclonal antibody (G49) specific to CPMV particles used at a concentration of 1:2000. The position of L and S coat proteins are indicated with the red arrows. Equal volumes of protein extracts were loaded for each sample: 10 μ l for western blot analysis and 6 μ l for gel Coomassie staining. 1: molecular marker (PageRuler™ Plus Prestained Protein Ladder, Thermo Scientific).

In the gel stained with Coomassie blue (figure 3-B) a signal corresponding to 35 kDa and two signals corresponding to 25-27 kDa are clearly visible in the lanes of extracts of leaves infiltrated for the expression of either CPMV eVLPs.p524 or unmodified CPMV eVLPs. Considering that these signals are not present in the lane corresponding to the negative control, they could be specific signal of the CPMV CPs. The western blot analysis (figure 3-A) highlight the presence of two specific bands in lane 1, but absent in the negative

control sample (lane 3). These two bands being in the position expected for the L and S CPMV CPs confirm the hypothesis and highlighted that the expression of CPMV eVLPs.p524 (1) appeared to be similar to that of unmodified eVLPs (2). The shift between the signals of the S CPs in this two samples indicates the presence of the fused peptide in CPMV eVLPs.p524 sample.

4. Purification of CPMV eVLPs.p524 and unmodified CPMV eVLPs for T1D peptide display

4.1. CPMV eVLPs.p524

A large-scale infection of *N. benthamiana* plants was carried out, to obtain infected tissue for particle purification. 20-30 plants (4 leaves per plant) were agroinfiltrated with a mixed suspension of agrobacteria carrying pEAQ-*HT*-24K or pEAQ-*HT*-VP60.p524 vector. Agroinfiltrated leaves (~25-30 g) were sampled 6 dpi and used for CPMV eVLPs.p524 purification.

TSP were extracted and clarified through filtration and centrifugation in order to remove cellular debris. An anion-exchange chromatography using the DEAE SephadexTM A-50 resin was performed in order to remove a large part of plant contaminant proteins present in the extract, first of all the Ribulose-1,5-bisphosphate carboxylase/oxygenase (Rubisco) that is one of the major contaminant.

In particular, DEAE SephadexTM A-50 is a resin containing the positively charged group diethyl-aminoethyl groups that allows the absorption of protein with smaller pI than the pH of the extraction buffer (pH 7) which are therefore proteins negatively charged.

The resin/sample ratio was optimized at 1/4 and a NaCl gradient starting from 50 mM to 1 M was used for the elutions.

In figure 4 the results of the chromatography steps analysed by SDS-PAGE and Commassie staining are reported.



Figure 4 SDS-PAGE and Coomassie staining on 12% polyacrylamide gel of 14 μ l of the following samples: total protein extract (E), sample loaded on anion-exchange chromatography (clarified sample) (L), Flow through (FT), wash (W), elution steps (1-6) done with NaCl gradients from 50 mM to 1 M, 4 μ g of purified unmodified CPMV eVLPs as positive control (P). The Rubisco's subunit molecular weight (55 kDa), the CPMV large and small coat proteins molecular weight (respectively 35 and 25 kDa) are indicated. M: molecular marker (PageRuler™ Plus Prestained Protein Ladder, Thermo Scientific).

The peptide p524 has a pI of 8.59 that makes the CPMV eVLPs.p524 positively-charged at pH 7 and therefore these particles do not interact with the chromatographic resin.

Indeed, only in the sample corresponding to the flow through (lane FT, figure 4) are visible two bands attributable to CPMV eVLPs.p524 large and small coat proteins that are completely absent in the sample derived from elution steps (lane 1-6, figure 4).

The FT (~ 120 ml) was concentrated 30 times (~4 ml) using a 100 kDa cut off Centricon® tube and, according with Alaa *et al.* (2013), injected into the HiPrep™ 16/60 Sephacryl™ S-500 HR (Akta Prime plus) size exclusion chromatography column.

The resulting chromatogram is characterized by six elution peaks (figura 5).

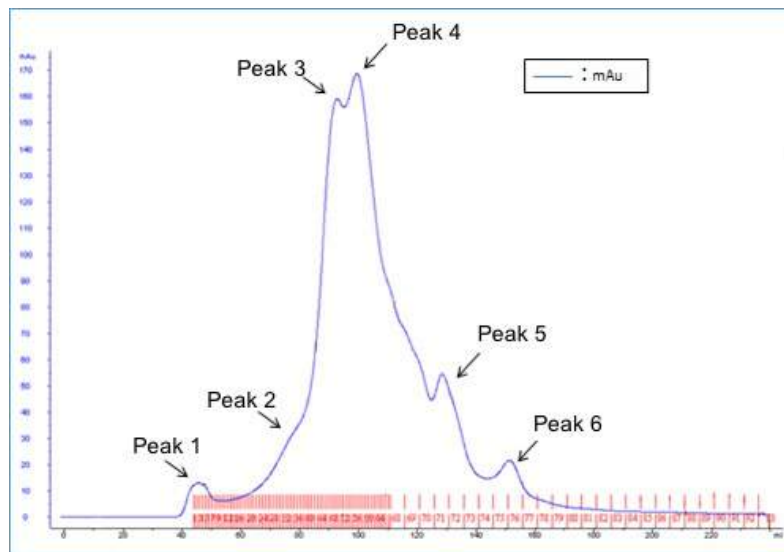


Figure 5 Elution chromatogram of the CPMV eVLPs.p524 purification process done through HiPrep™ 16/60 Sephacryl™ S-500 HR (Akta Prime plus) size exclusion chromatography column. The A₂₈₀ (mAu) and the elution volume (ml) are reported respectively on the y and x-axis. The arrows indicate the peak obtained from this analysis and in red the number of the collected fraction is indicated; the volume of the fraction from the number 1 to 67 is 1 ml, the following fractions are 5 ml.

A sample (20 μ l) of the central fraction of each peak was analysed by SDS-PAGE and silver staining in order to identify the CPMV eVLPs.p524 elution peak, the results of the size exclusion chromatography analysis are showed in the following figure 6.

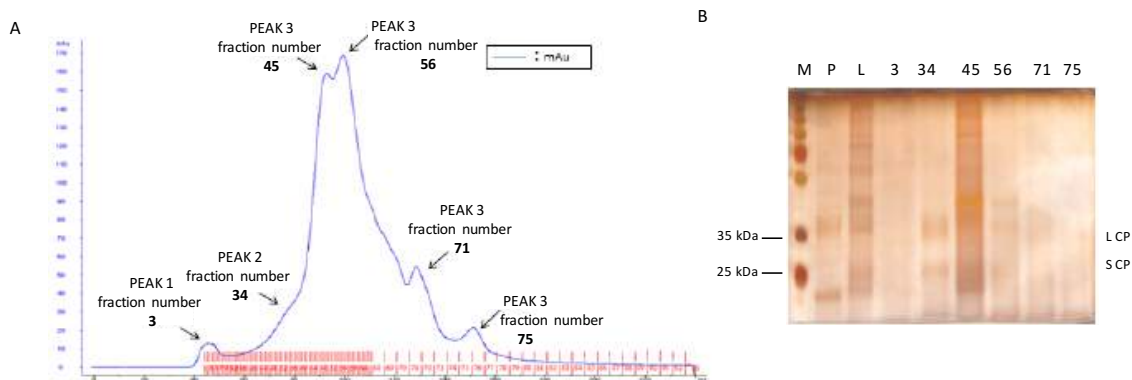


Figure 6 Elution chromatogram of the CPMV eVLPs.p524 purification process (A) in which the number of the selected fraction of each peak is reported. The A₂₈₀ (mAu) and the elution volume (ml) are reported respectively on the y and x-axis. In panel B SDS-PAGE and silver staining of the selected fraction corresponding to the central one of each peak (3, 34, 45, 56, 71 and 75) is shown. Thermo Scientific); 20 μ l of each selected fractions were loaded on 12% polyacrylamide gel. P: 1.5 μ g of unmodified purified CPMV eVLPs as positive control; L: 3 μ l of a dilution 1:10 of the protein extract loaded on size exclusion chromatography column. M: molecular marker (PageRuler™ Plus Prestained Protein Ladder); the expected molecular weight of the CPMV L and S CP are reported on the side of the gel.

In fraction 34 (figure 6) there are two bands corresponding to CPMV eVLPs L and S CPs expected sizes, therefore the peak containing the CPMV eVLPs.p524 particles is the number 2, corresponding to an elution volume from 65 to 80 ml. Considering that this region of the elution chromatogram it is not a well-define peak but there is a partial overlapping of peaks 2 and 3, samples from fractions of the peak 2 were analysed by SDS-PAGE and silver staining in order to remove possible contaminated fractions.

In the following figure 7 the results of peaks 2 fractions SDS-PAGE and silver staining analysis is reported.

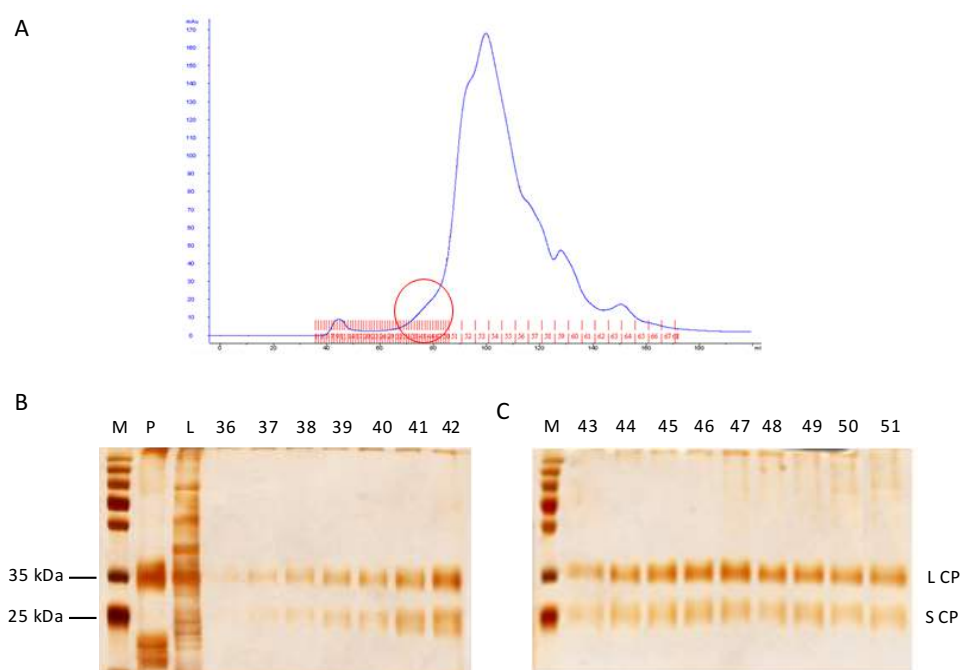


Figure 7 Elution chromatogram of the CPMV eVLPs.p524 purification process (A) in which the peak 2 is indicated with the red circles. In the panel B the SDS-PAGE and silver staining shows the analysis on the peak 2 fractions. 36-51: 20 μ l of each fraction were loaded on 12% polyacrylamide gel; P: 1.5 μ g of unmodified purified CPMV eVLPs as positive control; L: 3 μ l of a dilution 1:10 of the protein extract loaded on size exclusion chromatography column. M: molecular marker (PageRuler™ Plus Prestained Protein Ladder); the expected molecular weight of the CPMV L and S CP are reported on the side of the gel.

The results show that all the fractions are pure, therefore they were mixed and concentrated 10 times (\sim 0.4 ml) using a 100 kDa cut off Centricon® tube.

Purified CPMV eVLPs.p524 were stored at -80 °C because there were some evidences of peptide loss when particles are stored at 4 °C after purification. In order to assess the

suitability of the storage method an aliquot of the sample was analysed after 6 days at -80 °C.

The result of the SDS-PAGE and silver staining of CPMV eVLPs.p524 purified and stored at -80°C for 6 days is showed in figure 8.

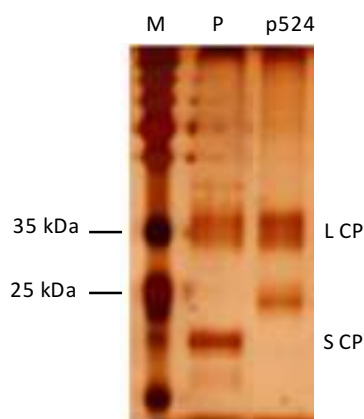


Figure 8 SDS-PAGE and silver staining analysis on 12% polyacrylamide gel of the purified CPMV eVLPs.p524 stored 6 days at -80°C. After thawing, 1,5 µ of the CPMV eVLPs.p524 (p524) purified through gel filtration (figure 7) are loaded on the gel. P: 1.8 µg of unmodified purified CPMV eVLPs as positive control; M: molecular marker (PageRuler™ Plus Prestained Protein Ladder. The expected molecular weight of the CPMV L and S CP are reported on the side of the gel.

The effective absence of proteolytic activity is confirmed as showed in figure 8.

Indeed, the S CP of the CPMV eVLPs.p525 shows a higher molecular weight in comparison to that of the unmodified CPMV eVLPs used as positive control, confirming the presence of p524 peptide fused on the small coat protein.

This analysis shows that the storage at -80 °C result to be a appropriate storage methods for CPMV eVLPs.p524.

Finally, the CPMV eVLPs.p524 sample do not have contaminant protein and particles result to have a higher level of purity.

4.2. Unmodified CPMV eVLPs

The procedure above-described was used also for the purification of unmodified CPMV eVLPs to be used afterwards as negative control in the tolerance induction studies in animal model.

The same results of CPMV eVLPs.p524 were obtained for unmodified CPMV eVLPs in the anion-exchange chromatography step, confirming the presence of CPMV eVLPs particles in the flow through (data not shown).

On the other hand, the size exclusion chromatography showed an elution pattern slightly different in comparison to that of particles displaying peptide p524.

The elution chromatogram is reported in figure 9.

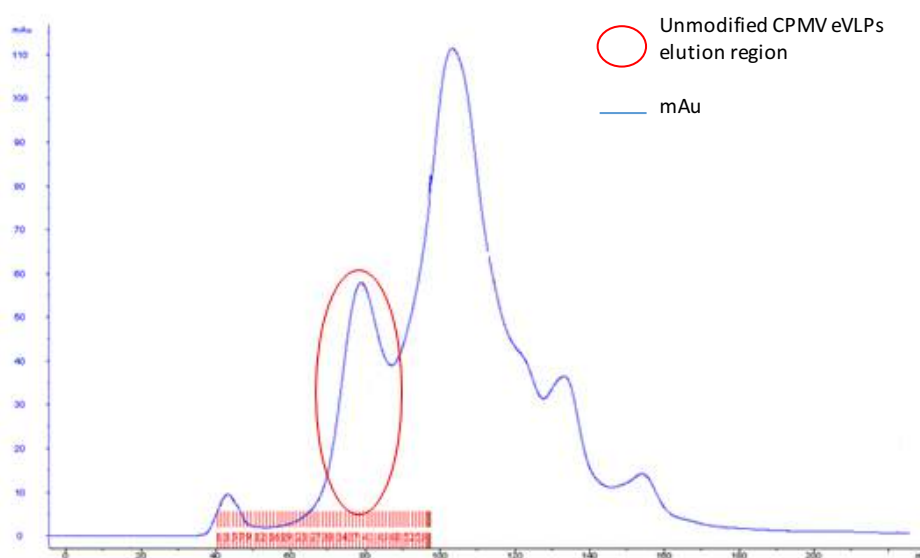


Figure 9 Elution chromatogram of the unmodified CPMV eVLPs purification process done through HiPrep™ 16/60 Sephacryl™ S-500 HR (Akta Prime plus) size exclusion chromatography column. The A280 (mAu) and the elution volume (ml) are reported respectively on the y and x-axis. The peak relative of the Unmodified CPMV eVLPs is indicated with the red circle and correspond to an elution volume from 65 to 80 ml.

Differently from CPMV eVLPs.p524, a well define peak is clearly visible in the region corresponding to unmodified CPMV eVLPs elution volume (65-80 ml). In order to confirm the effective presence of the particles of interest in these peaks and for the assessment of the purity level of the sample, an aliquot (20 μ l) of 7 random fractions which

are part of the peaks were analysed by SDS-PAGE and silver staining. The results are reported in figure 10.

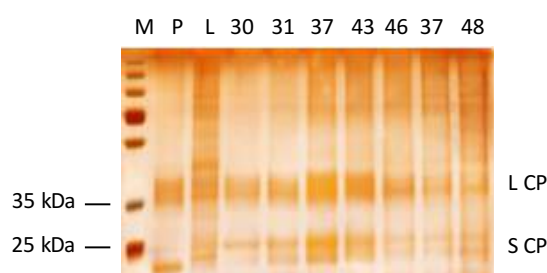


Figure 10 SDS-PAGE and silver staining of the analysis of the unmodified CPMV elution peak. 20 μ l of the selected fraction were loaded on 12% polyacrylamide gel; P: 1.5 μ g of unmodified purified CPMV eVLPs as positive control; L: 3 μ l of a dilution 1:10 of the protein extract loaded on size exclusion chromatography column. M: molecular marker (PageRuler™ Plus Prestained Protein Ladder). The expected molecular weight of the CPMV L and S CP are reported on the side of the gel.

The selected fractions did not show any contaminant protein (figure 10) and considering these fractions representative of the entire peak, all the fractions (from the number 28 to 46) which are part of it were mixed and concentrated at \sim 1 ml and then stored at -80°C . The difference between the elution pattern of the unmodified CPMV eVLPs and the CPMV eVLPs.p524 can be explained with the presence in the latter of the p524 peptide fused to the CP.

5. Characterization of purified CPMV eVLPs.p524 and unmodified CPMV eVLPs

The purified CPMV eVLPs.p524 and the unmodified CPMV eVLPs were quantified and then characterized by Dynamic Light Scattering (DLS) and LAL-test.

5.1. Quantification and yields

Purified CPMV eVLPs.p524 and unmodified CPMV eVLPs were quantified by reading of the 280 nm absorbance. Using the Lambert Beer law

$$A_{280} = \epsilon \times L \times C$$

ϵ : molar extinction coefficient ($\text{m}^2 \text{mol}^{-1}$);
L: path length (cm);
C: concentration (mg/ml).

and considering the CPMV eVLPs molar extinction coefficient ($1.28 \text{ m}^2 \text{mol}^{-1}$) the concentration (mg/ml) of the particle preparations was obtained.

The amount of purified CPMV eVLPs.p524 and unmodified CPMV eVLPs needed for the tolerance induction studies in NOD mice was respectively 3 mg and 2 mg.

320 g and 25 g of infiltrated leaves were necessary to purify respectively 3 mg of CPMV eVLPs.p524 and 2.4 mg of unmodified CPMV eVLPs. Thus, the final yields are 0.01 g/kg LFW for the CPMV eVLPs.p524 and 0.1 g/kg LFW for the unmodified CPMV eVLPs purification.

The CPMV eVLPs.p524 10-fold lower purification yield could be due to the presence of p524 peptide on particles surface that might interfere with their stability causing particles aggregation and subsequent precipitation.

5.2. Structural particles evaluation

In literature, a CPMV eVLPs diameter of 28 nm is reported (Montague *et al.*, 2011); knowing this data and exploiting DLS analysis, the appropriate assembly of the CPMV

eVLPs.p524 and the unmodified CPMV eVLPs and the absence of any aggregates was assessed.

For each sample, 3 measurements were done. Every measurement corresponds to the means of 12 analysis repetitions.

The DLS results regarding either the purified CPMV eVLPs.p524 or the unmodified CPMV eVLPs are reported in figure 11.

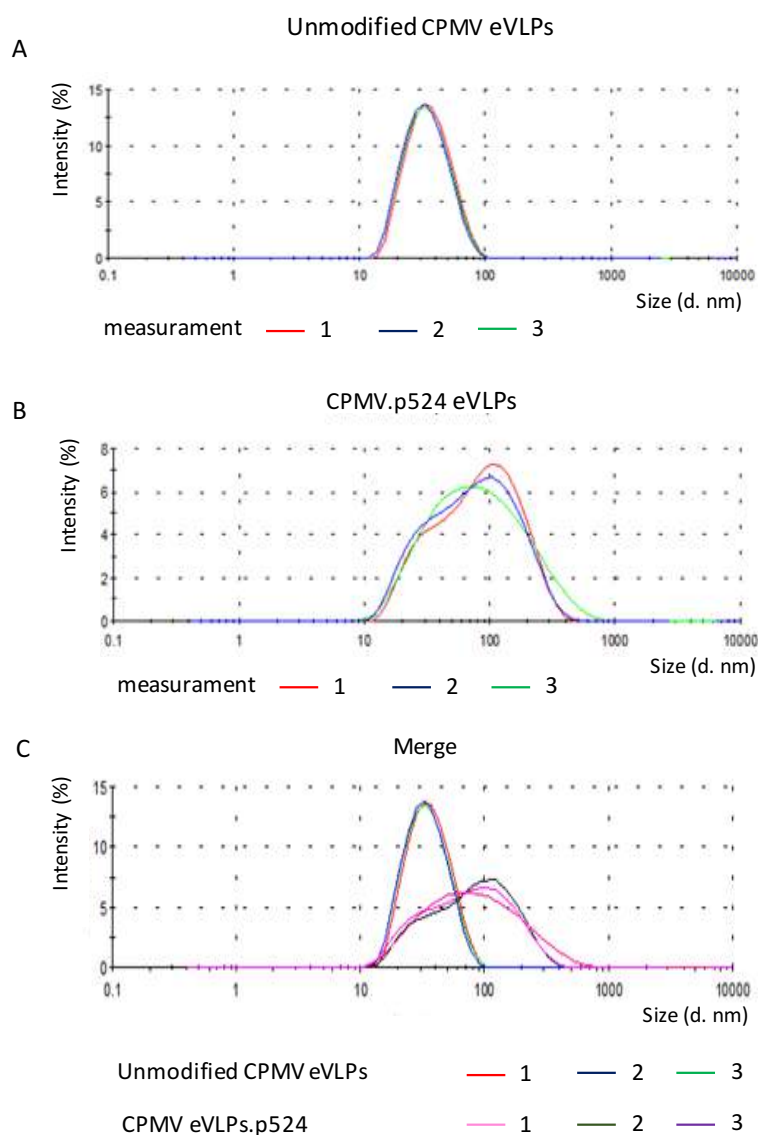


Figure 11 Dynamic light scattering analysis of the unmodified CPMV eVLPs (A), CPMS eVLPs.p524 (B) purified as described. The merge of the graphs A and B is reported in the panel C. For each sample, 3 measurements were done and every measurement corresponds to the means of 12 analysis repetitions. The intensity (%) and the diameter size (nm) are reported respectively on the y and x axis.

Figure 11-panel A demonstrates that purified unmodified CPMV eVLPs have the expected diameter (30 nm), indicating the proper assembly of the unmodified CPMV eVLPs sample and the absence of aggregates.

Figure 11-B reports DLS analysis of purified CPMV eVLPs.p524 displaying 2 peaks corresponding approximately to a diameter of 30 nm and 100 nm respectively. This sample is polydisperse and seems to be characterized by either well-assembled particles and particle aggregates. However, when the Intensity distribution is reported, the peak height is not indicative of the particles' quantity because more light scattered is produced by bigger particles. On the basis of this assumption, in order to understand which particles' species is the most representative of the sample, the data has to be reported as volume distribution.

The Intensity distribution can be converted, using Mie theory, to a volume distribution (figure 12) describing the relative proportion of multiple components in the same sample based on their volume rather than based on their scattering (Intensity).

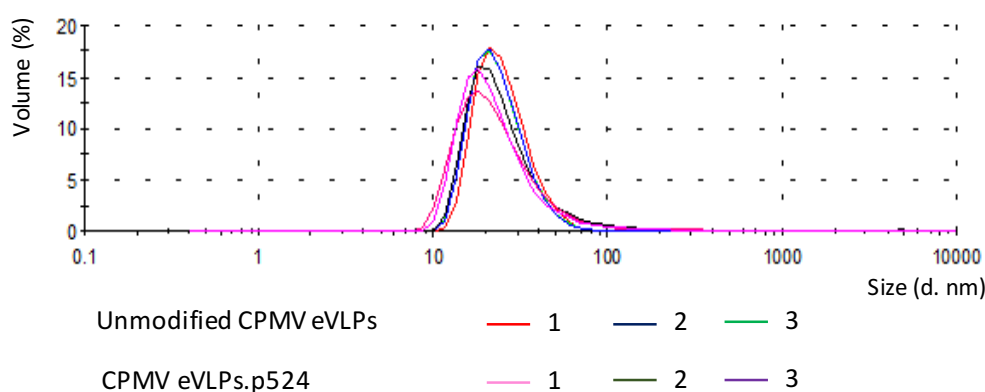


Figure 12 Dynamic light scattering analysis results from the merge of the measurements of CPMV eVLPs.p524 and unmodified CPMV eVLPs purified by gel filtration. For each sample 3 measurements were done and every measurement corresponds to the means of 12 analysis repetitions. The intensity (%) and the diameter size (nm) are reposted respectively on the y and x axis.

The Volume distribution (figure 12) confirmed the prevalent presence of well-assembled CPMV eVLPs.p524 in the purified sample, and the peaks representing these particles are overlapping those representing the unmodified CPMV eVLPs.

So, in conclusion, the conformation of the purified CPMV eVLPs.p524 and unmodified CPMV eVLPs is correct, thus they are structurally suitable for the pre-clinical trials in animal models.

5.3. Qualitative analysis

The LAL-test is a technique commonly used to ensure that a therapeutic product is endotoxins-free.

Diluted or undiluted CPMV eVLPs.p524 and unmodified CPMV eVLPs preparation have been subjected to this test.

The gel clot method was used with a sensitivity of 0.125 UE (endotoxin unit)/ml. Equal volumes of LAL reagents were mixed with diluted or undiluted samples and observed for gel clot formation, if the endotoxin concentration in the sample tested is higher than the test sensitivity, a gel clot is formed in the tube.

None of the samples showed any gel clot formation, including the undiluted sample. The endotoxin concentration in either CPMV eVLPs.p524 or unmodified CPMV eVLPs sample is lower than 0.125 UE/ml thereby confirming the suitability of the preparation to be used in pre-clinical studies.

6. Pre-clinical trials in T1D animal model

Administration of p524 synthetic peptide and CPMV eVLPs.p524 to NOD female mice
Groups of twenty female of NOD/SHILTJ mice were treated before the onset of insulinitis (4-week-old). When 2 doses were planned treatments were administered 2 weeks apart. The schedule of treatments was as follows:

- CPMV eVLPs.p524 50 µg (1 dose);
- CPMV eVLPs.p524 50 µg (2 doses);
- Unmodified CPMV eVLPs (2 doses);
- Original 15 aminoacids p524 synthetic peptide with IFA (table 2);
- Optimased 18 aminoacids p524 synthetic peptide with IFA (table 2).

GAD65 derived peptide p524 was first report to elicit T cell-proliferation responses in spleen cell culture prepared from NOD mice (Kaufman *et al.*, 1993) and prevent diabetes when it was administrated to NOD mice mixed with another GAD65 derived peptide (Tian *et al.*, 1996). Subsequently some evidence, showed that p524 peptide reduces cyclophosphamide-accelerated diabetes in NOD-mice.

In this work, for the first time, the p524 peptide was tested alone for the prevention of T1D in NOD-mice.

The survival curves obtained by weekly glycaemia measurements of the treated NOD-mice are shown in figure 13.

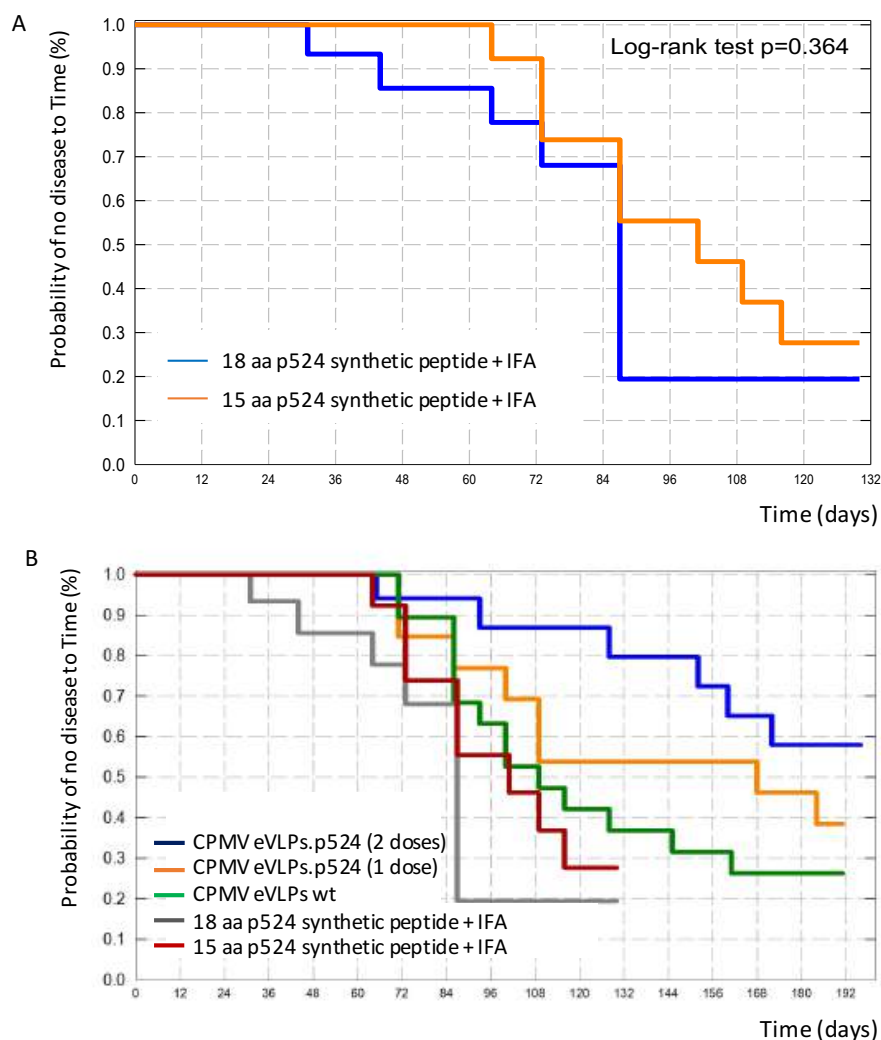


Figure 13 Overall survival curve for mice treated with the original 15 aminoacids (orange) and the optimised 18 aminoacids (blue) p524 synthetic peptides mixed

with IFA ($p=0.364$) (A), Overall survival curve for all mice groups of the T1D pre-clinical study (B), mice treated with 2 doses (blue) and 1 dose (orange) of CPMV eVLPs.p524, mice treated with unmodified CPMV eVLPs (green), mice treated with the original 15 aminoacids (red) and the optimised 18 aminoacids (grey) p524 synthetic peptides mixed with IFA ($p=0.01$). The probability of no disease and the Time (days) are reported respectively on the y and x axis.

The figure 13-A demonstrated that more than the 70% of the mice in both groups shows diabetic symptoms and have developed the disease; moreover, there are not significative differences in the use of the original p524 synthetic peptide upon the other ($p=0.364$). Indeed, the original 15 aminoacids nor the optimised 18 aminoacids p524 synthetic peptide showed a immunoregulative activity able to prevent the onset of T1D when they are injected alone mixed with IFA.

Instead, the use of CPMV eVLPs.p524 enhances the peptide immunological activity ($p=0.001$ and $p=0.008$ respectively for 18 and 15 aminoacids syntethic peptide) as shown in figure 13-B. It is important to underline that the CPMV eVLPs.p524 were injected without any adjuvant and the results obtained confirm the capability of the eVLPs to act as an adjuvant itself as reported in Jegerlehner *et al.* (2002). In conclusion, the results shown in figure 13 demonstrate that, compared to the treatment with the unmodified CPMV eVLPs, CPMV eVLPs.p524 partially protect mice from T1D onset. Finally, as expected, the treatment with two doses of CPMV eVLPs.p524 showed a partial protection higher ($p=0.04$) than the one obtained with the single dose ($p=0.398$).

6.1. Histopathological analysis of the pancreatic Langerhans islets

At 5 and 10 weeks after the treatments two mice per group were sacrificed and pancreatic sections were microscopically examined in order to assess the presence of lymphocytic infiltrates into the Langerhans islets indicating the presence of an insulitis process.

A pancreatitis score from 0 to 3 indicates the levels of lymphocytic infiltrates, with higher scores assigned to stronger infiltration; this score was used to evaluate mouse pancreatic sections.

Figure 14 shows the insulitis score and the analysis of the pancreatic section.

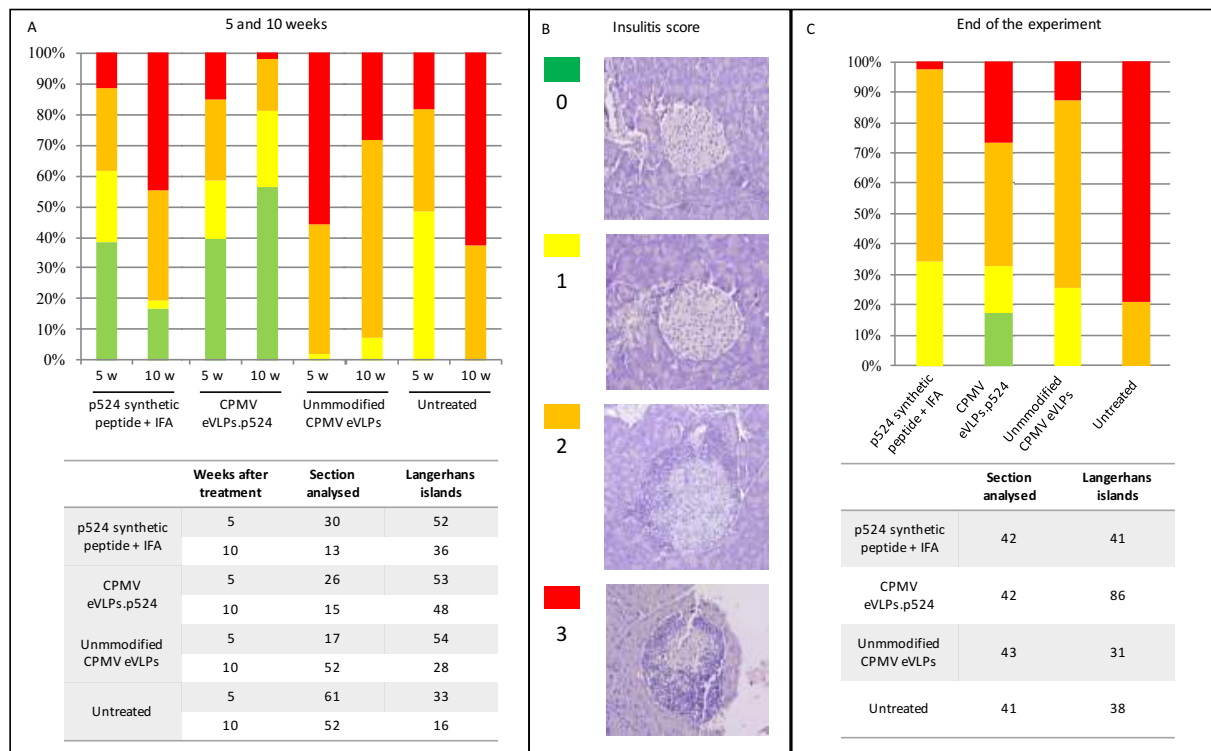


Figure 14 Histopathological analysis of lymphocyte infiltration in the pancreatic Langerhans islets of mice of the pre-clinical T1D study. Analysis of different sections of the pancreas of two mice per group at 5, 10 (A) and 27 weeks (C) from the second treatment are shown. The analysis were done considering the mice groups treated with the original 15 aminoacid p524 synthetic peptide mixed with IFA, with 2 doses of CPMV eVLPs.p524, with the unmodified CPMV eVLPs and as negative control an untreated mouse. In the table under the graph the number of pancreatic sections and the Langerhans islets observed is reported. Panel B shows the insulinitis score used for the evaluation of pancreatic sections.

At 5, 10 weeks and at the end of the experiments, the pancreata of the mice injected with the CPMV eVLPs.p524 have a pancreatitis score lower than the other sample confirming the results showed in the survival curve (figure 13-B).

6.2. Cytokines analysis in serum

All the Sera derived from mice were analysed in order to quantify 23 different cytokines using a commercial immunoassay method.

The cytokines analysed were:

Eotaxin	IL-2	IL-10	MCP-1 (MCAF)
G-CSF	IL-3	IL-12 (p40)	MIP-1 α
GM-CSF	IL-4	IL-12 (p70)	MIP-1 β
IFN- γ	IL-5	IL-13	RANTES
IL-1 α	IL-6	IL-17A	TNF- α
IL-1 β	IL-9	KC	

The data set regarding the quantification of the cytokines in sera of mice that did not developed T1D symptoms was explored in order to evaluate the presence of cytokine patterns in the sera analysed.

A Principal Component Analysis (PCA) was performed on data derived from 18 samples of the immune-analysis. In particular, 7 and 5 sera derived from mice treated respectively twice and once with CPMV eVLPs.p524, 6 sera derived from the mice group injected with optimised 18 aminoacids synthetic peptide p524 (+IFA) and 5 sera from mice treated with unmodified CPMV eVLPs.

The PCA was then used to supervise the best Orthogonal Bidirectional Projections to Latent Structures-Discriminant Analysis (O2PLS-DA). OPLS-DA is a discriminant analysis based on OPLS and employed to examine the difference between groups while neglecting the systemic variation.

A four-class O2PLS-DA model (3+7+0, UV, R²cum:0.944, Q²cum:0.764) corresponding to the four mice group analysed, was obtained (figure 14-A).

The first two principal components (PC) explained 44.7 % of the total variance of the model. The graph clearly showed a good clusterization of the four mice groups receiving different treatments. The second component could explain the immunoregulative action of the peptide. Figure 14-B shows the loading scatter plot relating to figure 14.

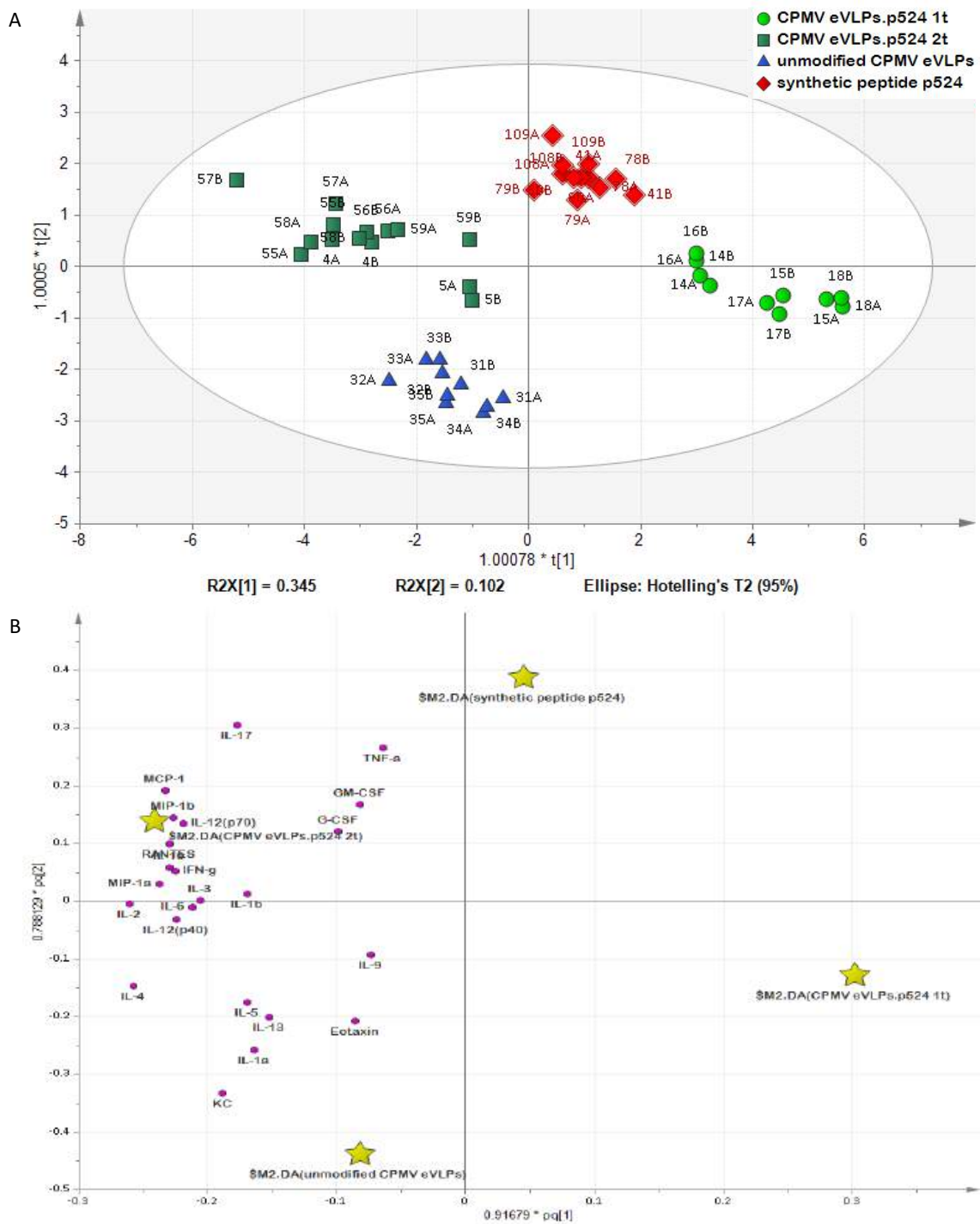


Figure 14 Plot of the O2PLS-DA (A) (3+7+0, UV, $R^2_{cum}:0.944$, $Q^2_{cum}:0.764$) of the mice treated with 2 doses (dark green square) and 1 dose (light green dot) of CPMV eVLPs.p524, with the unmodified CPMV eVLPs (blue triangle) and the original 15 aminoacids p524 synthetic peptide (red diamond) showing the first two principal component $t[1]=35.5\%$ and $t[2]=10.2\%$. In the panel B the corresponding loading scatter plot is reported. The yellow stars indicate the average position on the plot of the analysed mice groups; the purple dots show the contribution of each cytokines.

The loading scatter plot (figure 14-B) demonstrated that the group of mice treated with 2 doses of CPMV eVLPs.p524 that did not develop T1D is characterized by a strong activation of different cytokines.

Also in mice injected with unmodified CPMV eVLPs there seems to be a cytokines activation, this data it is not all that surprisingly because, miming a viral structure, particles injected are immunoactivators themselves.

Considering this overall results, more focused analyses were done.

The following figure 15 shows the two-classes O2PLS-DA (A) (1+3+0, UV, $R^2_{cum}:0.702$, $Q^2_{cum}:0.954$) corresponding to the mice groups treated with CPMV eVLPs.p524 and synthetic p524 peptide.

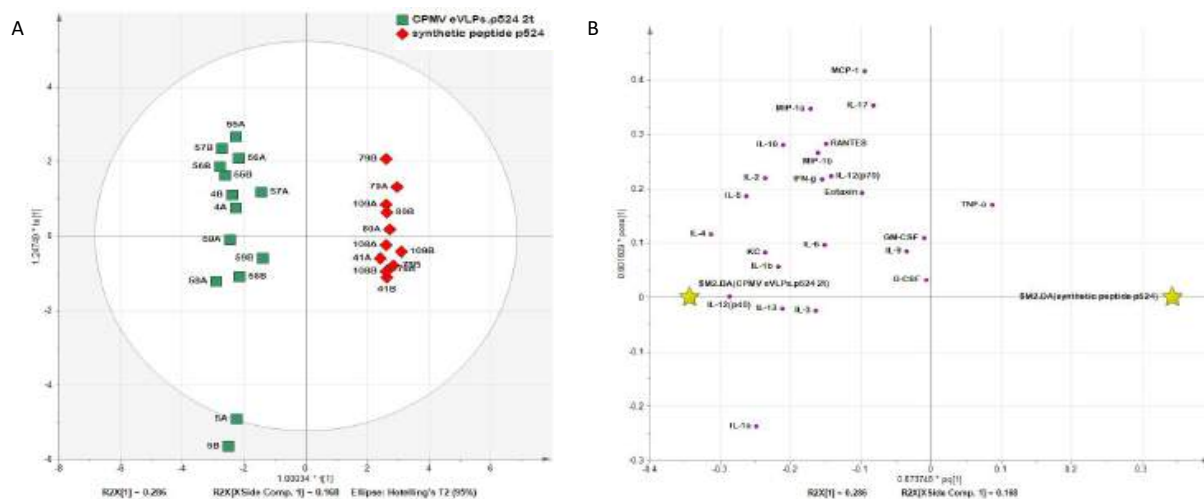


Figure15 Plot of the two classes O2PLS-DA (A) (1+3+0, UV, $R^2_{cum}:0.702$, $Q^2_{cum}:0.954$) of the mice treated with 2 doses (green square) and the original 15 aminoacids p524 synthetic peptide (red diamond) showing the first two principal component $t[1]=28.6\%$ and $t[2]=16.8\%$. In the panel B the corresponding loading scatter plot is reported. The yellow stars indicate the average position on the plot of the analysed mice groups; the purple dots show the contribution of each cytokines.

The first two PC explained 45.4 % of the total variance of the model. The graph clearly showed a strong clusterization of the two mice groups receiving different treatments.

The corresponding loading scatter plot (figure 15-B) underlines that the use of CPMV eVLPs for the p524 display allows to induce a strong activation of cytokines and the two groups analysed result to be separated only on the basis of the first component that is the one explaining the major variance (28.6%) of the model. In further detail, the immunological activation effects of CPMV eVLPs.p524 seem to be particularly due to

some cytokines IL-12(p40), IL-13 and IL-3. The role of the IL-12(p40) in the prevention of T1D result to be ambiguous because, on the contrary, in literature there are evidences of its involvement in the onset of the disease. In particular, IL-12 is the key cytokine driving Th1 cell development which is critical to the pathogenesis of T1D (Hsieh *et al.*, 1993). IL-12 stimulates the differentiation of CD4⁺ helper T lymphocytes into Th1 type, which themselves trigger IL-12 secretion by dendritic cells; Th1 usually produce high levels of INF-g and IL-2 which activate macrophages and CD8⁺ cytotoxic T lymphocyte. Upon activation, these cells secrete cytokines such as IL-1b and TNF-a that are potentially responsible of the pancreatic β cells destruction (Adorini, 2001).

In the light of above and considering the loading scatter plot of O2PLS-DA (figure 15-B), it is possible to assume that this mechanism is partially active in mice group treated with CPMV eVLPs.p524. Indeed, it is visible a strong activation of IL-12 (p40), that could lead to an activation of INF-g and IL-2 that are more activated in the mice group treated with CPMV eVLPs.p524 in comparison to the mice group treated with p524 synthetic peptide. On the other hand, even if IL-1b result to be again more activated in the mice group treated with CPMV eVLPs.p524 in comparison to the mice group treated with p524 synthetic peptide, the latter result to be characterised by a strong activation of TNF-a which is the only cytokine representing this group.

One possible explanation of the mechanism at the basis of this strong IL-12 activation is reported in Rabinovitch *et al.* (2007) in which is described the Th1 cytokines activate, but also downregulate immune responses. In other word, paradoxally the administration of IL-2 and INF-g actually prevent T1D, at least in animal models. A mechanism for the preventive effect of INF-g may be activation/induced cell death of pathogenic CD4⁺ Th1 cells (Raefaeliy *et al.*, 2002). Similarly, IL-2 has been recognized to be crucial for induction of immunological tolerance (Mallek *et al.*, 2004). In conclusion, the Th1 cytokines, IFNg and IL-2, have dual roles in the immune response, first activating and then downregulating autoimmune responses.

Regarding the IL-3, Akihiko *et al.* (1997) demonstrated that this cytokine plays an important role in delay the onset of T1D. In particular, the administration of IL-3 twice weekly starting at 2–4 weeks of age delayed the onset and reduced the overall incidence of diabetes.

In figure 16-A the O2PLS-DA model (1+2+0, UV, R^2 cum:0.884, Q^2 cum:0.682) explores the CPMV eVLPs.p524 effect of the two different doses used.

The first two PC explained 67.6 % of the total variance of the model. The graph clearly shows a clusterization of the two mice groups receiving different CPMV eVLPs.p524 doses.

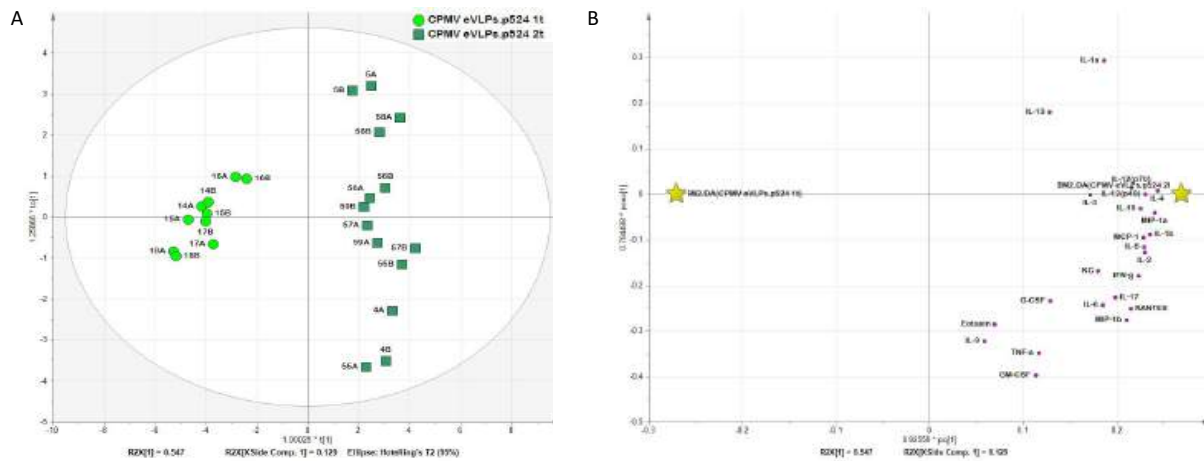


Figure 16 Plot of the two classes O2PLS-DA (A) (1+2+0, UV, R^2 cum:0.884, Q^2 cum:0.682) of the mice treated with 1 dose (light green dot) or 2 doses (dark green square) and the original 15 aminoacids p524 synthetic peptide (red diamond) showing the first two principal component $t[1]=54.7\%$ and $t[2]=12.9\%$. In the panel B the corresponding loading scatter plot is reported. The yellow stars indicate the average position on the plot of the analysed mice groups; the purple dots show the contribution of each cytokines.

The corresponding loading scatter plot (figure 16-B) highlights that there is a stronger activation of cytokines when mice were treated twice. Indeed, the two groups analysed result to be separated only on the basis of the first component that explains the major variance (54.7%) of the model and could represent the dose effects.

Finally, a two-class O2PLS-DA model (1+3+0, UV, R^2 cum:0.626, Q^2 cum:0.757) corresponding to mice treated twice with CPMV eVLPs.p524 that showed or not T1D symptoms was obtained (figure 16-A).

This analysis confirmed the strong activation of IL-12 as reported in the previous plot (figure 15), but the double doses seem to trigger the anti-inflammatory cytokines IL-4, IL-10 and IL-13. Numerous studies have revealed that treatment of NOD mice with these cytokines delays the onset of T1D and reduce its incidences (Rapoport *et al.*, 1993; Pennline *et al.*, 1991; Cameron *et al.*, 1997; Papaccio *et al.*, 2002). Moreover, in Rusell *et*

Morgan (2014) is reported the possible role of IL-4, IL-10 and IL-13 as citoprotective agents in the Langerhans pancreatic β -cell.

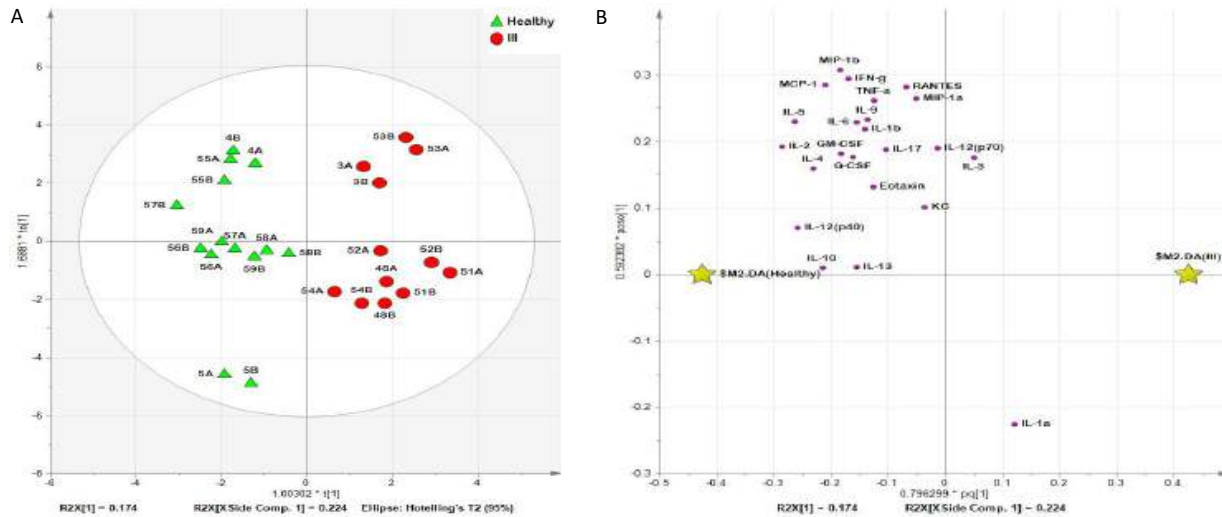


Figure 17 Plot of the two classes O2PLS-DA (A) (1+3+0, UV, R^2 cum:0.626, Q^2 cum:0.757) of the mice treated 2 doses of CPMV eVLPs.p524 that at the end of the pre-clinical trials result to be healthy (green square) or ill (red dot) showing the first two principal component $t[1]=17.4\%$ and $t[1]=22.4\%$. In the panel B the corresponding loading scatter plot is reported. The yellow stars indicate the average position on the plot of the analysed mice groups; the purple dots show the contribution of each cytokines.

The first two PC explained 39.8 % of the total variance of the model. The clusterization of the healthy and ill mice results to be less strong in comparison to the other O2PLS but the corresponding loading scatter plot (figure 17-B) confirms a strong cytokines activation in the healthy mice with a stronger contribute of IL-12(p40), IL-13 and IL-10. These cytokines result to be the most implicated in the preventive effects of CPMV eVLPs.p524 thus supporting the results showed in figures 15-B and 16-B.

6.3. Analysis of Treg cells

The population of regulative T cell (Treg) CD4+CD25+ having the phenotype FoxP3 have been characterised in the Langerhans islets of treated mice.

This analysis was performed since evidence in literature have been associated the Treg CD4+CD25+ FoxP3+ with T1D disease resistance. In particular, Foxp3 seems to act as a master regulator transcription factor for the induction of a regulatory differentiation program in T cells (Jaeckel *et al.*, 2008).

In figure 18 the results of the Treg CD4+CD25+ FoxP3+ analysis done in the Langerhans islets of mice treated with CPMV eVLPs.p524 in comparison with the ones treated with the unmodified CPMV eVLPs are reported.

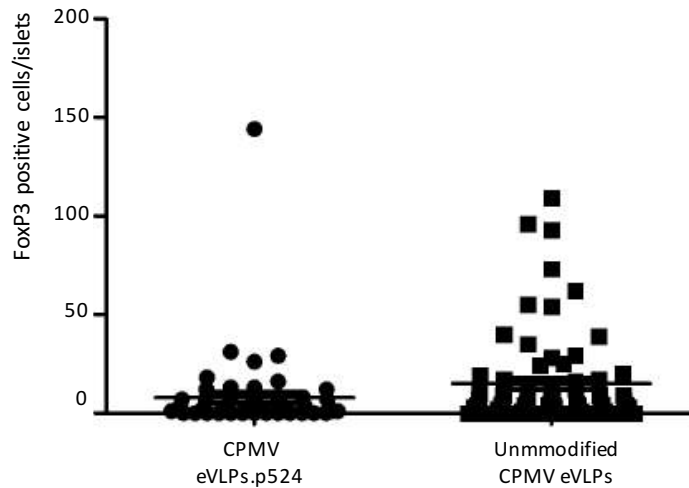


Figure 18 Cells count of the Treg CD4+CD25+ positive to the FoxP3 phenotype in the Langerhans islets of the pancreatic β -cell of mice treated with CPMV eVLPs.p524 or unmodified CPMV eVLPs. In the y axis the number of FoxP3 positive cells/islets is reported.

Figure 18 shows that the preventive effect of CPMV eVLPs.p524 seems not to involve changes in Foxp3 levels. On the other hand, mice treated with the unmodified CPMV eVLPs became diabetic despite increases in Foxp3 levels.

A similar result has been demonstrated in Lau *et al.* (2011) in which they demonstrated an Foxp3-independent inhibition of T1D correlated to a GAD-expressing lactobacillus. It could be concluded that that Foxp3 induction was not the primary mechanism mediated by CPMV eVLPs.p524.

EXPRESSION OF CPMV eVLPs.p524 IN EDIBLE PLANTS

1. Experimental design

Edible plants represent optimal biofactories for recombinant protein production. This strategy allows the production of oral biomolecule that can be assimilated in the diet, thus inducing immunological oral tolerance. The expression of eVLPs or CVPs in edible plants has never been reported in literature thus, in this work, the expression of CPMV eVLPs.p524 has been tested.

8 spinach and red beet plants 6 weeks old were infiltrated with a mix of *A. tumefaciens* LBA4404 strains carrying one the vector pEAQ-*HT*-VP60.p524 and the other the plasmid pEAQ-*HT*-24K. Starting from 3 dpi to 7 dpi the infiltrated leaves of one plant per species per day were collected. The CPMV eVLPs.p524 expression was assessed by SDS-PAGE, Commassie staining and western blot analysis.

2. Analysis of the expression in Spinach and Red beet of CPMV eVLPs displaying p524

4 leaves of 7 plants of either spinach or red beet were infiltrated with a mixed suspension of *A. tumefaciens* carrying pEAQ-*HT*-24K or pEAQ-*HT*-VP60.p524 plasmids.

As negative control, 4 leaves of either spinach or red beet were infiltrated with the infiltration buffer used for the resuspension of bacterial cells (MMA)

The agroinfiltrated leaves of one plant per species per day were collected and the TSP were extracted from them and analysed by western blot, using a polyclonal antibody specific to CPMV particles for the detection of specific signals. Results of this analysis are reported in figure 19.

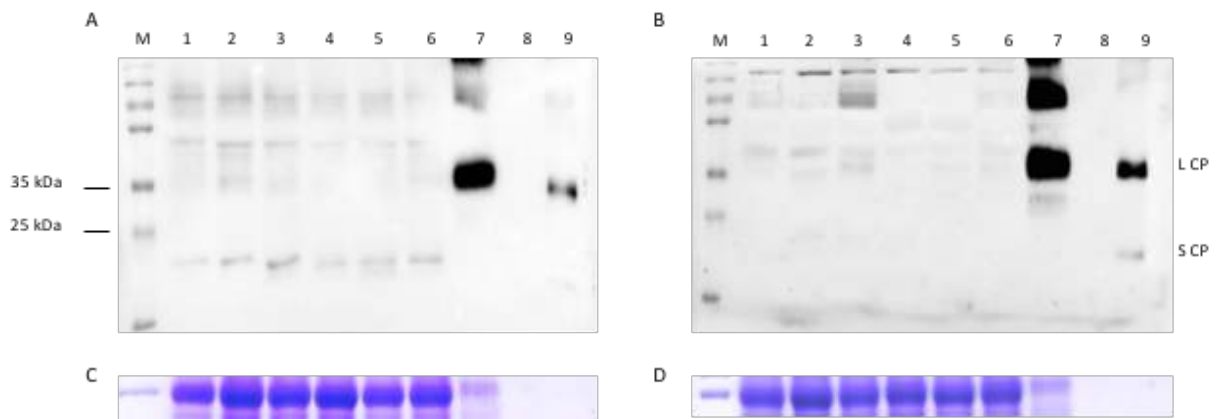


Figure 19 SDS-PAGE and western blot analysis of the analysis of the expression of CPMV eVLPs.p524 in spinach (A) and red beet (B). 20 μ l of the total protein extract of each sample were obtained using PBS buffer pH 7.2 and loaded on 12% polyacrylamide gels then blot was probed with a polyclonal antibody (G49) specific to CPMV particles used at a concentration of 1:2000. M: molecular marker (PageRuler™ Plus Prestained Protein Ladder, Thermo Scientific); 1: negative control, protein extract from leaves infiltrated with infiltration buffer; 2: protein extract of infiltrated leaves for the expression of CPMV eVLPs.p524 at 3 dpi; 3: protein extract of infiltrated leaves for the expression of CPMV eVLPs.p524 at 4 dpi; 4: protein extract of infiltrated leaves for the expression of CPMV eVLPs.p524 at 5 dpi; 5: protein extract of infiltrated leaves for the expression of CPMV eVLPs.p524 at 6 dpi; 6: protein extract of infiltrated leaves for the expression of CPMV eVLPs.p524 at 7 dpi; 7: positive control, protein extract from *N. benthamiana* expressing CPMV eVLPs.p524; 8:- ; 9: positive control, 1 μ g of purified unmodified CPMV eVLPs. Coomassie stained gels of Rubisco large subunit (C: spinach samples and D: red beet sample) are reported as loading control.

The analysis reported in figure 18 shows that CPMV eVLPs.p524 are not expressed neither in spinach nor in red beet. Indeed, no specific signals is visible in the samples relative to the time course expression analysis (lanes 2-6 figure 19-A/B) but there are only some aspecific bands clearly visible also in the negative control protein extract (lane 1 figure 19-A/B). In conclusion, the CPMV eVLPs expression system, which was developed for the transient expression of these particles in *N. benthamiana*, is unsuitable for the expression of them in the tested edible plants.

RHEUMATOID ARTHRITIS TREATMENT

1. Experimental design

There are several animal models of autoimmune arthritis that have proven to be valuable research tools for testing new therapies, including spontaneous models and those that require immunization. Among the latter, CIA (collagen-induced arthritis) mice has been the most widely studied model of rheumatoid arthritis (RA).

In DBA-1 mice, RA is induced by immunization with an emulsion of complete Freund's adjuvant (CFA) and type II collagen (CII). Typically, the first signs of arthritis appear 21-28 days after immunization and identification of the arthritic limbs is not difficult (Brand *et al.*, 2007).

The identification of new putative immunodominant peptides involved in RA was performed in collaboration with Dr. Elisa Tinazzi's research group of the Department of Medicine in the University of Verona.

A FliTrx random dodecamer peptide library was used according to the manufacturer's instruction (FliTrx Panning Kit Invitrogen) and following the methods reported in Navone *et al* (2005), three novel peptides (table 1) were identified to be putatively involved in seronegative RA.

Table 1: Novel peptide identified to be putatively involved in seronegative RA.

Name	Sequence	Features of the protein at which belongs the peptide
LIP₁	ASVLANVAQAFE	The Liprin-alpha-1 protein may regulate the disassembly of focal adhesions. It may localize receptor-like tyrosine phosphatases type 2A at specific sites on the plasma membranes, possibly regulating their interaction with the extracellular environment and their association with substrates. (Serra-Pags <i>et al.</i> , 1995)
FADK₂	AKVLANLAHPPA	The protein-tyrosine kinase 2-beta is a non-receptor protein-tyrosine kinase that regulates the reorganization of the actin cytoskeleton, cell polarization, cell migration, adhesion, spreading and bone remodelling. It plays a role in the regulation of the humoral immune response and it is required for normal levels of marginal B-cells in the spleen and normal migration of splenic B-cells. It is also required for normal macrophage polarization and migration towards inflammation sites. It regulates cytoskeleton rearrangement and cell spreading in T-cells, contributing to the regulation of T-cell responses. It promotes osteoclastic bone resorption and it may inhibit differentiation and activity of osteoprogenitor cells. It functions in signalling downstream of integrin and collagen receptors, immune receptors, G-protein coupled receptors (GPCR), cytokine, chemokine and growth factor receptors, mediating responses to cellular stress. Furthermore, it regulates numerous signalling pathways (Sun <i>et al.</i> , 2008; Ruusala <i>et al.</i> , 2008; Collins <i>et al.</i> , 2010; Lipinski <i>et al.</i> , 2010).
BANK₁	DMILANLSIKKK	The B-cell scaffold protein with ankyrin repeats is involved in B-cell receptor (BCR)-induced Ca ²⁺ mobilization from intracellular stores. It promotes Lyn-mediated phosphorylation of IP3 receptors 1 and 2. It is involved in Systemic lupus erythematosus (SLE). (Yokoyama <i>et al.</i> , 2002; Kozyrev <i>et al.</i> , 2008)

Among the 3 peptides identified, the former two, LIP₁ and FADK₂, were considered the most interesting ones from an immunological point of view, hence they were selected to be tested in pre-clinical studies in DBA-1/CIA mice.

The TBSV CVPs expression system was used for the expression of viral particles displaying either LIP₁ or FADK₂ peptides on their surface.

Following the method reported in Grasso *et al.* (2013), a small scale infection 3 *N. benthamiana* plants (2 leaves/plants), with the infectious RNA in vitro synthesized from pTBSV vectors, was carried on to check the expression of TBSV particles displaying the two peptides of interest (TBSV CVPs.FADK₂ and TBSV CVPs. LIP₁).

In order to assess the genetic stability of TBSV CVPs particles displaying the peptides of interest, for the following infections, sap from symptomatic leaves was used for other 2 cycles. 6-10 days after each infection when the viral symptoms are clearly visible, symptomatic leaves (either local or systemic ones) of the infected plants were collected and analyzed: RNA was extracted, retro-transcribed and the cDNA was used for PCR and following sequencing to ensure that viral genome is stable.

Since these particles were properly produced and TBSV CVPs.FADK₂ and TBSV CVPs. LIP₁ are genetically stable, a large scale infection was performed and, as reported by Grasso *et al.* (2013), extracted and purified from symptomatic leaves.

The unmodified TBSV CVPs (i.e. lacking heterologous peptides on their surface) are essential in the perspective of animal trials as negative control and they were expressed and purified as well.

After purification and characterization to confirm the correct assembly and shape, the TBSV CVPs.FADK₂ and TBSV CVPs. LIP₁ were used in pre-clinical studies in DBA-1/CIA mice in order to assess the potential of these particles to be used for the treatment RA.

2. Cloning of LIP₁ and FADK₂

The expression vectors for the production of pTBSV.LIP₁, pTBSV.FADK₂ and pTBSV were generously provided by the Prof. Luca Santi (Department of Agriculture and Forestry Science (DAFNE) of the University of Tuscia).

The sequence of the two peptide of interest are reported in table 2.

Table 2: LIP₁ and FADK₂ sequence for their expression with the TBSV CVPs system

LIP₁	
Aminoacid sequence	ASVLANVAQAFE
Nucleotidic sequence	GCT TCT GTT CTT GCT AAT GTT GCA CAA GCA TTT GAA
Length (aminoacids)	12
FADK₂	
Aminoacid sequence	AKVLANLAHPPA
Nucleotidic sequence	GCT AAG GTT CTT GCT AAT CTT GCA CAT CCA CCT GCT
Length (aminoacids)	12

Starting from the sequences reported in table 2 oligonucleotide pairs for both the peptides were designed to obtain DNA fragments *ApaI* and *PacI* compatible ends that were ligated in the pTBSV *ApaI-PacI* digested vector.

After the ligation of the DNA fragments encoding for LIP₁ or FADK₂ peptide into the pTBSV vector, the resulting pTBSV.LIP₁ and pTBSV.FADK₂ plasmids were independently transformed in *E. coli* XL1-Blue strain competent cells by electroporation. *E. coli* were plated in ampicillin (100 µg/ml) containing medium and PCR selected using vector- and peptide-specific primers (TBSV-2Back/LIP₁-For and TBSV-2Back/FADK₂-For).

All the colony tested result to be correctly transformed (data not shown).

Selected pTBSV-LIP₁ and pTBSV-FADK₂ were propagated in selective broth and plasmids were extracted, PCR analysed and sequenced to assess that the inserts were correct.

3. Analysis of the expression in plant of TBSV CVPs.FADK₂ and TBSV CVPs.LIP₁

A small scale infection of 3 plants per TBSV CVPs.FADK₂ and TBSV CVPs.LIP₁ was performed, in order to verify the expression of the modified particles.

The vectors pTBSV.LIP₁ and pTBSV.FADK₂ were linearized and the infectious RNAs were *in vitro* transcribed. The RNA quality was assessed using BioAnalyzer (data non shown) and the resulting infectious viral RNAs were used to infect 2 leaves per plants. 8 dpi, when viral symptoms appeared, symptomatic leaves were collected and analysed by retrotranscription-PCR (RT-PCR). The cDNAs were then sequenced to verify the stability of the peptide expressed on the viral surface.

After the first cycle of infection, another cycle was performed inoculating 2 leaves/plants using sap derived from symptomatic leaves of the first infection cycle. 6-10 dpi, the local and systemic symptomatic leaves were collected and analysed as describe before.

- First infection cycle

The symptomatology was constantly monitored; an example of a plant inoculated with the infectious RNA derived from pTBSV.FADK₂ is shown in figure 1.

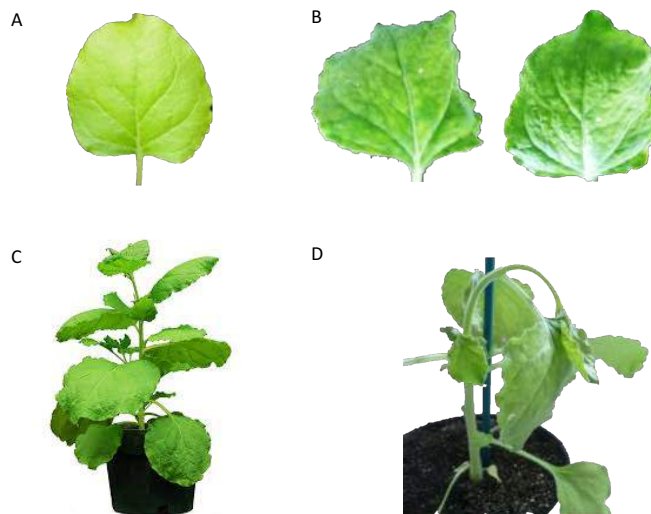


Figure 1 *N. bethamiana* leaves showing chlorotic symptoms 3-4 dpi after the infection with TBSV CVPs.FADK₂ (B) and their effects on the whole plant 8 dpi (D). In panels A and C a respectively wild type leaf and plant is showed.

Plants infected showed the characteristic chlorotic lesion onto inoculated leaves at 3-4 dpi (figure 1-A). At 5-6 dpi symptoms appeared systemically showing mottling, distortions and stunting leaves (figure 1-B and 1-D).

Symptomatology of plants inoculated with infectious TBSV RNAs harbouring LIP₁ peptide showed the same behaviour of the ones shown in figure 1.

At 8 dpi local and systemic leaves were collected in order to avoid the coming necrosis of the apical shoots.

RT-PCR analysis was done on the latter being the viral concentration higher than in the local one.

The RT-PCR reactions were performed using the SuperScript III (Promega) and 2 PCR analysis were performed. The first was carried out with primers specific for the actin constitutive gene (ACT1 and ACT2) in order to assess cDNA synthesis. The latter, was done using TBSV specific primers (RTPCR1For and TBSV-2back) to amplify the 3' CP region, in which the peptide sequence was cloned.

The results of the PCR are reported in figure 2.

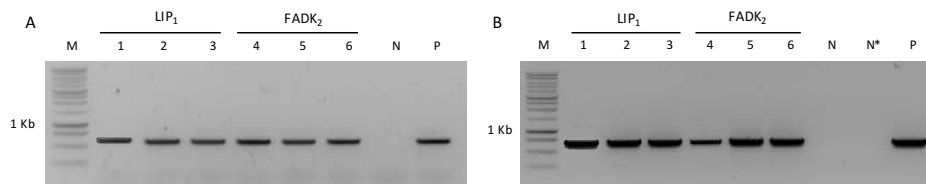


Figure 2 RT-PCR analysis of the symptomatic leaves collected from plant infected with the infectious RNA derived from pTBSV.LIP1 (1-3) and pTBSV.FADK2 (4-6). The PCR analysis done on the cDNAs using primers for a constitutive gene (ACT1 and ACT2) (A) and TBSV specific primers (RTPCR1For and TBSV-2back) (B) are reported. PCR amplification products obtained were loaded on a 2% agarose gel. M: molecular marker (BenchTop 1Kb DNA ladder – Promega); N: negative control of the PCR; N*: negative control (using cDNA derived from a wild type *N. bethamiana* as template); P: positive control (using a pTBSV vector display a well-know peptide as template).

An amplicon of approximately 700 bp is clearly visible in all cDNA samples (figure 2-B) confirming the specific presence of the viral TBSV RNA in analysed plants.

The fragments resulting from the PCR with TBSV specific primers, were sequenced and the resulting sequence was aligned with the expected one; the results are summarized in table 3.

Table 3: Genetic stability results for the primary infection of *N. benthamiana* plants with infectious RNA derived from pTBSV.LIP₁ and pTBSV.FADK₂. V: the genetical stability is conferred.

Primary infection	TBSV CVPs.LIP ₁	TBSV CVPs.FADK ₂
<i>N. benthamiana</i> 1	V	V
<i>N. benthamiana</i> 2	V	V
<i>N. benthamiana</i> 3	V	Problems in the sequencing

5 of the 6 samples analysed resulted to have the expected sequence and no mutations were present.

- *Second infection cycle*

Sap obtained from the systemic symptomatic primary infection leaves was used for inoculating 5 plants, either for the expression of TBSV CVPs.LIP₁ or TBSV CVPs.FADK₂. When the infection is performed with a plant extract containing TBSV particles, viral symptoms appear faster than when the primary infection is carried out with infectious TBSV RNA, hence 6 dpi the symptomatic leaves were collected in order to avoid necrosis and plant death.

RT-PCRs were conducted on the symptomatic systemic leaves and the results confirmed the presence of TBSV particles in infected plants, either for TBSV CVPs.LIP₁ or TBSV CVPs.K (data not shown). The PCR products obtained with TBSV specific primers, were sequenced and the resulting sequences were aligned with the expected one.

All the resulting sequences, TBSV CVPs.LIP₁ and TBSV CVPs.FADK₂ had a 100% identity with the reference one.

In conclusion, TBSV CVPs.LIP₁ and TBSV CVPs.FADK₂ are correctly expressed in *N. benthamiana* plants and they resulted to be genetically stable.

For the purpose of the production of TBSV CVPs.LIP₁ and TBSV CVPs.FADK₂ in view of pre-clinical trials, in literature there are many evidences (Grasso *et al.*, 2013) of higher

particles yields in the second infection cycle than the primary, thus allowing to avoid the need of third infection cycles

4. Purification of TBSV CVPs.LIP₁, TBSV CVPs.FADK₂ and unmodified TBSV CVPs

4.1. TBSV CVPs.LIP₁ and TBSV CVPs.FADK₂

The TBSV CVPs displaying either LIP₁ or FADK₂ peptides were purified following the method reported in Grasso *et al.* (2013) starting from 30-40 g of mixed symptomatic and local infected leaves derived from the second infection cycle.

An aliquot of every purification step was collected in order to monitor the process. Purified particles were eventually resuspended in 0.7% NaCl buffer.

SDS-PAGE and silver staining analysis were performed on the final purified particles TBSV CVPs.LIP₁, TBSV CVPs.FADK₂ and aliquots were collected during the purification in order to confirm particles purification; in figure 3 the results of these analysis are reported.

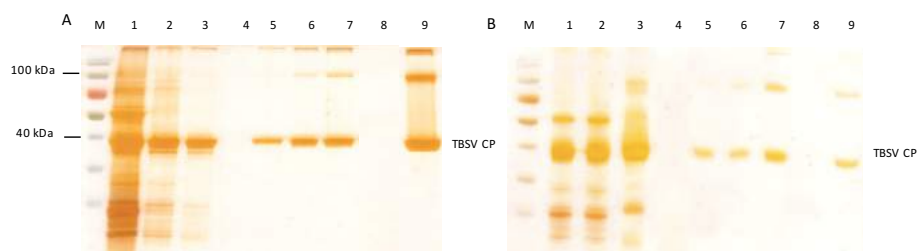


Figure 3 SDS-PAGE and silver staining analysis of the purified TBSV CVPs.FADK₂ (A) and TBSV CVPs.LIP₁ (B). 1: 2.5 μ l of total protein extract derived from symptomatic leaves; 2-3: 2.5 μ l of sample from progressive purification steps; 4: - ; 5: 2.5 μ l of a dilution 1:100 (A) and 1:50 (B); 6: 5.0 μ l of a dilution 1:100 (A) and 1:50 (B); 7: 7.5 μ l of a dilution 1:100 (A) and 1:50 (B); 8: - ; 9: 0.25 μ l of the purified TBSV CVPs.FADK₂ (A) and TBSV CVPs.LIP₁ (B). The samples were loaded on 14% polyacrylamide gel. The TBSV CP molecular weight (40 kDa), is indicated. M: molecular marker (PageRuler™ Plus Prestained Protein Ladder, Thermo Scientific).

This analysis highlighted the progressive purification of TBSV CVPs.LIP₁ (A) TBSV CVPs.FADK₂ (B) particles. Lanes 5-7 show pure viral particles, corresponding to a band of approximately 40 kDa. In both lane 6 and 7 there is also a signal at approximately 90 kDa corresponding to a dimer of TBSV CP that was probably not denatured during the

treatment before electrophoresis, probably due to high TBSV CVPs particles concentration. The purity of the samples was confirmed in lane 9 corresponding to the non-diluted purified TBSV CVPs.LIP₁ (figure 3-A) and TBSV CVPs.FADK₂ (figure 3-B).

4.2. Unmodified TBSV CVPs

Following the same procedure, unmodified TBSV CVPs from infected *N. benthamiana* leaves were successfully purified. SDS-PAGE and silver staining analysis were performed on the final pure unmodified TBSV CVPs in order to confirm the particles purification; in figure 4 the results of these analysis are reported.

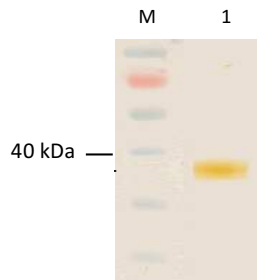


Figure 4 SDS-PAGE and silver staining analysis of the purified unmodified TBSV CVPs 1: 7.5 μ l of 1: 50 diluted TSP derived from 40 g of symptomatic leaves. The samples were loaded on 14% polyacrylamide gel. The TBSV CP molecular weight (40 kDa), is indicated. M: molecular marker (PageRuler™ Plus Prestained Protein Ladder, Thermo Scientific).

Figure 4 underlines that the unmodified TBSV CVPs were successfully purified and they will be used as negative control in the subsequent pre-clinical studies.

5. Characterization of purified TBSV CVPs.LIP₁, TBSV CVPs.FADK₂ and unmodified TBSV CVPs

Purified TBSV CVPs.LIP₁, TBSV CVPs.FADK₂ and unmodified TBSV CVPs were quantified, analysed by Dynamic Light Scattering and subjected to a LAL test in order to exclude the presence of any endotoxin in the purified particle preparations and to assess their suitability to be used in pre-clinical studies.

5.1. Quantification of purified TBSV CVPs.LIP₁, TBSV CVPs.FADK₂ and unmodified TBSV CVPs

The Bradford protein assay with known quantities of bovine serum albumin (BSA) as standards was used for the quantification of purified TBSV CVPs.LIP₁, TBSV CVPs.FADK₂ and unmodified TBSV CVPs.

1.750 mg of each purified TBSV CVPs particles were necessary for pre-clinical study and twice of the amount (3.5 mg) were prepared.

The amount of symptomatic leaves (leaf fresh weight; LFW) needed to achieve 3.5 mg of TBSV CVPs displaying the peptide of interest were specific for each sample and yields are reported in table 4.

Table 4: TBSV CVPs.FAK₂, TBSV CVPs.LIP₁ and unmodified TBSV CVPs purification yields.

	LFW (g) to achieve 3.5 mg	Yields (µg/g)
TBSV CVPs.FADK ₂	31	114
TBSV CVPs.LIP ₁	49	72
Unmodified TBSV CVPs	54	65

5.2. Limulus Amebocyte Lysate-test (LAL-test)

Purified TBSV CVPs.LIP₁, TBSV CVPs.FADK₂ and unmodified TBSV CVPs were subjected to a LAL-test.

The gel clot method was used and LAL-test showed a sensitivity of 0.125 UE (endotoxin units)/ml.

None of the samples of TBSV CVPs.LIP₁ and TBSV CVPs.FADK₂ showed any gel clot formation indicating that endotoxin concentration in these samples is lower than 0.125 UE/ml. As a consequence, particles were suitable to be injected in animal models.

On the other hand, the undiluted unmodified TBSV CVPs formed a gel clot indicating an endotoxin concentration higher than 0.125. A resin for the endotoxin removal (EndoTrap® HD) was then used. After the treatment with EndoTrap, the resulting unmodified TBSV CVPs sample was subjected again to LAL-test resulting negative, thereby indicating particles suitability to be used in pre-clinical study.

6. Pre-clinical trials in RA animal model

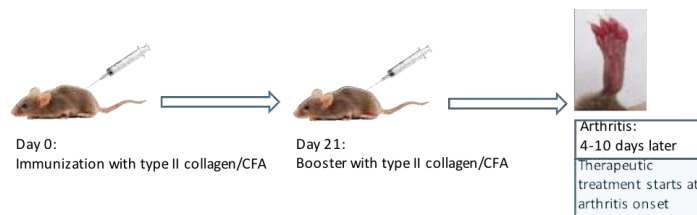
6.1. Induction of autoimmune arthritis in mice with type II collagen (CII)

Collagen-induced arthritis (CIA) mouse model is the most commonly studied autoimmune model of rheumatoid arthritis. The original “gold standard” of the CIA model are DBA-1 (Dilute Brown Non-Agouti) mice that have to be immunized using type II collagen.

DBA-1 mice were immunized or not with an emulsion of complete Freund’s adjuvant (CFA) and type II collagen (CII) at day 0 and 21 in order to develop arthritis.

The immunization was done as reported in scheme 1:

Scheme 1 CIA induction



Results showing the kinetics of arthritis development in DBA-1 mice immunized with CII are reported in figure 5.

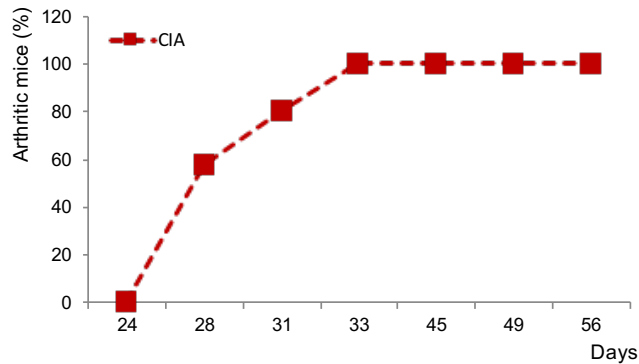


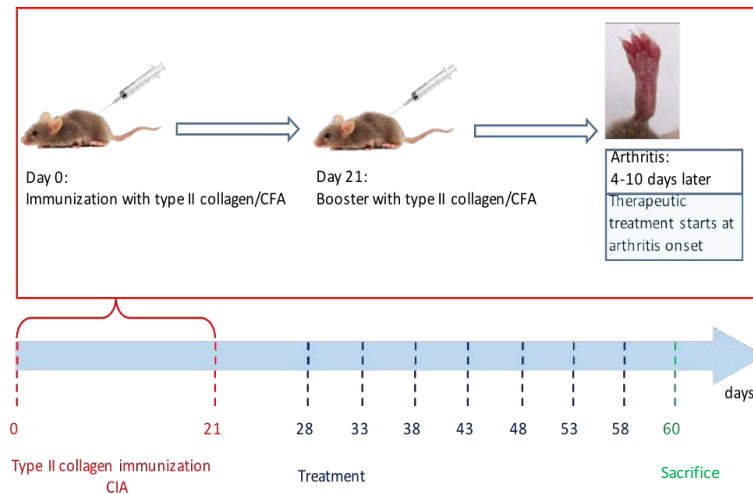
Figure 5 Kinetics of arthritis development in DBA-1 mice immunized with CII. The percentage of arthritic mice and the time (days) are respectively reported on y and x axis.

Figure 5 shows that 28 days post-immunization 60 % of immunized mice were arthritic and 33 days post-immunization 100% of immunized mice showed signs of RA.

6.2. Injection of LIP₁ and FADK synthetic peptides, TBSV CVPs.LIP₁, TBSV CVPs.FADK₂ and unmodified TBSV CVPs in CIA mice

The pre-clinical study was scheduled as reported in scheme 2:

Scheme 2 RA pre-clinical study in CIA mice.



Each experimental group was treated 7 time, 5 days apart, starting from day 28 after the first immunization.

The experimental groups of the pre-clinical study were:

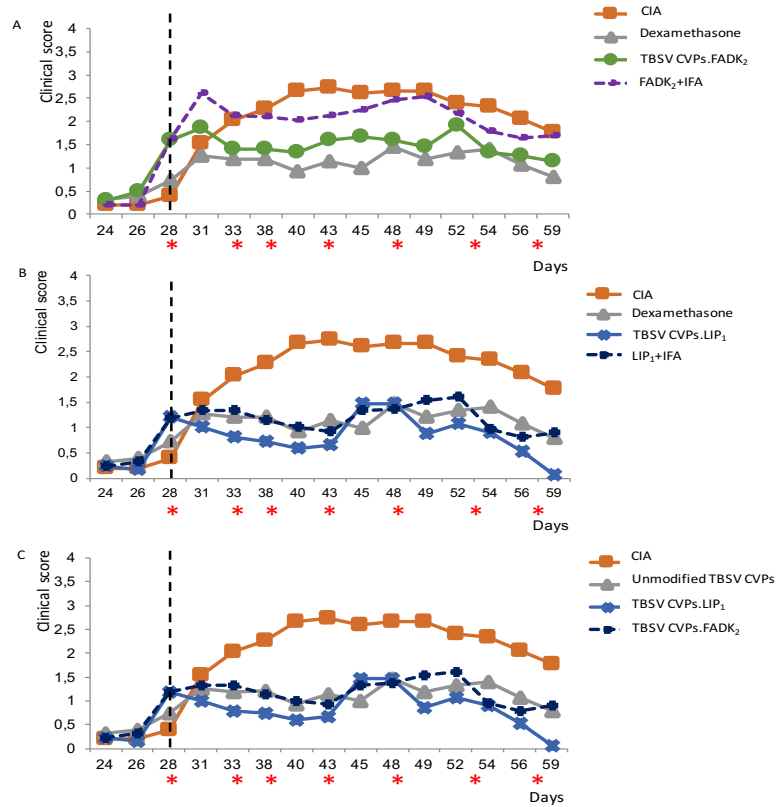
- No CIA mice;
- CIA mice treated with 50 µg of TBSV CVPs.LIP₁;
- CIA mice treated with 50 µg of TBSV CVPs.FADK₂;
- CIA mice treated with 50 µg of synthetic peptide LIP₁ mixed with IFA;
- CIA mice treated with 50 µg of synthetic peptide FADK₂ mixed with IFA;
- CIA mice treated with 50 µg of unmodified TBSV CVPs;
- CIA mice treated with saline buffer as negative control;
- CIA mice treated with Dexamethasone as positive control.

Each experimental group was composed by 5 mice.

Clinical assessment of CIA was done using a macroscopic score system based on visual identification of arthritic limbs; the RA index for each mouse was expressed as the mean of the four scores of individual paws.

The clinical score, reported in the vertical axis, was constructed by dividing the total score by the number of animals used for each experimental group.

Therapeutic effects of different treatments are reported in figure 6.



Clinical score:

- 0: no signs of RA
- 1: Swelling and/or redness of the paw or one digit
- 2: Two joints involved
- 3: more than two joints involved
- 4: severe RA of the entire paws and digits

Figure 6 Clinical score of the pre-clinical RA study. The results of the treatments done with the TBSV CVPs.FADK₂ (green circle- A) and TBSV CVPs.LIP₁ (blue cross - B) and the corresponding synthetic peptides mixed with IFA (FADK₂; purple dot - A and LIP₁; dark blue cross - B) are reported respectively in panel A and B in comparison with the negative

control CIA mice group (orange square) and mice treated with dexamethasone as positive control (grey triangle). The panel C shows the clinical score of mice treated with TBSV CVP.LIP₁ (dark blue cross) and TBSV CVP.FADK₂ (light blue cross) in comparison with the negative control CIA mice group (orange square) and mice group treated with the unmodified TBSV CVPs. On the bottom of the figure the clinical score used for the evaluation of mice clinical symptoms is reported. The clinical score and the time (days) are showed in each graph respectively on the y and x axis. The red starts under the x axis indicate the mice treatments that were started at day 28 as indicated by the blu dotted line.

Results in figure 6-panel A shows that the mice group treated with TBSV CVPs.FADK₂ has a similar behaviour of the positive control group injected with dexamethasone. It is important to underline that at the end of the immunization (day 28; dotted black line in figure 6) the mice group treated with TBSV CVPs.FADK₂ had a higher clinical score then the positive control group, so the therapeutic effects of the TBSV CVPs.FADK₂ is relevant. Moreover, at day 28 the clinical score of the mice group treated with TBSV CVPs.FADK₂ is exactly the same of the one injected with the synthetic FADK₂ peptide (+IFA) but, at the end of experiment, the clinical score of the group injected with TBSV CVPs.FADK₂ is lower then the one treated with the synthetic peptide confirming a higher therapeutic effect of TBSV CVPs.FADK₂.

The results were more robust in the treatments made with TBSV CVPs.LIP₁. Results in panel B of figure 6 showed that synthetic peptide LIP₁ had a similar behaviour of the positive control group (dexamethasone-treated mice) and, notably, at the end of the experiment the mice group injected with TBSV CVP.LIP₁ did not show any arthritic symptoms.

Finally, in figure 6-panel C it is shown the clinical score of the groups treated with TBSV CVPs.FADK₂, TBSV CVPs.LIP₁ and the unmodified TBSV CVPs, in comparison with the negative control group, the injection with the unmodified TBSV CVPs seems to induce a partial mice protection as reported even in the T1D clinical trials done using CPMV eVLPs expression system; it is clearly visible that the treatments with TBSV CVPs.LIP₁ resulted to be the most effective; the injection with TBSV CVPs.FADK₂ seems to have similar effects of those of the treatments with the unmodified TBSV CVPs but it is important to consider that at day 28 the mice group treated with TBSV CVPs.FADK₂ had a clinical score higher than the group treated with unmodified TBSV CVPs.

These data clearly confirmed the effectiveness of the viral structure in boosting an immunoregulative activity of the novel discovered immunodominant peptides and the capability of the viral scaffold to work as an adjuvant itself.

6.3. Treg determination in lymph nodes

At the end of the experiment (day 60) Treg were determined in lymph nodes and the analysis results are reported in figure 7.

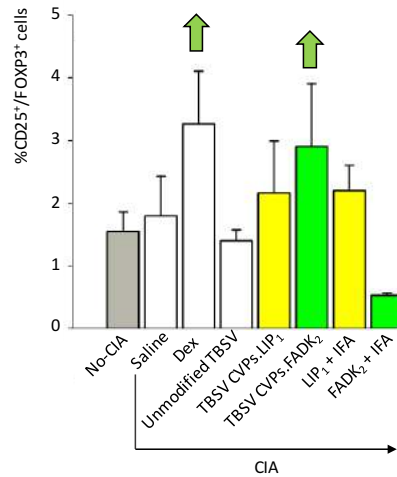


Figure 7 Treg CD25⁺/FOXP3⁺ analysis in lymph nodes of the mice treated in the pre-clinical RA study. The CD25⁺/FOXP3⁺ percentage is reported on the y axis.

Regulatory T cells (Tregs) are also considered suppressor T cells being responsible for immune system regulation retaining tolerance to auto-antigens and eliminating autoimmunity. CD4⁺ CD25⁺ suppressor T cells are well-known Tregs that express the transcription factor fork head box P3 (Foxp3); they are indispensable for the maintenance of immune self-tolerance and homeostasis by suppressing aberrant or excessive immune response (Haque *et al.*, 2014).

Figure 7 underlines a higher percentage of CD25⁺/FOXP3⁺ cells in lymph nodes of mice treated with TBSV CVPs.FADK2 and dexamethasone as well. These results suggest that the Treg mechanism could be at the basis of the therapeutic effect of TBSV CVPs.FADK2. Interestingly, the use of synthetic peptide FADK₂ (+IFA) did not activated any Treg

response confirming a strong viral particle contribution in the immunoregulative action. On the other hand, the CD25⁺/FOXP3⁺ percentage in the lymph nodes of the mice injected with either TBSV CVPs.LIP₁ or synthetic peptide LIP₁ is similar to that of the negative control CIA-mice group treated with the saline buffer.

6.4. Cytokines analysis in different sites

The more important cytokines involved in the immune response associated to this treatment were determinate in lymph nodes, joints and serum.

The following table 5 summarises the results of the treatment done with dexamethasone (positive control), TBSV CVPs.LIP₁, TBSV CVPs.FADK₂ and the synthetic peptide LIP₁ or FADK₂ (both with IFA) in comparison with the negative control CIA-mice group treated with saline buffer.

Results in table 5 shows a general decrease of the pro-inflammatory cytokines production (indicated as negative cytokines in table 5 –A) either in the groups of mice treated with TBSV particles displayed the peptides of interest or with the synthetic LIP₁ and FADK₂ mixed with IFA.

Table 5 Overview of the cytokines activation/repression in different tissue of mice group treated with dexamethasone as positive control, TBSV CVPs.LIP₁, TBSV CVPs.FADK₂ and synthetic peptide LIP₁ or FADK₂ mixed with IFA in relation to CIA mice control group treated with saline buffer.

A										
Negative cytokines	TNF- α			IL-17a		IL-1 β			IFN- γ	
	LN	J	S	LN	J	LN	J	S	LN	J
Dexamethasone	↓	↓	↓	↓	=	↓	↓	↓	↓	↓
TBSV CVPs.LIP ₁	↓	=	↓	↓	=	↓	=	↓	↓	=
TBSV CVPs.FADK ₂	=	=	=	↓	↓	↓	↑	↓	=	=
Synthetic peptide LIP ₁	↓	=	=	↓	=	↓	=	↓	↓	↓
Synthetic peptide FADK ₂	↓	↓	=	↓	↓	↓	=	=	↓	↓

B		
Positive cytokines	TGF- β 1	IL-10
	Serum	
Dexamethasone	↑	=
TBSV CVPs.LIP ₁	=	↑
TBSV CVPs.FADK ₂	=	↑
Synthetic peptide LIP ₁	=	=
Synthetic peptide FADK ₂	↑	=

Table 5 underlines that the treatment with TBSV CVPs.LIP1 seems to be more effective in lymph nodes and serum; in particular, the viral structure seems to improve, in serum, the immunosuppression effect of the LIP1 peptide against the TNF- α , cytokines involved in the acute phase reaction of the systemic inflammation.

On the other hand, by comparing the treatment with TBSV CVPs.LIP₁ with the positive control (mice treated with dexamethasone) the former seems to have no effects in the joints. Conversely, looking at the results of the treatment performed with FADK₂ synthetic peptide is more effective than the respective TBSV CVPs FADK₂ in pro-inflammatory cytokines suppression. FADK₂ synthetic peptide resulted to be very effective in dampen pro-inflammatory cytokines production in joints.

Table 5-B highlights the activity in serum of either TBSV CVPs.LIP₁ or TBSV CVPs.FADK₂ in inducing the production of Interleukin-10 (IL-10) involved in the inhibition of the synthesis of pro-inflammatory cytokines. This activity has not been relived neither in treatments done with the synthetic peptides nor in the positive control mice.

The treatment with dexamethasone and with the synthetic FADK₂ peptide seem to activate a therapeutic effect driven by the transforming growth factor β (TGF- β), a pleiotropic cytokine with potent regulatory and inflammatory activity. Regarding the TGF- β regulatory activity, it has been demonstrated that it plays a central role in the induction of peripheral tolerance (Kronenberg *et al.*, 2005). This cytokine is essential for the survival of naïve T cells and for inhibiting the proliferation and differentiation of self-reactive CD4⁺ and CD8⁺ T cells (Li *et al.*, 2008; Lii *et al.*, 2006).

On the other hand, the treatment with TBSV CVPs.LIP₁ and TBSV CVPs.FADK₂ seems to activate the IL-10 mediated pathway. IL-10 is essential for homeostasis of the immune system by limiting the inflammatory response and has a particular role especially in the gastrointestinal tract following the action mechanism shown in the figure 8.

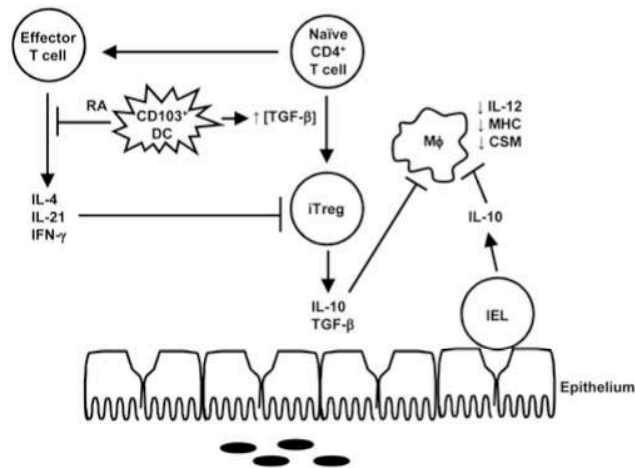


Figure 8 IL-10 mediated pathway in the gastrointestinal tract (Sanjabi *et al.*, 2009).

In figure 8 it is reported the IL-10 mediated pathway in the gut: in the gastrointestinal tract commensal bacteria/flora and food antigens are constantly sampled by intestinal dendritic cells (DCs). Tolerogenic CD103⁺ DCs produce retinoic acid which inhibits effector cytokine production by CD4⁺CD44⁺ T cells. In the absence of effector cytokines and in the presence of high concentrations of TGF- β , naïve CD4⁺ T cells are converted into Foxp3⁺ iTregs that produce TGF- β and IL-10. IL-10 produced by Intraepithelial lymphocytes (IEL) and iTregs regulates activation of intestinal lymphocytes, and reduces the expression of IL-12 and downregulates costimulatory molecules on macrophages.

CHAPTER 2: DIAGNOSIS

INTRODUCTION

1. Autoimmune disease diagnosis

There are 80-100 different autoimmune diseases (American Autoimmune Related Diseases Association) and many of them show similar symptoms, making their diagnosis challenging.

An early and precise diagnosis is decisive for autoimmune diseases because it allows to manage and stem the negative effects of the disorders before they cause other complications and lead to a total tissue and/or organ target destruction.

Most of autoimmune diseases cause fatigue, fever and general malaise affecting many parts of the body. The most common organs and tissues affected are joints and connective tissue, muscles, skin, red blood cells, blood vessels and endocrine glands.

Diagnosis is often based on the investigation of the presence in the blood of either autoantibodies able to recognize specific tissues or organs that are involved in the autoimmune disease.

Antinuclear antibodies (ANAs) are used as diagnostic marker for many autoimmune diseases. ANA are antibodies directed against structure within the nucleus of the cells found in many autoimmune, inflammatory and infective disorders such as Systemic Lupus Erythematosus (SLE), RA, SjS (Cervera *et al.*, 2000), scleroderma (Barnett *et al.*, 1993), polymyositis, dermatomyositis, primary biliary cirrhosis, autoimmune hepatitis (Obermayer-Straub *et al.*, 2000), multiple sclerosis, discoid lupus, thyroid disease, antiphospholipid syndrome, juvenile idiopathic, psoriatic arthritis, juvenile dermatomyositis, idiopathic thrombocytopenic purpura and cancer.

There are many prototype of ANAs, such as anti-La or anti-Ro antibodies which recognize different proteins or protein complexes within the nucleus.

Moreover, there is a group of autoantigens called extractable nuclear antigens (ENA) associated to autoimmune disease. They are termed ENA because they can be extracted from cell nucleus with a saline buffer (Kavanaugh *et al.*, 2000). They consist in ribonucleoproteins and non-histone proteins, called either with the name of the donor who

provides the prototype serum (La, Ro, Sm, Ja) or name of the disease setting in which they were found (SS-A, SS-B, Scl-70) (Wanzel *et al.*, 2001).

Other diagnostic procedure currently used in autoimmunity consists in red and white blood cells measurements because when an autoimmune disease is established the number of this blood cells varies compared to healthy individual.

Also high level of C-reactive protein (CRP) in blood plasma may indicate the establishment of an autoimmune disease because CRP level rises in response to inflammation throughout the body and the indication of the inflammation rate can be obtained through the measurement of the erythrocyte sedimentation rate (ESR).

1.1. Sjögren's syndrome diagnosis

The largest problem associated with SjS diagnosis is the absence of specific and unique diagnostic tools. At present, diagnosis consists of several steps based on classifying main SjS symptoms like ocular and oral dryness. Having symptoms common to most other widespread diseases, SjS is thus often underdiagnosed, and/or consequently diagnosed too late when the disease has already begun to damage the organism. It has been estimated that on average it takes up to 4 years to diagnose SjS (The British Sjögren's Syndrome Association).

The current diagnostic criteria up to now used for SjS diagnosis is the one drawn up by the American European Consensus Group (AECG) and the American college of Rheumatology (ACR).

In 2002 AECG proposed criteria for the classification of SjS:

- I. Ocular Symptoms (dry eyes);
- II. Oral Symptoms (dry mouth);
- III. Ocular Signs (evaluated through Schirmer's test);
- IV. Histopathology: lip biopsy showing focal lymphocytic sialoadenitis;
- V. Oral Signs (Unstimulated whole salivary flow (< 1.5 mL in 15 minutes);
- VI. Autoantibodies ANA.

Any 4 of the 6 criteria must be fit to diagnose SjS; but they must include either item IV (Hystopathology) or VI (Autoantibodies). Or any 3 of the 4 objective criteria (III, IV, V, VI).

In 2012 ACR proposed simplified criteria for the classification of SjS:

The classification of SjS, which applies to individuals with signs/symptoms that may suggest SjS, will be met in patients having at least 2 of the following 3 objective features:

1. positive serum anti-SSA/Ro and/or anti-SSb/La or (positive rheumatoid factor and ANA titer 1:320);
2. labial salivary-gland biopsy exhibiting focal lymphocytic sialoadenitis;
3. keratoconjunctivitis sicca with ocular staining score 3.

Either on the basis of AECG or ACR criteria, one of the major diagnostic methods is the serological test for detecting antinuclear antibodies (ANA). However, 40-25% of SjS patients are ANA-negative (Nardi *et al.*, 2006).

Moreover, anti-SSA/Ro and Anti-SSA/La is found in 30–60% of Sjögren's syndrome; anti-Ro antibodies alone are found in 50–70% of Sjögren's syndrome (Kumar *et al.*, 2009; Hernández-Molina *et al.*, 2011).

For ANA-negative patients, labial salivary gland biopsy is needed. This method is invasive and such an irreversible diagnostic technique can cause negative effects such as intolerance to anesthetics, bleeding and infection of damaged tissues.

1.2. Rheumatoid arthritis diagnosis

Rheumatoid arthritis can be difficult to diagnose because, especially early stage symptoms are common to other diseases or are typical manifestation of healthy elderly people.

The current diagnostic procedure consists of several steps to evaluate physical and serological parameters. First of all, a physical evaluation of swelling, redness and warmth of joints allow to achieve a general valuation of the principal RA target. This analysis is in-depth verified using X-rays and magnetic resonance imaging (MRI) scan or ultrasound scan to assess the presence of damage in joints.

In order to evaluate the presence of inflammation, CRP and ESP blood tests are used linked with the investigation of autoantibodies typically present in sera of RA patient. These autoantibodies are rheumatoid factor (RF) and anti-citrullinated protein antibody (ACPA). RF is an antibody against the Fc portion of IgG (Falkenburg *et al.*, 2015).

However, about 4 out of 5 people with rheumatoid arthritis have positive tests for RF, but about 1 in 20 people without RA also have positive results. Only about half of all people with RA have a positive RF when the disease starts (Arthritis Research UK – arthritisresearchuk.org).

Moreover, 38 % of RA patients are diagnosed with seronegative RA being negative to RF and ACPA serological tests (De Winter *et al.*, 2016).

The goal of this part of the PhD thesis work is the use of plant viruses for the display of new specific serological SjS and RA markers for the development of reagents to be used in an indirect ELISA test. These innovative diagnostic kits could avoid the current SjS and RA diagnostic obstacles due to the presence of a subgroup of seronegative patients. The development of these new tools could substantially reduce the time needs for a definitive diagnosis allowing a earlier disease identification thus avoiding further complications.

RESULTS AND DISCUSSION

SJÖGREN'S SYNDROME DIAGNOSIS

Adapted from:

Frontiers in Plant Science 2015, **6**: 1080.

Plant-derived chimeric virus particles for the diagnosis of primary Sjögren Syndrome.

Tinazzi E., Merlin M., Bason C., Beri R., Zampieri R., Lico C., Bartoloni E., Puccetti A., Lunardi C., Pezzotti M., Avesani L.

1. Experimental design

The heterogeneity of Sjögren Syndrome (SjS) symptoms often delays diagnosis (Patel *et al.* Shahane, 2014) and many cases are overlooked due to the absence of sensitive and specific disease markers and other definitive criteria for classification.

In Navone *et al.* (2005) a novel autoantigen target in SjS derived from tear lipocalin has been identified. This peptide, called lipo, is specifically recognized by the antibodies present in SjS patient sera and for this reason could be exploited for the development of a diagnostic kit.

The sequence of lipo peptide is FEKAAGARGLST.

The most widely used diagnostic immunoassays are based on the enzyme linked immunosorbent assay (ELISA), in which a passively adsorbed antigen is used to identify samples containing reactive antibodies. This is a simple and rapid technique which is routinely applied in many laboratories (Engvall *et al.* Perlmann, 1972).

One major drawback of peptide ELISAs is the inefficient binding of peptides to solid substrates such as microtiter plates (Griesmann *et al.*, 1991). Binding depends on the mass of the peptide and its amino acid composition, and if much of the peptide is involved in non-specific absorption then the relevant epitopes can be obscured (Sallberg *et al.*, 1995; Gregorius *et al.*, 1999; Gregorius *et al.* Theisen, 2001).

To overcome this obstacle, lipo peptide were cloned in the pPVXSma, pTBSV and pEAQ-HT-VP60 vectors in order to express in *N. benthamiana* plant PVX CVPs, TBSV CVPs

and CPMV eVLPs displaying lipo peptide.

After purification from plant tissues these particles were used as coating reagent in ELISA and sensitivity, specificity, reproducibility and stability of diagnostic ELISAs building up with the different virus particle displaying lipo peptide were compared to each other and to the ELISAs based on the synthetic lipo peptide. The use of PVX CVPs-, TBSV CVPs-CPMV eVLPs- based systems, characterized by different viral shapes, peptide display context and peptide position on the viral surface, allows to evaluate the influence of viral structures on ELISA performance.

2. Production of PVX CVPs.lipo, CPMV eVLPs.lipo and TBSV CVPs.lipo

2.1. PVX CVPs.lipo expression in plant and purification

The PVX CVPs.lipo were produced by introducing the lipo synthetic peptide sequence into the vector pPVXSma to yield pPVXSma.lipo in which the peptide was fused to the N-terminus of a truncated CP in order to be displayed on the particle surface. The peptide sequence was optimized for *N. benthamiana* codon usage, and virus movement was promoted by adding a serine residue between the initiator codon and the first native residue (Betti *et al.*, 2012). The production of PVX CVPs particles depends on virus replication, so the genetic stability of the virus genome was verified after several reinfection cycles. The plants were infected using pPVXSma.lipo plasmid DNA to initiate the first cycle, followed thereafter by infection using sap from symptomatic leaves obtained 12 days after each round of infection. The chimeric CP gene remained stable through several passages as demonstrated by RT-PCR and sequencing (data not shown). The presence of PVX CVPs.lipo and unmodified PVX CVPs was verified by western blot analysis of infected leaf extracts as show in figure 1.

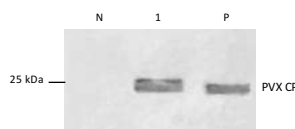


Figure 1 Western blot of *N. benthamiana* leaf TSP extracts, 24 μ l per lane separated by SDS-PAGE and detected with an alkaline phosphatase conjugated anti-PVX CP antibody. N: non-infected leaf extract, 1: PVX CVPs lipo leaf extract, and 2: unmodified PVX CVPs control leaf extract.

In figure 1 is evident a single band corresponding to the viral CP, with a molecular weight shift in the PVX CVPs.lipo sample in comparison to unmodified PVX CVPs, corresponding to the lipo peptide fused to the CP.

A larger number of plants were infected to obtain sufficient leaf material for particle purification. A yield of 0.11 mg/g LFW of PVX CVPs.lipo and the purity of the particles was verified by SDS-PAGE and silver staining. The result of this analysis is shown in figure 2.

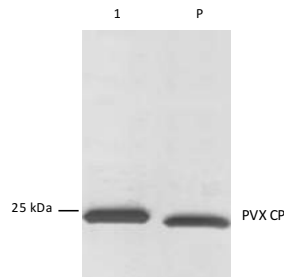


Figure 2 Silver staining of 750 ng purified particles separated by SDS-PAGE. 1: PVX CVPs.lipo and 2: unmodified CVPs PVX as positive control. The position of the 25 kDa molecular marker is indicated.

N. benthamiana plants were also infected with pPVX201 to obtain leaf material for the production of unmodified PVX control particles (Figures 1 and 2). The yield was 0.62 mg/g FLW.

2.2. CPMV eVLPs.lipo expression in plant and purification

The CPMV eVLPs.lipo were produced using the pEAQ-*HT* system. The VP60 CP precursor and the 24K protease were expressed on two separate pEAQ constructs allowing the production of eVLPs structurally identical to wild-type CPMV particles (Saunders *et al.*, 2009). The sequence encoding the target peptide was inserted into vector pEAQ-*HT*-VP60, within the β B- β C loop of the small CP. *N. benthamiana* leaves were agroinfiltrated simultaneously with both vectors. Leaf extracts were prepared 6 dpi for analysis by western blot using anti-CPMV antibodies, revealing the presence of specific signals corresponding to the large and small and a molecular weight shift accounting for the modified small CP, thus confirming the insertion of the foreign peptide (figure 3).

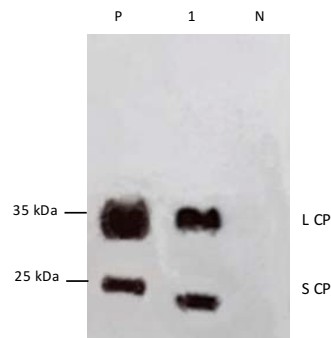


Figure 3 Western blot of *N. benthamiana* leaf TSP extracts, 11 μ l per lane separated by SDS-Page and detected with a polyclonal antibody (G49) specific to CPMV particles used at a concentration of 1:2000. N: non-infected leaf extract, 1: CPMV eVLPs.lipo leaf extract, and P: unmodified eVLPs CPMV control leaf extract.

A larger number of plants were infiltrated to obtain leaf material for the purification of unmodified CPMV eVLPs and CPMV eVLPs.lipo. Clarified leaf protein extracts were processed by anion exchange chromatography column to remove phenolic compounds. The flow through fraction containing the eVLPs was concentrated and then purified by size-exclusion chromatography. A final yield of ~ 0.04 mg/g and ~ 0.05 mg/g FLW for respectively the modified and unmodified CPMV eVLPs was achieved. The purity of the eVLPs was confirmed by SDS-PAGE and silver staining as shown in figure 4.

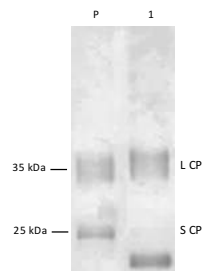


Figure 4 Silver staining of 2 μ g purified particles separated by SDS-page. 1: CPMV eVLPs.lipo particles and 2: unmodified CPMV eVLPs as positive control. The position of the 25 and 35 kDa molecular markers is indicated.

2.3. TBSV CVPs.lipo expression in plant and purification

The TBSV CVPs.lipo were produced by introducing the lipo synthetic peptide sequence into the vector pTBSV to yield pTBSV.lipo in which the peptide was fused to the C-terminus of the TBSV CP in order to be display on the particle surface. The genetic stability of the TBSV CVPs.lipo genome was verified after several reinfection cycles. The plants were infected using pTBSV.lipo RNA infectious retrotranscribed from plasmid DNA to initiate the first cycle, followed thereafter by infection using sap from symptomatic leaves obtained 12 days after each round of infection. The chimeric CP gene remained stable through several passages as demonstrated by RT-PCR and sequencing (data not shown). TBSV CVPs.lipo and unmodified TBSV CVPs was purified from symptomatic leaves and analysed by SDS-PAGE and silver staining in order to assess the purity of particles. The result of this analysis is shown in figure 5.

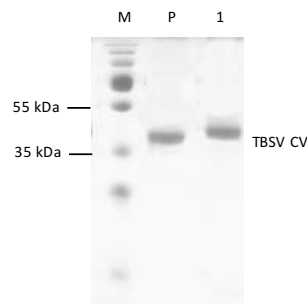


Figure 5 Silver staining of 1 μ g purified particles separated by SDS-PAGE. 1: TBSV CVPs.lipo particles and P: unmodified TBSV CVPs as positive control; M: molecular marker (PageRuler™ Plus Prestained Protein Ladder, Thermo Scientific). The position expected for the TBSV CP is indicated.

Figure 5 confirms the correct purification of the TBSV CVPs.lipo particles and the shift in the molecular weight in comparison to the unmodified TBSV CVPs particles indicates the effective presence of lipo peptide fused to the CP.

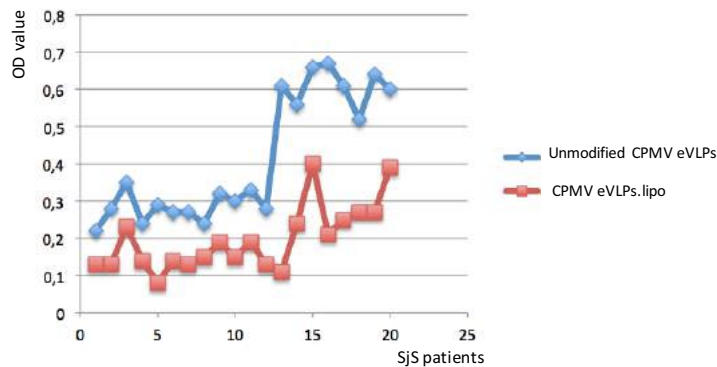
3. Development of an indirect ELISA using PVX CVPs.lipo, CPMV eVLPs.lipo and TBSV CVPs.lipo

The suitability of modified viral particles for the diagnosis of SJS was tested by comparing ELISAs based on the free synthetic peptide to the different VNP formats, and also by

comparing modified and unmodified CVPs and eVLPs, using sera from SjS patients, healthy controls and patients with other systemic autoimmune diseases.

Preliminary comparative analysis of the modified and unmodified eVLPs allowed to discard the CPMV platform because the unmodified CPMV eVLPs generated a stronger signal than the CPMV eVLPs.lipo as shown in graph 1.

Graph 1 OD value of ELISA based diagnostic kit set up with CPMV eVLPs.lipo.



This result could be due either to the icosahedral viral structure or to the peptide position on the viral surface that is rigid into a loop. In order to understand which characteristic was the most important for the recognition between the lipo peptide and the antibodies present in SjS sera patient the TBSV CVPs-based expression platform was tested. This expression platform allows to express icosahedral particles based on TBSV in which the peptide being fused on CP C-terminal is flexible on the viral surface. However, also with the TBSV CVPs expression system the unmodified TBSV CVPs generated a stronger signal than the TBSV CVPs.lipo (data not shown).

The difference in performance between the three platforms may reflect their distinct structures. PVX particles comprise ~ 1300 copies of identical CPs arranged in a helical configuration (Atabekov *et al.*, 2007) whereas the icosahedral CPMV particle comprises 60 copies each of the small and large CP subunits, only the former of which is modified, resulting in the display of 60 lipo peptides. The icosahedral TBSV particles comprise ~ 180 copies of identical CPs forming particles of 30 nm of diameter.

The CPMV particles are 28 nm in diameter, compared to PVX with a diameter of 12 nm

but a length of ~ 550 nm. This means that PVX and TBSV particles display approximately 10 times as many peptides in the same unit of surface area (PVX = 6.2×10^{-2} peptides/nm², and CPMV = 6.1×10^{-3} peptides/nm² and TBSV = 6.4×10^{-2} peptides/nm²). Furthermore, the rigid icosahedral structure of CPMV and the position of the peptide within the β -loop of the small CP subunit may constrain its ability to be displayed whereas the peptides displayed on the surface of PVX and TBSV are fused respectively to the N- and C-terminus of the CP, leading to a more flexible and mobile structure maintaining the linear conformation, which correctly promotes antibody recognition.

The flexible and filamentous PVX CVPs structure seem to be decisive for the diagnostic application of the particles in ELISA.

The ELISA based on the PVX CVPs.lipo showed greater sensitivity than the corresponding assay with synthetic peptide. This may reflect the relatively flat nature of the synthetic peptide ELISA, with the synthetic peptide passively adsorbed to the two-dimensional polystyrene surface of the microtiter plate, compared to the three-dimensional nature of the PVX CVPs.lipo, which form a nanomolecular scaffold that increases the surface area of the plate available for peptide display.

The ELISA based on PVX CVPs platform was compared with the one based synthetic peptide to evaluate the sensitivity and specificity of each ELISA. 90/91 patients with SjS were correctly shown to possess serum antibodies against lipo peptide using the PVX CVPs.lipo, whereas 79/91 were identified using the lipo peptide alone. These results corresponded to a sensitivity of 86.8% for the synthetic peptide and 98.8% for the PVX CVPs.lipo.

Neither the synthetic peptide nor the PVX CVPs.lipo particles were recognized by sera from healthy donors. Autoimmune reactivity against the lipo peptide therefore appears to be largely confined to the SjS patient population. The specificity of quantitative analysis was 90% for both the PVX CVPs.lipo and synthetic lipo peptide ELISAs.

Moreover, results showed that sera from the ANA-negative subgroup of SjS patients with diagnostic salivary gland histology (25/91 patients) reacted toward the PVX CVPs.lipo particles with a sensitivity of 98.7%, compared to 75% sensitivity in the peptide ELISA (table 1).

Table 1 The sensitivity and specificity (expressed as a percentage) ELISAs based on the synthetic lipo peptide and PVX CVPs.lipo considering all SjS patients or the SjS subgroup without ANA as a diagnostic serological marker.

	All SjS patients		ANA-negative SjS patients	
	Sensitivity	Specificity	Sensitivity	Specificity
Synthetic lipo peptide	86.8	90.0	75.0	90.0
PVX CVPs.lipo	98.8	90.0	98.7	90.0

The PVX CVPs.lipo based ELISA was more reproducible than the synthetic lipo peptide ELISA (data not shown), reflecting the nature of interaction between the binding reagent and the solid substrate. Synthetic lipo peptides are passively and non-covalently adsorbed to the solid substrate, an interaction which is weak due to the shortness of the peptide, and the structure of the peptide is randomly oriented with respect to the surface plane (Griesmann *et al.*, 1991). In contrast, large and complex multimeric proteins such as PVX CVPs adsorb strongly to the surface, and regardless of orientation, there remain plenty of peptides projecting freely into solution to permit interactions with serum antibodies. This increases the robustness and reproducibility of the ELISA regardless of the chemical structure of the peptide. However, synthetic peptide-based ELISA can be improved by chemical modifications, such as biotinylation, that may help in maintaining peptide conformation and improve their adsorption to solid substrates.

There was also a positive correlation between ANA titers and the ELISA outcome. Patients with an ANA titer exceeding 1:160 produced strong signals in the ELISA ($p = 0.023$), although there was no statistically significant relationship between ANA titers and the presence of anti Ro-SSA or anti La-SSB antibodies. Moreover, there was a strong correlation between the ELISA outcome and exocrine gland symptoms ($p < 0.001$) but not with the involvement of other organs, e.g., pulmonary fibrosis, neurological pathology, or vasculitis. This may reflect the small proportion of patients in our SjS cohort presenting with these symptoms.

4. Stability of ELISA test over the time

To demonstrate the stability and reproducibility of the PVX CVPs.lipo-based ELISA, microtiter plates were coated with PVX CVPs.lipo, stored at 4°C and then used after 1, 15, 30, and 60 days to test the sera from 18 SjS patients.

The results of these analysis are shown in figure 6.

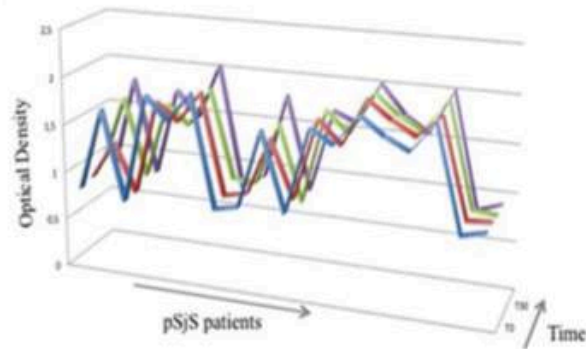


Figure 6 PVX CVPs.lipo ELISA results using sera from a subgroup of 18 SjS patients at four time points to determine assay stability. Each serum sample was tested three times at each time point; average values of optical density are graphed on the y axis. Blue: 24 h, red: 15 days, green: 30 days, and purple:60 days.

The results of these tests did not change regardless of the duration of storage, confirming the stability of the PVX-based ELISA format and the reproducibility of the assay (figure 6).

RHEUMATOID ATHRITIS DIAGNOSIS

1. PVX CVPs expression system

1.1. Experimental design

RA is one of the most widespread autoimmune disease; although serological AR markers are well established (e.g. RF and ACPA), 38 % of RA patient are seronegative to these (De Winter et al., 2016) and for that difficult to diagnose.

In Tinazzi *et al.* (2015) and as reported in the previous section (RESULTS – SJÖGREN'S SYNDROME DIAGNOSIS – page 115), filamentous and flexible viruses result to be excellent tools for the development of innovative diagnostic kit based on indirect ELISA. PVX CVPs and TuMV CVPs expression systems were selected for the expression of novel peptides identified to be putatively involved in seronegative RA (table 1 – page 92).

The LIP₁, FADK₂ and BANK₁ nucleotidic sequence were independently cloned in pPVXSma viral vector and purified through maxi purification from bacteriological culture. Once obtained a sufficient amount of pPVXSma.LIP₁, pPVXSma.FADK₂ and pPVXSma.BANK₁, experimental procedure was divided in two infection phases: a small and large phase. The first phase consists in three infection cycle of 5 *N. benthamiana* plants: at the first cycle, plants are infected using plasmid DNA, while for the following infections, sap from symptomatic leaves is used. The aim of the small scale infection is to assess whether recombinant virus remains genetically stable despite the insertion of the peptide sequence in the CP gene.

If PVX CVPs displaying peptide of interest result to be genetically stable a large phase infection (50 plants) was carried out for obtaining sufficient material for PVX CVPs.LIP₁, PVX CVPs.FADK₂ and PVX CVPs.BANK₁ purification.

In collaboration with the research group of professor Fernando Ponz Ascaso (Centro de Biotecnología Y Genómica de plantas – Madrid – Spain). LIP₁ and FADK₂ were selected to be expressed with the viral system based on TuMV.

LIP₁ and FADK₂ were cloned in p35Tunos-vec01-NAT1 vector and used for *N. benthamiana* inoculation. The genetic stability of TuMV display peptides of interest were assessed by immunocapture-RT-PCR (IC-RT-PCR) and sequencing.

After the assessment of the TuMV CVPs.LIP₁ and TuMV CVPs.FADK₂ genetic stability, sap derived from symptomatic *N. benthamiana* leaves were used for the infection of *Brassica juncea* plants. This plant results to be more suitable for the expression of TuMV CVPs in comparison to *N. benthamiana* and it allows to reach higher biomass yield. TuMV CVPs.LIP₁ and TuMV CVPs.FADK were purified from *B. juncea* infected plants.

1.2. Cloning of LIP1, FADK2 and BANK1 with the PVX CVPs expression system

The sequence of the novel peptides identified to be putatively involved in seronegative RA (table 1 – Results of RA therapy) were optimised as reported in table 1 in order to fit the parameters for the expression with the PVX CVPs expression system (rif introduzione PVX).

Table 1 optimised sequence for the expression of novel peptides putatively associated with seronegative RA with the PVX CVPs system

Peptide	Sequence	Length (aminoacids)	pI	W (%)	S + T (%)
LIP ₁	ASVLANVAQAFE	12	4.00	0	8.3
Optimized LIP ₁	MASVLANVAQAFEKST	16	5.75	0	18.8
Nucleotidic sequence	ATG GCT TCT GTT CTT GCT AAT GTT GCT CAA GCT TTT GAA AAG TCT ACT				
FADK ₂	AKVLANLAHPPA	12	8.80	0	0
Optimized FADK ₂	MSEAKVLANLAHPPAT	16	6.50	0	12.5
Nucleotidic sequence	ATG TCT GAA GCT AAG GTT CTT GCT AAT CTT GCT CAT CCT CCT GCT ACT				
BANK ₁	DMILANLSIKKK	12	9.70	0	8.3
Optimized BANK ₁	MSDMILANLSIKKKTE	16	8.25	0	18.8
Nucleotidic sequence	ATG TCT GAT ATG ATT CTT GCT AAT CTT TCT ATT AAG AAG AAA ACT GAA				

The methionine (M) at the beginning of the sequence was added in order to introduce the translation start site. Moreover, serine (S) and threonine (T) residues were added because these phosphorylated residues promote virus disassembling and viral RNA replication. Finally, the absence of tryptophan was assessed because the presence of this aminoacid in peptide sequence could critically affect cell-to-cell and phloem movement of the virus.

The peptide sequences reported in table 1 were used for the design of oligonucleotide pairs *NheI*-compatible 5'- and *XmaI*-compatible 3'- end DNA fragments that were ligated into the *NheI-XmaI* digested vector.

The resulting pPVXSma.LIP₁, pPVXSma.FADK₂ and pPVXSma.BANK₁ were transformed in *E. coli* TOP10 strain competent cells by heat-shock, plated on ampicillin containing medium and PCR selected using vector-specific primers annealing respectively at the 5' and at the 3' of the insertion site (pCP for - CP rev). The length of the amplification fragments obtained is 360 bp plus the length of the inserted sequence. Results of this analysis on 4 colonies transformed with pPVXSma.LIP₁, pPVXSma.FADK₂ and pPVXSma.BANK₁ are reported in figure 1.

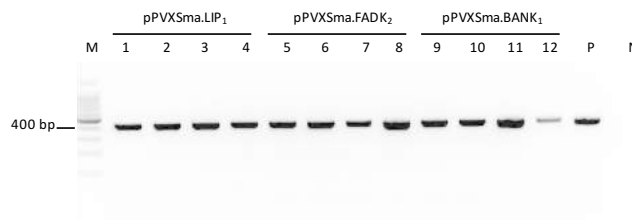


Figure 1 Colonies transformed with pPVXSma vector after ligation with LIP₁, FADK₂ and BANK₁ oligonucleotides. PCR amplification products obtained with two vector-specific primers (pCP for – CP rev) were loaded on a 2% agarose gel. M: molecular marker (BenchTop 100bp DNA ladder - Promega); 1-4: number of *E. coli* TOP10 colonies transformed with pPVXSma.LIP₁ vector; 5-8: number of *E. coli* TOP10 colonies transformed with pPVXSma.FADK₂ vector; 9-12: number of *E. coli* TOP10 colonies transformed with pPVXSma.BANK₁ vector; P: positive control (using as template pPVXSma harboring a 12 aminoacid length peptide); N: negative control.

Figure 1 shows that all colonies analysed presumably contained the vector with peptides sequence insertion; indeed specific amplicons of approximately 380 bp were visible in all the samples loaded on the gel.

Positive bacterial colonies were propagated in selective broth and plasmids were extracted, PCR analysed and sequenced to assess that the insert was correct. One colony for each insert type was selected and propagated in selective medium for the extraction of plasmid by maxi-preparation. Plasmids obtained were used for the small scale phase infection cycle.

1.3. Analysis of the expression and genetic stability of PVX CVPs.LIP₁, PVX CVPs.FADK₂ and PVX CVPs.BANK₁

A small scale infection of 5 plants using vectors pPVXSma.LIP₁, pPVXSma.FADK₂ and pPVXSma.BANK₁ was performed, in order to verify the expression of the modified particles.

13 days post infection (dpi), local and systemic symptomatic leaves were collected and analysed by retrotranscription-PCR (RT-PCR). The cDNAs were then sequenced to verify the stability of the peptide expressed on the viral surface.

After the first cycle of infection, other two cycles were performed inoculating 2 leaves/plants using sap derived from symptomatic leaves of the first infection cycle. 10-13 dpi, the local and systemic symptomatic leaves were collected and analysed as describe before.

- First infection cycle

A small scale infection of 5 plants for PVX CVPs.LIP₁, PVX CVPs.FADK₂ and PVX CVPs.BANK₁ was performed, in order to verify the expression of the modified particles. The symptomatology was constantly monitored; an example of a plant inoculated with pPVXSma.LIP₁ is shown in figure 2.

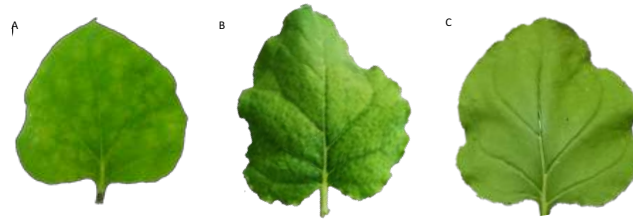


Figure 2 Inoculated (A) and systemic (B) leaves of a *N. benthamiana* plant infected with pPVXSma.LIP₁ 13 days post infection (dpi), in comparison with a wild type leaf (C).

Figure 2 highlights the typical PVX chlorotic symptom on local leaves (A); after the mechanical inoculation on 2 leaves, the PVX CVPs moves from cell to cell in the infected tissue through the plasmodesmata and spreads systemically in the upper leaves through the phloem vein network. As shown in figure 2-B, PVX produces typical mosaic symptoms on systemic leaves.

Either plants infected with PVX CVPs.LIP₁ or PVX CVPs.BANK₁ showed these typical symptoms, whereas plants infected with PVX CVPs.FADK₂ did not developed neither chlorosis nor mosaic symptoms.

RT-PCR analysis was done on systemic symptomatic leaves being the viral concentration higher than in the systemic one.

The RT-PCR reactions were performed using the SuperScript III (Promega) and 2 PCR analysis were performed. The first was carried out with primers specific for the actin constitutive gene (ACT1 and ACT2) in order to assess cDNA synthesis. The latter, was done using PVX specific primers (pCP for – CP rev) to amplify the 3' CP region, in which the peptide sequence was cloned.

The results of the PCR are reported in figure 3.

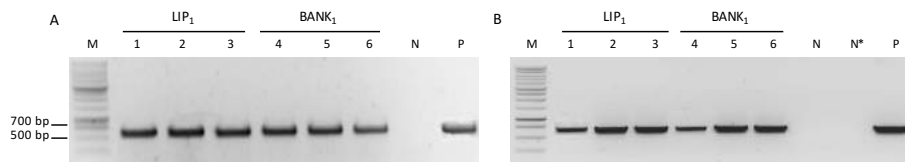


Figure 3 RT-PCR analysis of the symptomatic leaves collected from plant infected with pPVXSma.LIP₁ (1-3) and pPVXSma.BANK₁ (4-6). The PCR analysis done on the cDNAs using primers for a constitutive gene (ACT1 and ACT2) (A) and PVX

specific primers (pCP for – CP rev) (B) are reported. PCR amplification products obtained were loaded on a 2% agarose gel. M: molecular marker (BenchTop 1Kb DNA ladder – Promega); N: negative control of the PCR; N*: negative control (using cDNA derived from a wild type *N. bethamiana* as template); P: positive control (using a pPVXSma vector display a well-know peptide as template).

An amplicon of approximately 700 bp is clearly visible in all cDNA samples (figure 2–B) confirming the specific presence of the viral PVX RNA in the analysed plants.

The fragments resulting from the PCR with PVX specific primers, were sequenced and the resulting sequence was aligned with the expected one; all the plants infected either with pPVXSma.LIP₁ or pPVXSma.BANK₁ expressed PVX CVPs in which the sequence of the peptide is genetically stable.

- *Second and third infection cycle*

Sap from symptomatic leaves of plants infected with pPVXSma.LIP₁ and pPVXSma.BANK₁ was used for the infection of 5 plants/peptide.

At 10-12 dpi symptomatic leaves were collected and analysed by RT-PCR and sequencing in order to assess the genetic stability of the cloned peptide.

The results of these analysis are summarized in table 2.

Table 2 genetic stability of PVX CVPs.LIP₁ and PVX CVPs.BANK₁ in the 2nd and 3th infection cycle. V: particles were expressed in plants and were genetically stable; X: particles were not expressed in plants or were not genetically stable.

	2 nd infection	3 th infection
PVX CVPs.LIP₁	V	X
PVX CVPs.BANK₁	V	V

PVX CVPs.BANK1 results to be stable among 3 infection cycle, whereas PVX CVPs.LIP1 in the 3rd infection cycle showed a mutation in a aminoacid that result in the shift of Leucine (L) in Proline (P).

1.4. Purification of PVX CVPs.LIP₁ and PVX CVPs.BANK₁

PVX CVPs.LIP₁ and PVX CVPs.BANK₁ were purified starting from 50 g of symptomatic local and systemic leaves respectively from the 2nd and 3th infection cycle.

The purification of particles was performed following the protocol described in Uhde *et al.* (2005). Purification fractions were analyzed by SDS-PAGE on a 14% polyacrylamide gel and the gel was silver stained. The results of this analysis are reported in figure 4.

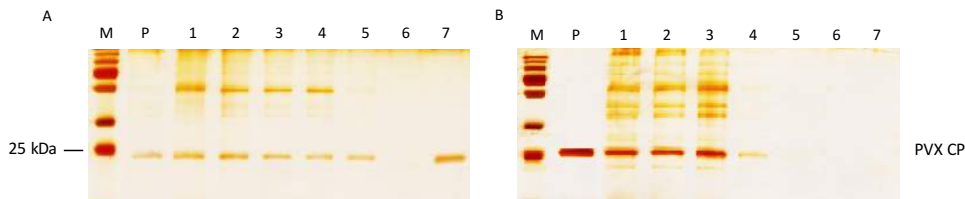


Figure 4 SDS-PAGE and silver staining analysis of the PVX CVPs.LIP₁ (A) and PVX CVPs.BANK₁ (B) purification steps. 1: 1.4 μ l of total protein extract derived from symptomatic leaves; 2-3: 1.4 μ l of sample from progressive purification steps; 4-5: 1.6 μ l of sample from progressive purification steps 6: - ; 7: 0.5 μ l of the final purified PVX CVPs particles; P: 750 ng of unmodified PVX CVPs particles purified in a previous PhD thesis work (Merlin, 2013) from *N. benthamiana* infected with pPVX201 vectors. The samples were loaded on 14% polyacrylamide gel. The PVX CP molecular weight (25 kDa), is indicated. M: molecular marker (PageRuler™ Plus Prestained Protein Ladder, Thermo Scientific).

The silver staining analysis allows to confirm the correct purification of PVX CVPs.LIP₁; indeed, in figure 4-A (lane 7) it is clearly visible a signal corresponding to the PVX CP protein without the presence of any other contaminant proteins. This signal is comparable to that of positive control, without any shift in the molecular weight. Positive control used in this analysis were unmodified PVX CVPs purified from *N. benthamiana* plants infected with pPVX201 vector during another PhD thesis work (Merlin, 2013). The resulting unmodified PVX CVPs are composed by CPs of 25 kDa. As reported in the previous sections, for the expression of PVX CVPs.LIP₁ pPVXSma, which encodes for a 21 aminoacids (aa) N-terminal truncated version of the CP, were used; however, the presence of 16 aminoacid LIP₁ peptide cloned at the N-terminal of the CP sequence in the pPVXSma vector explained the same migration pattern of the unmodified PVX CVPs (figure 4-A, lane P) and the PVX CVPs.LIP₁ (figure 4-A, lane 7) in the SDS-PAGE analysis.

On the contrary, the PVX CVPs.BANK₁ were not successfully purified because were lost during the purification steps. In particular, PVX CVPs.BANK₁ seem to precipitate in the centrifugation step after the adding of silver nitrate, indeed no signal are present in the lane 5 of the figure 4-B in which supernatant derived from this centrifugation step were loaded.

In order to find the suitable protocol for PVX CVPs.BANK₁ purification, several procedures were tested changing centrifugation time and speed, using other published purification protocol (Leiser-Richter *et al.*, 1978) or chromatography methods but none of them allowed to purified the PVX CVPs.BANK₁ (data not shown).

1.4.1. PVX CVPs.LIP₁ purification yield

Purified PVX CVPs.LIP₁ were quantified by reading of the 280 nm absorbance.

Using the Lambert Beer law:

$$A_{280} = \epsilon \times L \times C$$

ϵ : molar extinction coefficient ($\text{m}^2 \text{mol}^{-1}$)
L: path length (cm)
C: concentration (mg/ml)

and considering the CPMV eVLPs molar extinction coefficient ($1.25 \text{ m}^2 \text{mol}^{-1}$) the concentration (mg/ml) of the particle preparations was obtained.

The PVX CVPs.LIP₁ purification yield result to be 0.36 mg/g LFW.

2. TuMV expression system

2.1. Cloning of LIP₁ and FADK₂ with the TuMV CVPs expression system

Considering the results obtained with the expression system based on PVX, it was chosen to focus the attention on the expression of LIP₁ and FADK₂ using the expression system based on TuMV.

This part of the work was carried out in collaboration with the research group of professor Fernando Ponz Ascaso (Centro de Biotecnología Y Genómica de plantas – Madrid – Spain).

The sequence of optimised LIP₁ and FADK₂ reported in table 1 were successfully cloned in the p35Tunos-vec01-Nat1 vector following the procedure reported in Sánchez *et al.* (2013).

Nicotiana benthamiana plants inoculation with p35Tunos-vec01-Nat1.LIP₁ and p35Tunos-vec01-Nat1.FADK₂

N. benthamiana plants were infected with p35Tunos-vec01-Nat1.LIP₁ or p35Tunos-vec01-Nat1.FADK₂ when necrotic symptoms were visible leaves were collected, analyzed by IC-RT-PCR and sequenced in order to assess the genetic stability of the peptides displayed on TuMV surface.

Either *N. benthamiana* infected with p35Tunos-vec01-Nat1.LIP₁ or p35Tunos-vec01-Nat1.FADK₂ result to express genetically stable respectively TuMV CVPs.LIP₁ and TuMV CVPs.FADK₂ (data not shown).

2.2. Expression of TuMV CVPs.LIP₁ and TuMV CVPs.FADK₂ in *Brassica juncea*

Sap derived from *N. benthamiana* plants expressing TuMV CVPs.LIP₁ and TuMV CVPs.FADK₂ were used for inoculate *B. juncea* plants.

B. juncea is the best model plant for TuMV CVPs production because allow to reach higher yield in comparison to the expression in *N. benthamiana* in which necrotic symptoms cause strong interference in the plant fitness. On the contrary, the first inoculation of plant with p35Tunos-vec01-Nat1.LIP₁ or p35Tunos-vec01-Nat1.FADK₂ were conducted in *N. benthamiana* because it is more susceptible.

At 7-10 dpi *B. juncea* inoculated either for the expression of TuMV CVPs. LIP₁ or TuMV CVPs.FADK₂ plants showed typical chlorotic and necrotic TuMV symptoms as shown in figure 5.



Figure 5 Inoculated leaves expressing TuMV CVPs.FADK₂ (A) and TuMV CVPs.LIP₁ (B) of a *B. juncea* plant 10 days post infection (dpi), in comparison with a wild type leaf (C).

A large scales infection of 30 plants for each peptide were carried out in order to obtained sufficient material for TuMV CVPs.FADK₂ and TuMV CVPs.LIP₁ purification.

2.3. TuMV CVPs.LIP₁ and TuMV CVPs.FADK₂ purification

The purifications of TuMV CVPs.LIP₁ and TuMV CVPs.FADK₂ were performed following the procedure reported in Sánchez *et al.* (2013).

The last step of the purification protocols consists in a CsCl gradient that results in a thick white band forming in the tube below the green contaminant protein.

The result of the CsCl gradient performed during the TuMV CVPs.LIP₁ and TuMV CVPs.FADK₂ purification steps is shown in figure 6.

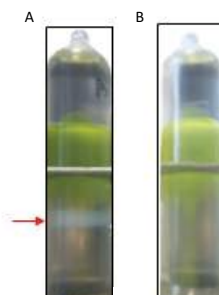
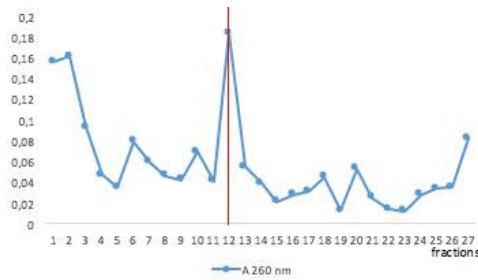


Figure 6 CsCl gradient step of the procedure for the purification of TuMV CVPs.FADK₂ (A) and TuMV CVPs.LIP₁ (B).

The purification was successful only for the TuMV CVPs.FADK₂ indeed the expected white band is visible only in figure 6-A as indicated with the red arrow.

The band corresponding to the purified TuMV CVPs.FADK₂ were picked up, whereas the CsCl gradient in which sample derived from the TuMV CVPs.LIP₁ infection were loaded were fractionated and numerated from 1 to 27 from the bottom to the top. The resulting fraction were analyzed measuring the absorbance at 260 (A_{260}); the results of this analysis is reported in the graph 1.

Graph 1 A_{260} nm analysis of CsCl gradient fractions of the TuMV CVPs.LIP₁ purification experiment



Beside the high value of A_{260} that characterise the first fraction that usually contain high molecular weight contaminant (Rubisco, lipids, ..), graph 1 shows a peak in the A_{260} at the fraction number 12.

This fraction and an aliquot derived from the white band of the TuMV CVPs.FADK₂ purification were loaded on 14 % polyacrylamide gel and silver stained in order to assess the effective presence of TuMV CVPs particles and their purification level.

The result of this analysis is showed in figure 6.

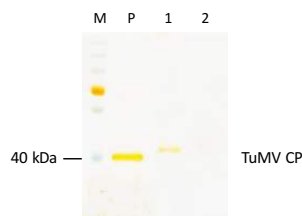


Figure 6 SDS-page and silver staining analysis of the TuMV CVPs.FADK₂ (1) and TuMV CVPs.LIP₁ (2). 10 μ l of aliquots derived from white band of the TuMV CVPs.FADK₂ (1) and fraction number 12 of CsCl gradient of TuMV CVPs.LIP₁ the purification were loaded on 14% polyacrylamide gel. P: 800 ng of unmodified TuMV CVPs as positive control (gently provided by professor Fernando Ponz Ascaso). The TuMV CP molecular weight (33-35 kDa), is indicated. M: molecular marker (PageRuler™ Plus Prestained Protein Ladder, Thermo Scientific).

Figure 6 underlines the presence of a signal (lane 1) corresponding to TuMV CVPs.FADK₂. These particles were successfully purified indeed no other contaminant protein are present. The shift in the molecular weight of the TuMV CVPs.FADK₂ (lane 1) in comparison to the unmodified TuMV CVPs used as positive control (lane 2) indicate the presence of FADK₂ fused to the TuMV CP.

On the other hand, no signal is visible in lane 2 indicating that fraction 12 did not contain TuMV CVPs.LIP₁. The purification of these particle has failed.

CHAPTER 3: OTHER APPLICATIONS

INTRODUCTION

1. eVLPs internalization

Cell-penetrating peptides (CPPs) have attracted attention due to their ability to deliver functionally cargo into cells in non-destructive manner (Langel *et al.*, 2006; Seebach *et al.*, 2004).

CPPs usually are short cationic sequences with amphiphilic nature that are attracted by the anionic cell surface and can eventually penetrate through the hydrophobic lipid bilayer. The exact mechanism is still poorly understood, but it seems to be independent of classical receptor-mediated intake and, in some cases, it might involve endocytosis as the initial step (Fonseca *et al.*, 2009).

A drawback of CPPs is their difficult synthesis and the fact that they are not accessible for recombinant expression.

This peptide can be described as a cluster of arginine and lysine that provides the cationic nature to the peptide.

1.1. Tat peptide

Tat peptide is derived from the small nuclear protein of HIV. This protein is required for optimal HIV viability (Fisher *et al.*, 1986) and transcription (Peterlin *et al.*, 1986). Tat peptide is one of the most common used CPPs, indeed it has been successfully shown to deliver a large variety of cargos, from small particles to proteins, peptides and nucleic acids.

Despite the high number of studies and biological application using this peptide, the precise mechanism of entry still appears controversy and requires further investigations.

2. Antimicrobial Peptides (AMPs)

Pesticides are widely used in agricultural production to reduce crop yield losses and maintain high product quality. However, serious concerns have been raised about health

risks and their impacts on environment. Thus there is a current need for alternative crop protection systems with improved safety propriety.

A class of peptide called antimicrobial peptides (AMPs) is a key component of the innate immune system in almost all living organisms and has attracted attention as potential agents able to help plant species to fight microbial diseases.

AMPs are sequence long less then 50 aminoacids with unique propriety in terms of biocompatibility, moderate biodegradability and low resistance developed on target microorganism (Badosa *et al.*, 2013).

Thanks to these characteristics they can be exploited in several fields: they can substitute or complement antibiotics in animal feed, they can be used as biopreservatives in food, cosmetics, biomaterials and antifouling (Cleveland *et al.*, 2001).

However, AMPs are produced at low concentration in living organisms and have low stability.

2.1. BP100 peptide

BP100 peptide is a AMPs designed through combinatorial chemistry approaches. BP100 is derived from a 125-member library of chimeric peptides, hybrids of two natural AMPs (cecropin and A-melittin).

BP100 has a strong cationic charge and amphipathic arrangements that allow it to interact and destroy cell membranes of target microorganisms.

Several studies have demonstrated that BP100 has significant *in vitro* activity against *X. axonopodis* pv. *Vescicatoria*, *P. syringae* pv *syringae* and *E. amylovora* (MIC of 2.5-7.5 μ M) and low hemolysis showing a minimal cytotoxicity (22% at 150 μ M) (Badosa *et al.*, 2007).

Finally, its efficacy is comparable to standard antibiotics and it is highly biocompatible, as assessed by acute oral toxicity tests in mice (Montesinos and Bardaji, 2008).

Besides the therapeutic and diagnostic applications, eVLPs displaying functional peptides can be useful reagents and tools in the industrial and biotechnological fields.

In particular, in this part of the work CPMV eVLPs have been used for the expression of CPP Tat peptide in order to develop eVLPs able to vehicle peptides inside the cell either for therapeutic purpose or for studying specific interaction.

Finally, CPMV eVLPs system has been exploited for the expression of BP100 peptide in order to produce eco-friendly pesticides.

RESULTS AND DISCUSSION

DEVELOPMENT OF A SYSTEM FOR CELLULAR PEPTIDE INTERNALIZATION

1. Experimental design

CPMV eVLPs expression system could be exploited as a biotechnological tool for peptide internalisation into the cells. This could be particularly useful in several fields, from targeting therapeutics or imaging agents to functional studies by targeting selected peptide inside specific cell types.

In particular, the aim of this part of the work was the study of an interaction between a ligand and a receptor located inside the endothelial cell of the central nervous system. The strategy was to express the ligand on the surface on CPMV eVLPs, so the capability of these particle to penetrate the neuroblastoma cells had to be assess.

The penetration capability of purified unmodified CPMV eVLPs was tested *in vitro* culture. *In vitro* culture of neuroblastoma cells were treated with unmodified CPMV eVLPs. At different times, unmodified CPMV eVLPs were removed and the neuroblastoma cells treated were lysate using a detergent. The cellular lysate was then analysed by SDS-PAGE and western blot using a polyclonal antibody specific for CPMV particles for the detection of specific signals.

At the same time, the HIV-Tat derived peptide has been selected to be cloned into the pEAQ-*HT*-VP60 vector in correspondence of the β B- β C loop of the CPMV S CP which is the main exposed one.

The pEAQ-*HT*-VP60 was engineered and two restriction sites were created at the ends of the sequence encoding for the second main exposed loop of the same CP (β C'- β C'' loop) in order to obtain a new pEAQ-*HT*-VP60 whit an insertion site for peptide cloning into β C'- β C'' loop.

Tat sequence was modified in order to optimize the peptide pI to be expressed with the CPMV eVLPs expression system.

The modified sequence was cloned into newpEAQ-*HT*-VP60 used for agroinfiltrated *N. bethamiana* plants.

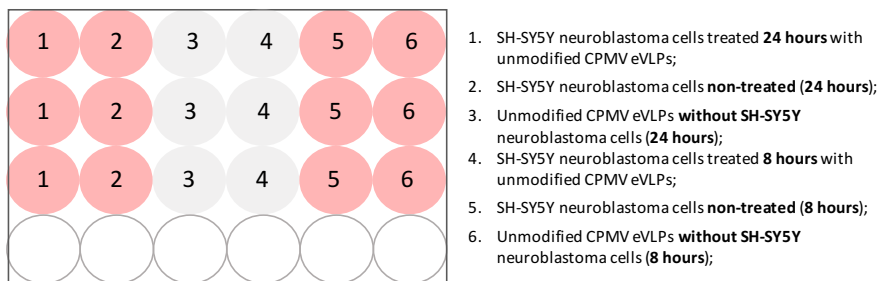
The expression of CPMV eVLPs displaying Tat peptide (CPMV eVLPs.Tat) was assessed and the purification strategy was set up in order to test CPMV eVLPs.Tat penetration in neuroblastoma cells.

2. Unmodified CPMV eVLPs internalisation experiments in neuroblastoma SH-SY5Y cells

30-40% confluent neuroblastoma cells SH-SY5Y were transferred in plate wells and incubated at 37 °C until 70% confluency was reached.

The treatments were done as reported in the following scheme in which every circle represent a wells with 70% confluent SH-SY5Y cells.

Scheme 1 SH-SY5Y neuroblastoma cells treatment with unmodified CPMV eVLPs



Some preliminary experiments showed that the sodium phosphate buffer (0.1 M + 0.15M NaCl), in which unmodified CPMV eVLPs were resuspended, could interfere with neuroblastoma cells stability; thus the unmodified CPMV eVLPs were concentrated and mixed with the DMEM culture medium without FBS (fetal bovine serum) to reach the particles concentration of 0.05 mg/ml in order to minimise the presence of that buffer. 350 µl of the unmodified CPMV eVLPs prepared as described, were added to wells with 70% confluent SH-SY5Y neuroblastoma cells and incubated at 37 °C for different time points (8 and 24 hours).

As negative control, 4 wells containing 70% confluent SH-SY5Y neuroblastoma cells were treated with DMEM culture medium without FBS (fetal bovine serum) without the eVLPs and 4 empty wells (without neuroblastoma cells) were treated with DMEM culture medium

without FBS (fetal bovine serum) containing unmodified CPMV eVLPs at a final concentration of 0.05 mg/ml.

After the incubation, the culture medium was picked up and the neuroblastoma cells attached on the bottom of the wells were washed in order to remove unmodified residual CPMV eVLPs and treated with SDS 1% to obtain a cellular lysate.

Neuroblastoma cells incubated 24 hours with unmodified CPMV eVLPs, at the end of the experiment resulted to be in solution and not attached on the bottom of the well. The corresponding negative control, in which neuroblastoma cells were treated 24 hours with culture medium without unmodified CPMV eVLPs did not show any stress signal.

This observation indicated that the presence of unmodified CPMV eVLPs end/or the residual of the sodium phosphate buffer (0.1 M + 0.15M NaCl) for this timeframe interfere with cell stability. Anyway, the cells were transferred into a tube pelleted and resuspended with SDS 1% as well.

The resulting lysate was analysed by SDS-PAGE and western blot using a polyclonal antibody specific to CPMV particles for the detection of specific signals; results are reported in the figure 1.

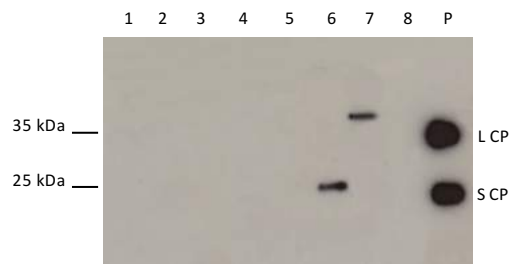


Figure 1 SDS-PAGE and western blot analysis of the cellular lysate obtained from the neuroblastoma cells internalization experiment done with the unmodified CPMV eVLPs. 1: negative control, cellular lysate obtained from non-treated SH-SY5Y neuroblastoma cells (24 hours); 2, 4, 5: cellular lysate obtained from SH-SY5Y neuroblastoma cell treated 24 hours with unmodified CPMV eVLPs; 3: negative control, unmodified CPMV eVLPs without SH-SY5Y neuroblastoma (24 hours); 6: negative control, unmodified CPMV eVLPs without SH-SY5Y neuroblastoma (8 hours); 7: negative control, cellular lysate obtained from non-treated SH-SY5Y neuroblastoma cells (8 hours); 8: cellular lysate obtained from SH-SY5Y neuroblastoma cell treated 8 hours with unmodified CPMV eVLPs; P: 875 ng of purified unmodified CPMV eVLPs as positive control. 20 μ l of each sample were loaded on 12% polyacrylamide gels then blot was probed with a polyclonal antibody (G49) specific to CPMV particles used at a concentration of 1:2000. The expected position of CPMV L and S CPs is indicated on the side of the figures.

Figure 1 showed no specific signals in the lane corresponding to the cellular lysates indicating that unmodified CPMV eVLPs are not able to penetrate neuroblastoma cells.

3. Design of new insertion site in the pEAQ-HT-VP60 vector and development of newpEAQ-HT-VP60/Tat

It is well known (Porta *et al.*, 2003) that for the exposition in the BC'-BC'' loop peptide sequence have to be inserted between the Val42 and Gly43 of the pEAQ-HT-VP60. Thus the sequence of this vector was studied in order to find possible sequences in the region above mentioned that, through silent mutation or by adding an aminoacid could be transformed into a unique restriction site.

In figure 2 the selected sequence and the mutations done are reported.

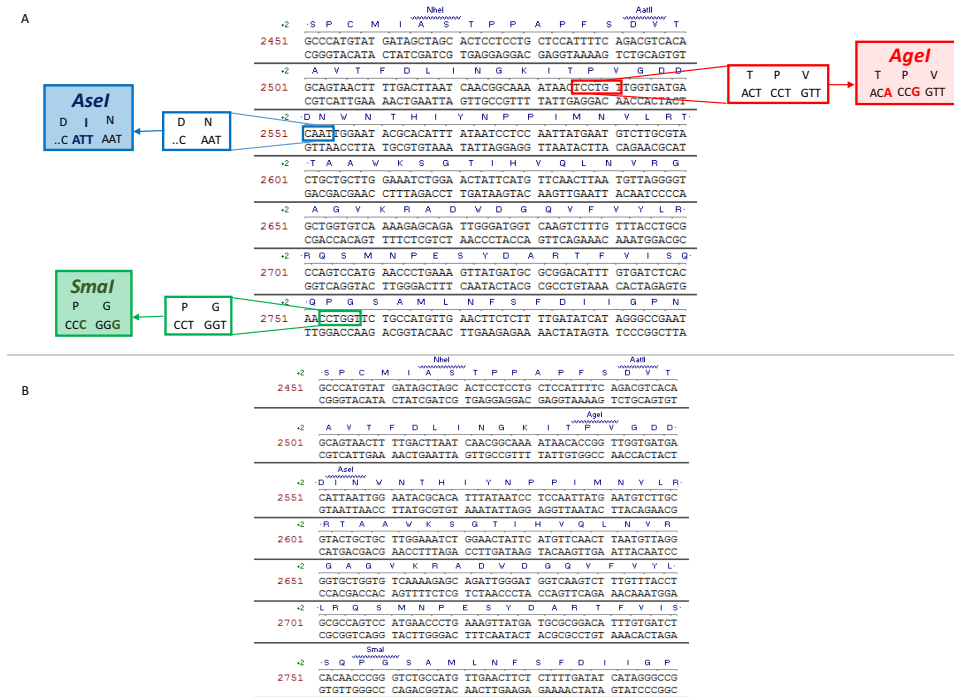


Figure 2 pEAQ-HT-VP60 2451-2801 bp region. A: mutation done to obtained AgeI (red boxes), AseI (blue boxes) and SmaI (green boxes) restriction site. B: newpEAQ-HT-VP60 final sequence.

As explained in figure 2-A, new AgeI and SmaI unique restriction sites have been created by introducing two silent mutations and the AseI restriction site was obtained by the

addition of one aminoacid. These three new restriction sites were created to allow the insertion of the peptide of interest in the $\beta C'$ - $\beta C''$ loop located between the Val42 and Gly43. In particular, in this new vector sequence, the insertion can be obtained either through classic cloning procedure involving two oligonucleotides that are ligated between *AgeI* and *AseI* restriction sites or by designing a gene string to be inserted between *AgeI* and *SmaI*.

In panel B-figure 2 the final newpEAQ-*HT*-VP60 vector sequence is reported.

In order to express the Tat peptide with the CPMV eVLPs system its sequence has been optimized (table 1) to decrease its pI, too high for the expression with this platform.

Table 1 Optimization of Tat peptides for its expression with CPMV eVLPs system

Aminoacids sequence	CGRKKRRQRRRPPQ
Nucleotidic sequence	TGT GGT AGA AAG AAG AGA CGA CAA AGA CGT AGA CCT CCA CAA
Peptide length (aminoacids)	pI
14	12.30
Optimized aminoacids sequence	DEDESCGRKKRRQRRRPPQTDEDD
Optimized nucleotidic sequence	GAT GAA GAT TCT TGT GGT AGA AAG AAG AGA CGA CAA AGA CGT AGA CCT CCA CAA ACT GAT GAA GAT GAT
Peptide length (aminoacids)	pI
23	8.20

The modified Tat sequence reported in table 1 was inserted between the Ala22 and Pro23 of the newpEAQ-*HT*-VP60, as reported in figure 3, in order to obtain a vector for the expression of CPMV eVLPs in which Tat peptide is exposed on the viral surface in the small CP into the βB - βC loop.

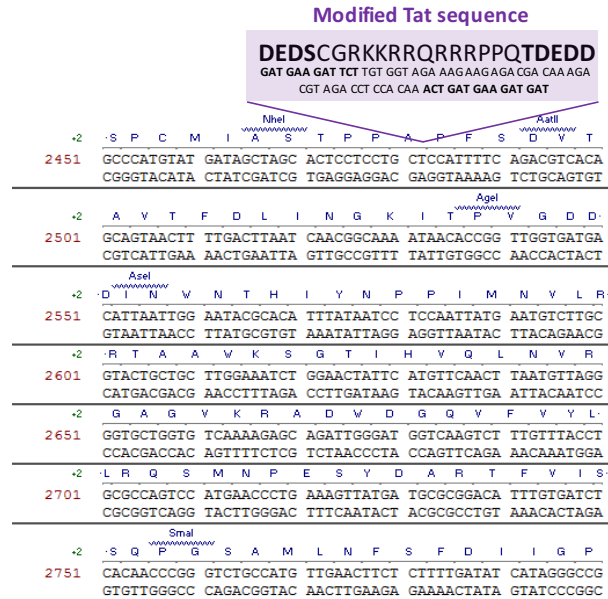


Figure 3 newpEAQ-*HT*-VP60/Tat 2451-2801 bp region . In the purple box is reported the Tat sequence inserted between the Ala22 and Pro 23 into the sequence corresponding to the βB - βC loop of the CPMV small CP.

In view of the above, a gene string started from the *NheI* until the *StuI* (restriction site not reported in figure 3 but present in pEAQ-*HT*-VP60 original vector approximately 600 bp downstream the *NheI* restriction site) was synthesized. Original pEAQ-*HT*-VP60 vector was restricted using *NheI* and *StuI* restriction enzymes and the new gene string harbouring all the modifications described was ligated resulting in the new vector called newpEAQ-*HT*-VP60/Tat.

4. CPMV eVLPs. Tat expression in *N. benthamiana* plants

A small scale first trial was carried out in order to assess the expression in planta of CPMV eVLPs. Tat.

4 leaves of *N. benthamiana* were infiltrated with a mixed suspension of *A. tumefaciens* carrying pEAQ-*HT*-24K or newpEAQ-*HT*-VP60/Tat plasmids.

The agroinfiltrated leaves sampled at 6 days post infiltration (dpi) did not show viral symptoms as expected.

TSP were extracted from infiltrated leaves and analysed by SDS-PAGE and western blot, using a polyclonal antibody specific to CPMV particles for the detection of specific signals and the results confirmed the effective expression of CPMV eVLPs.Tat in plants.

Afterwards a large scale infection of *N. benthamiana* plants was carried out, to obtain infected tissue for particles purification. 20-30 plants (4 leaves per plant) were agroinfected. Agroinfiltrated leaves (~25-30 g) were sampled 6 dpi and used for CPMV eVLPs.Tat purification experiments.

5. CPMV eVLPs.Tat purification

5.1. Chromatography based protocol

Considering that CPMV eVLPs.Tat was meant to be used in sterile culture of neuroblastoma cells the purification procedure is very important and the first protocol chosen was the purification based on size exclusion chromatography.

TSP were extracted from 25 g of agroinfiltrated leaves and clarified through filtration and centrifugation in order to remove cellular debris. An anion-exchange chromatography using DEAE Sephadex™ A-50 resin was performed in order to remove a large part of plant contaminant proteins present in the extract before their injection into HiPrep™ 16/60 Sephacryl™ S-500 HR (Akta Prime plus).

Considering the positive charge of the Tat peptide an elution step with buffer containing 1 M NaCl was performed in order to understand if particles interact with resin.

The resin/sample ratio was optimized at ¼.

Before injecting the sample into the HiPrep™ 16/60 Sephacryl™ S-500 HR (Akta Prime plus) the aliquots collected in all purification steps were analysed by SDS-page and Coomassie staining (figure 4).

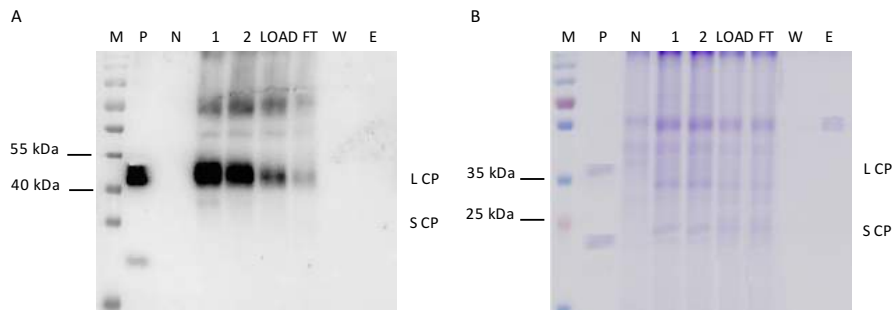


Figure 4 SDS-page, western blot (A) and coomassie staining of the purification step based on anion-exchange chromatography using DEAE SephadexTM A-50. 1: 10 μ l of TSP extracted from leaves infiltrated with *A. tumefaciens* harbouring the newpEAQ-*HT*-VP60/Tat; 2: 10 μ l of clarified extract; LOAD: 10 μ l of sample that has been loaded on the DEAE-chromatography; FT: 15 μ l of the DEAE-chromatography flow trough; W: 15 μ l of the DEAE-chromatography wash step; E: 15 μ l of the DEAE-chromatography elution step done with sodium phosphate buffer 0.1M NaCl 1 M; N: 10 μ l of TSP extracted from wild type *N. benthamiana* leaves; P: purified unmodified CPMV eVLPs as positive control (A: 875 ng, B: 7.5 μ g). M: molecular marker (PageRulerTM Plus Prestained Protein Ladder, Thermo Scientific). Samples were loaded on 12% polyacrylamide gels then blot was probed with a polyclonal antibody (G49) specific to CPMV particles used at a concentration of 1:2000. The expected position of CPMV L and S CPs is indicated on the side of the figures.

Figure 4 shows that most of the CPMV eVLPs.Tat precipitate in the centrifuge before the DEAE chromatography step, indeed the signal corresponding to the sample that was loaded on DEAE column (lane LOAD) has an intensity visibly weaker than the TSP sample. Moreover, the passage into DEAE resin seems to increase the CPMV eVLPs.Tat loss as underlined by lane FT of figure 4 in which the signal corresponding to the particles is faint. Considering these results and in order to avoid CPMV eVLPs.Tat loss, other two experiments using different pH were conducted. In particular, either sodium phosphate 0.1 M pH 6 or pH 8 were used either for the extraction of TSP or for anion-exchange chromatography steps but none of these pH allowed to improve the stability of the CPMV eVLPs.Tat. Using the pH 6 extraction buffer the particles precipitation was even more pronounced, while using pH 8 extraction buffer the behaviour of the CPMV eVLPs.Tat was exactly the same of the one obtained with pH 7 (data not shown).

On the basis of the obtained results, other purification experiments using hydrophobic interactions chromatography (HIC) were done. Different HIC resins based on different adsorbent medium (phenyl-, butyl- and octyl-sepharose) were tested.

The first experiment done at atmospheric pressure gave promising results; indeed, the western blot analysis done on aliquots corresponding to every step of the purification procedure showed that CPMV eVLPs.Tat were collected in the elution step of every HIC column tested. On the other hand, the coomassie staining analysis demonstrated that the elution fraction in which CPMV eVLPs.Tat were present resulted to be contaminated by other high molecular weigh proteins. In order to avoid these contaminations, more elution steps were tested but the yield of purified particles was too low and the loss in comparison to the initial protein extract was too high to consider this protocol suitable for CPMV eVLPs.Tat purification (data not shown).

5.2. Double sucrose cushion and Nycodenz gradient

Given the above mentioned results, the purification protocol described in Peyret *et al.* (2015) was tested, which is based on either a sucrose cushion or nycodenz gradient and, as a consequence, it could be suited for the purification of those particles that tend to aggregates, as is the case of CPMV eVLPs.Tat.

A purification test was conducted starting from 30 g of agroinfiltreted leaves, the TSP were extracted and clarified through filtration and centrifugation in order to remove cellular debris. The clarified extract was loaded on double sucrose cushion prepared with sucrose 25% (2/13) and 70% (0.25/13).

After centrifugation, a thick green band was visible at the interface between the 25% and 70% sucrose layers. CPMV eVLPs typically co-sediment slightly below the green band with a partial overlapping with it.

On the bottom of the tube a white pellet was formed, it was resuspended and collected.

Thus the double sucrose cushion was fractionated collecting the following aliquots:

- A. The green band of the sucrose cushion, corresponding to the 70% sucrose layer;
- B. the surnatant of the sucrose cushion;
- C. the resuspended pellet.

In order to remove the sucrose, the aliquot A (7 ml) was dialyzed over night against 20 mM ammonium bicarbonate pH 8.5. Due to the high osmotic pressure of the sucrose the volume of the CPMV eVLPs.Tat dialysate was raised to 20 ml.

The dialysate was then concentrate to 5 ml using a 100 kDa cut off Centricon® tube.

The results of the western blot and coomassie staining analysis of an aliquot of all the steps described before are reported in figure 5.

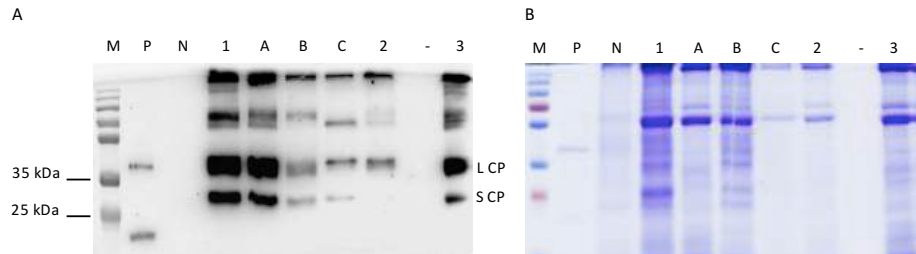


Figure 5 SDS-page, western blot (A) and coomassie staining of the sucrose cushion step of the CPMV eVLPs.Tat purification. N: TSP extracted from wild type *N. bethamiana*; 1: TSP extracted from leaves infiltrated with *A. tumefaciens* harbouring the newpEAQ-HT-VP60/Tat; A: green band of the sucrose cushion corresponding to the 70% sucrose layer; B: surnatant of sucrose cushion; C: resuspended pellet obtained from the centrifugation of the sucrose cushion; 2: CPMV eVLPs.Tat dialysate; 3: concentrated CPMV eVLPs.Tat. 10 μ l (A) and 15 μ l (B) of each sample were loaded on 12% polyacrylamide gels then blot was probed with a polyclonal antibody (G49) specific to CPMV particles used at a concentration of 1:2000 ; P: purified unmodified CPMV eVLPs as positive control (A: 875 ng, B: 7.5 μ g). M: molecular marker (PageRuler™ Plus Prestained Protein Ladder, Thermo Scientific). The expected position of CPMV L and S CPs is indicated on the side of the figures.

Figure 5-A showed that the CPMV eVLPs.Tat are correctly present in the concentrated dialysate (lane 3); however, as underlined by the coomassie staining this sample resulted to be contaminated by other proteins so further purification steps are required.

Further purification can be achieved with a Nycodenz gradient. Solutions of Nycodenz at 20, 30, 40, 50, and 60% were prepared and the gradient was set up. The concentrated dialysate CPMV eVLPs.Tat was loaded on the Nycodenz gradient and an ultracentrifugation at 40,000 rpm for 3 h at 4 °C was performed. After ultracentrifugation, a green band and a brown band were visible.

Peyret *et al.* (2015) reported that after ultracentrifugation, the green contaminants usually sedimented towards the top of the gradient, while CPMV eVLPs typically sediment usually below the green impurities sometime in a more diffuse brown band.

Unexpectedly, the position of the green and brown band resulted to be inverted in comparison with that reported in Peyret *et al.* (2015).

The Nycodenz gradient was fractionated and 500 μ l aliquot were collected following the scheme reported (figure 6-A). The collected fractions were then analysed by western blot and coomassie staining analysis as reported in figure 6-B and C.

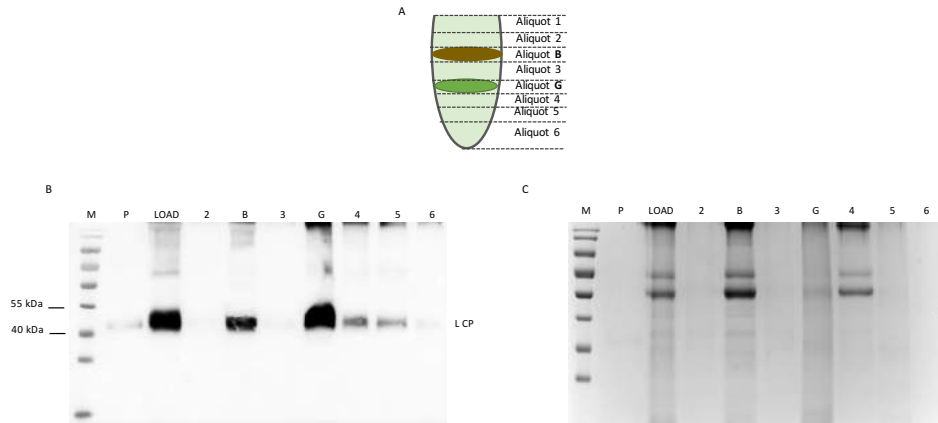


Figure 6 Nycodenz gradient of the CPMV eVLPs.Tat. Schematic representation of the Nycodenz gradient after the ultracentrifugation (A) with the name and the number of collected aliquots. SDS-PAGE and subsequently western blot analysis (B) and coomassie staining (C) of the aliquots collected aliquots. Aliquots were loaded on 12% polyacrylamide gels then blot was probed with a polyclonal antibody (G49) specific to CPMV particles used at a concentration of 1:2000. 2-B-3-G-4-5-6: aliquots collected from the Nycodenz gradient as reported in panel A, 15 μ l of each aliquots were loaded on gel; LOAD: sample loaded on Nycodenz gradient (12 μ l); P: purified unmodified CPMV eVLPs as positive control (A: 875 ng, B: 7.5 μ g). M: molecular marker (PageRuler™ Plus Prestained Protein Ladder, Thermo Scientific). The expected position of CPMV L CP is indicated on the side of the figure in panel A.

CPMV eVLPs.Tat was present either in the green band (lane G) and in the brown one (lane B), indeed a strong signal corresponding to the CPMV L CP are visible in both samples. The possible interaction between CPMV eVLPs and contaminant protein due to the presence of strong charged Tat peptide on particles surface could explain the lower position of the green band in comparison to the brown one. Unexpectedly figure 11-B underlines a strong specific signal in lane G corresponding to the green band that seems to contain the most of CPMV eVLPs.Tat.

Moreover, the coomassie staining analysis (figure 6-C) showed that CPMV eVLPs.Tat in the green band showed an higher degree of purity than the ones in the brow band, indeed in lane B two strong signals are visible at higher molecular weight that are not present in the lane G. On the other hand, some faint bands are visible even in lane G indicating the presence of some contaminant proteins.

Considering that the use of CPMV eVLPs.Tat in vitro test with SH-SY5Y neuroblastoma cells require a higher purification level, the green band of the Nycodenz gradient were 0.2 m filtrated in order to remove the contaminant protein. The filtrated sample was analysed by western blot but no signal corresponding to CPMV eVLPs.Tat was visible indicating the particles loss in the filtration step. These results could be explained with the presence of the Tat peptide on CPMV eVLPs surface that could promote particle aggregates formation.

DEVELOPMENT OF AN ECO-PESTICIDE

1. Experimental design

Pesticides are widely used in agriculture to maintain high product quality and reduce crop yield losses caused by plant diseases. However, several concerns have been raised about the pesticides impact on environment and human health. In the search for alternative solution, antimicrobial peptide (AMPs) have proven to be optimal candidates.

BP100 AMPs is a cecropin A-mellitin hybridis derived from a undecapeptide peptide library obtained through combinatory chemistry approaches (Badosa *et al.*, 2009). This peptide results to have bactericidal activity and antifungal properties, being at the same time high biocompatible (Badosa *et al.*, 2007; Montesinos *et al.*, 2008).

Here we evaluate the use of the CPMV eVLPs for the expression of BP100; indeed, the final application of these particles requires a no-replicative system in order to avoid the viral infection of plants that will be treated with particles displaying the anti-microbial peptide.

BP100 peptide is characterised by a strong positive charge at neutral pH that facilitate the electrostatic attraction to phospholipid membranes of target microorganisms, thus making its pI out of the desirable range for the expression with the CPMV eVLPs expression system. As a consequence, the BP100 sequence was optimized in order to decrease its pI. Vectors used for this part of the work were kindly provided by professor George P. Lomonosoff from the Department of Biological Chemistry at the John Innes Centre, (Norwich, UK)

After cloning the BP100 peptide sequence in the expression vector pEAQ-*HT*-VP60, a small scale agroinfection of 1-2 *N. benthamiana* plant (4 leaves/plants) was carried on to check the expression of CPMV eVLPs displaying BP100 peptide (CPMV eVLPs.BP100).

2. Cloning of BP100 peptide for the expression of CPMV eVLPs.BP100

The BP100 peptide aminoacidic sequence was optimized (table 2) by the addition of one acid aminoacid at the peptide N-terminus and two at the C-terminus in order to decrease the peptide pI.

Table 2 Optimization of BP100 peptides for its expression with CPMV eVLPs system

Aminoacids sequence	KKLFFKKILKYL
Nucleotidic sequence	AAG AAA CTT TTT AAG AAA ATT CTT AAG TAT CTT
Peptide length (aminoacids)	pI
11	10.30
Optimized aminoacids sequence	DKKLFKKILKYLED
Optimized nucleotidic sequence	GAT AAG AAA CTT TTT AAG AAA ATT CTT AAG TAT CTT GAA GAT
Peptide length (aminoacids)	pI
14	9.31

The pI of the modified BP100 peptide results to be still higher than the optimal one, but considering the high presence of positive charge aminoacids (Lys) in the sequence, adding more acid aminoacids at the N- and/or C- terminus of the sequence could interfere with the assemble and the stability of the CPMV eVLPs particles and we proceed with the described modification.

For the expression with the CPMV eVLPs system the nucleotidic optimized sequence encoding for BP100 peptide was cloned in the pEAQ-*HT*-VP60 vector within the sequence of the S CP located into the VP60 precursor sequence.

Oligonucleotide pairs were designed to obtain *NheI*-compatible 5'- and *AatII*-compatible 3'-end DNA fragments that were ligated into the *NheI*-*AatII*-digested vector.

After ligation of the DNA fragments encoding BP100 peptide into pEAQ-*HT*-VP60 vector, the resulting pEAQ-*HT*-VP60.BP100 plasmid was transformed in *E. coli* DH5a strain competent cells by heat-shock. *E. coli* cells were plated on kanamycin containing medium (50 µg/ml) and PCR selected using vector-specific primers CPMV Seq-for and CPMV Seq rev, annealing respectively upstream and downstream of the insertion site. The length of the amplification fragments obtained is 200 bp plus the length of the BP100 inserted sequence, making in total of 242 bp.

Results of the PCR analysis on the colonies growth on selection medium after transformation with pEAQ-*HT*-VP60.BP100 vector are reported in figure 7.

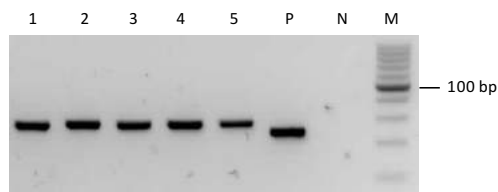


Figure 7 *E. coli* colonies transformed with pEAQ-*HT*-VP60 vector after ligation with BP100 oligonucleotide. PCR amplification products obtained with two vector-specific primers (CPMV Seq for – CPMV Seq rev) were loaded on a 2% agarose gel. M: molecular marker (BenchTop 100bp DNA ladder - Promega); 1-5: number of *E. coli* DH5a colonies tested; P: positive control (using pEAQ-*HT*-VP60 vector as template); N: negative control.

The PCR results showed that all the colonies tested were transformed; indeed, the resulting bands correspond to an amplicon of approximately 242 bp as expected.

It is clearly visible the shift between the positive control and the amplicons derived from the colonies transformed with the pEAQ-*HT*-VP60.BP100 confirming the presence of the BP100 insert that increased the length of the fragment.

Colonies were propagated in selective broth and plasmids were extracted, PCR analysed and sequenced to assess that the sequence of the insert was correct.

Selected pEAQ-*HT*-VP60.BP100 resulting suitable from the PCR and sequencing analysis was transformed in competent cells of *A. tumefaciens* LBA4404 strain by electroporation and plated on kanamycin (50 µg/ml), rifampicin (50 µg/ml) and streptomycin (100 µg/ml) containing medium. After three days 28 °C incubation, colonies were PCR selected using vector-specific primers CPMV Seq-for and CPMV Seq rev to assess their effective transformation. Positive *A. tumefaciens* LBA4404 colonies were propagated in selective broth and used for the next expression step.

3. Analysis of the expression in plant of CPMV eVLPs displaying BP100

A small scale first trial was carried out in order to assess the expression in planta of CPMV eVLPs.BP100.

4 leaves of *N. benthamiana* were infiltrated with a mixed suspension of *A. tumefaciens* carrying pEAQ-*HT*-24K or pEAQ-*HT*-VP60.BP100 plasmids.

The agroinfiltrated leaves sampled at 6 dpi did not showed viral symptoms, obtaining the same result reported in figure 2 of the chapter 1 (page 65).

TSP were extract from infiltrated leaves and analysed by SDS-page and western blot, using a polyclonal antibody specific to CPMV particles for the detection of specific signals.

Results of this analysis are reported in figure 8.

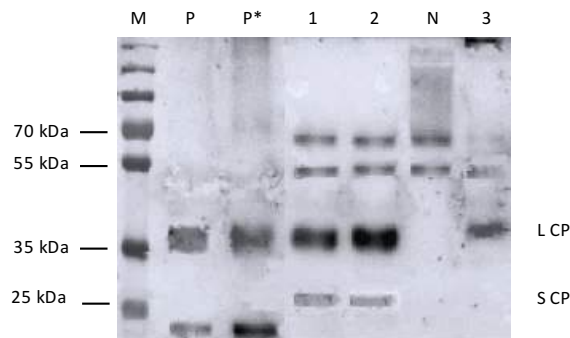


Figure 8 Western blot analysis of the TSP extracted from leaves agroinfiltrated for the expression on CPMV eVLPs.BP100. Samples were loaded on 12% polyacrylamide gels then blot was probed with a polyclonal antibody (G49) specific to CPMV particles used at a concentration of 1:2000. 1-2: 12 and 15 μ l of TSP extracted from pEAQ-*HT*-VP60.BP100 infiltrated leaves; 3: pellet obtained from the centrifugation in order to obtain the TSP, pellet was resuspended in running buffer and loaded on gel (12 μ l) P:875 ng of purified unmodified CPMV eVLPs as positive control; P*: TSP extracted from pEAQ-*HT*-VP60 infiltrated leaves; M: molecular marker (PageRuler™ Plus Prestained Protein Ladder, Thermo Scientific). The expected position of CPMV L and S CPs are indicated on the side of the figure.

The results show in figure 8 confirmed the expression of CPMV eVLPs.BP100 in plant.

Indeed, a strong signal corresponding to 35 kDa and two signals corresponding to 25-27 kDa are clearly visible in lanes 1-2 corresponding to the protein extract of the leaves infiltrated for the expression of CPMV eVLPs.BP100. Other two signals are visible at molecular weight of approximately 55 and 70 kDa, but being present also in the negative control (lane N: protein extract obtained from *N. benthamiana* plant inoculated with

infiltration buffer MMA) they could be considered aspecific signals. Finally, the tendency of this particles to aggregate is underlined by the presence of CPMV eVLPs.BP100 (lane 3) that precipitated in the pellet obtained after the following centrifugation step.

Considering the results, a large scale infection of *N. benthamiana* plants was carried out, to obtain infected tissue for particle purification.

4. Purification of CPMV eVLPs.BP100

4.1. PEG 6000 precipitation based protocol

A first small scale purification starting from 10 g of agroinfiltrated *N. benthamiana* plants was carried out in order to verify if the standard purification protocol based on the precipitation of CPMV eVLPs with Poly(ethylene)glycol (PEG) 6000 was suitable for the CPMV eVLPs.BP100. TSP were extracted and clarified through filtration and centrifugation in order to remove cellular debris.

Polyethylene glycol 6000 (PEG 6000) to a final concentration of 4% and NaCl to 0.2 M were added to the supernatant; the sample was then stirred o/n at 4 °C to precipitate the CPMV eVLPs.BP100 and then spinned to pellet the PEG precipitate. Other centrifugation steps were performed in order to further purified the precipitated particles.

At every purification steps an aliquot of the sample was collected. At the end of the experiments all the aliquots collected were analysed by SDS-PAGE and western blot using a polyclonal antibody specific to CPMV particles for the detection of specific signals.

At the same time, the purification protocol was carried out for the purification of unmodified CPMV eVLPs from *N. benthamiana* plant infiltrated with a mix containing *A. tumefaciens* carried pEAQ-HT-VP60 or pEAQ-HT-24K.

The results of this analysis are reported in the figure 9.

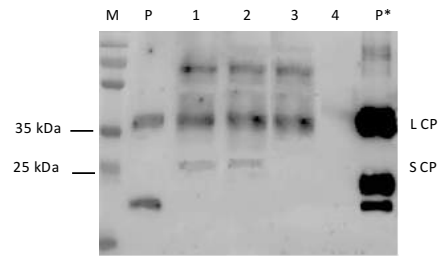


Figure 9 Western blot analysis of the CPMV eVLPs.BP100 standard purification steps. Samples were loaded on 12% polyacrylamide gels then blot was probed with a polyclonal antibody (G49) specific to CPMV particles used at a concentration of 1:2000. 1: 20 μ l of TSP extracted from pEAQ-*HT*-VP60.BP100 infiltrated leaves; 2: 20 μ l of the supernatant of the first centrifugation done for a extract clarification; 3: 20 μ l of sample with PEG6000 and NaCl before the centrifugation; 4: 6 μ l of the pellet resuspended in $\frac{1}{2}$ of the initial volume after the centrifugation of the sample 3; P: 875 ng of purified unmodified CPMV eVLPs as positive control; P*: 20 μ l of TSP extracted from pEAQ-*HT*-VP60 infiltrated leaves as positive control; M: molecular marker (PageRuler™ Plus Prestained Protein Ladder, Thermo Scientific). The expected position of CPMV L and S CPs are indicated on the side of the figure.

The standard protocol based on the precipitation with PEG 6000 is not suitable for the purification of CPMV eVLPs.BP100. Indeed, in figure 9 it is possible to follow the presence of the particles until the step corresponding to the sample in which PEG 6000 and NaCl were added over night (lane 3) whereas, in the following samples corresponding to the pellet precipitated after centrifugation, CPMV eVLPs.BP100 are not present. The use of PEG 6000 is not sufficient to precipitate the CPMV eVLPs.BP100 that remains in solution.

Considering the results further purification experiments were carried out as describe in the following section.

4.2. CPMV eVLPs.BP100 precipitation experiments

In order to overcome the problem arose with the standard protocol, the strategies planned in order to precipitation the CPMV eVLPs.BP100 are summarised below:

- A. Increase in the concentration of PEG 6000;
- B. Increase in the centrifugation speed after the over night step with PEG;
- C. PEG and ionic strength variation: particles precipitation experiments with PEG with differently either molecular weight or ionic strength;
- D. Increase in the centrifugation time after the over night with PEG.

Starting from A and B strategies, they have been applied to the surnatant of the centrifugation done after the over night step at 4°C with PEG 6000 that, as reported in the previous section (Standard protocol: PEG 6000 precipitation), contains the CPMV eVLPs.BP100 that did not precipitate. This sample was divided into 2 aliquots in order to pursue the strategies A and B. In one of the two aliquots 4% of PEG 6000 was added in order to reach twice the concentration previously used and after the over night step at 4 °C the sample was spinned at 13 000 g for 20 minutes as reported in the standard protocol. The other aliquot was spinned for 20 minutes at a higher velocity (27 000 g) in comparison with that provided for by the standard protocol (13 000 g) following the strategy B.

Aliquots derived from all the steps of the strategies A and B were collected and analysed by SDS-page and western blot. The western blot analysis underlines that neither the strategy A nor B allowed to precipitate the CPMV eVLPs.BP100 that remained in the surnatant (data not shown).

Moving on strategy C, the TSP were extracted from 10 g of *N. bethamiana* pEAQ-HT-VP60.BP100 infected leaves and divided into 6 independent sample which were incubated over night at 4 °C at different ionic strengths and PEG types.

The details of this experiment are reported in table 3.

Table 3 strategy a for the CPMV eVLPs.BP100 precipitation

Sample	PEG molecular weight	Ionic strength (NaCl M)
1	3350	Normal (0.2 M)
2	3350	Twice (0.4 M)
3	4000	Normal (0.2 M)
4	6000	No NaCl (0 M)
5	6000	10 fold lower (20 mM)
6	6000	Twice (0.4 M)
7	8000	Normal (0.2 M)
9	8000	Twice (0.4 M)
10	20000	Normal (0.2 M)

After the incubation over night at 4 °C in the condition reported in table 1, samples were spun and either the resulted supernatant or pellet were analysed by SDS-page and western blot. The behaviour of the CPMV eVLPs.BP100 in the different conditions are shown in figure 10.

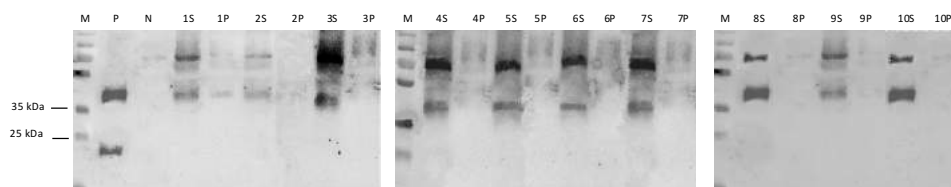


Figure 10 Western blot analysis of the 10 purification strategies schedule in table 3. 20 μ l of each sample were loaded on 12% polyacrylamide gels then blots were probed with a polyclonal antibody (G49) specific to CPMV particles used at a concentration of 1:2000. The number indicated the strategy (table 3), and supernatant (S) and resuspended pellet (P) of every strategy were analysed. P: 1 μ g of purified unmodified CPMV eVLPs as positive control. M: molecular marker (PageRuler™ Plus Prestained Protein Ladder, Thermo Scientific).

The figure 10 highlights the presence of CPMV L CP specific signals at approximately 40 kDa in all the supernatants loaded on the gel; only sample 1 is characterised by a faint signal in the pellet sample obtained from the centrifugation after the over night precipitation with peg 3350. However, this signal is too faint in comparison with the one of the supernatant to be considered relevant.

Considering that all the signals corresponding to the CPMV eVLPs.BP100 are present in the surnatants, they have been spinned at 30 000 g for 16 hours in the attempt to precipitate them. The pellets formed were resuspended and loaded on polyacrillamide gel to be analysed by western blot but again all the signals corresponding to the CPMV eVLPs.BP100 were clearly visible only in the surnatants (data not shown).

4.3. Double sucrose cushion and Nycodenz gradient

As reported in the previous section regarding CPMV eVLPs. Tat the protocols reported in Peyret *et al.*, 2015 were tested to purify CPMV eVLPs.BP100 from 3 g of infiltrated *N. benthamiana* leaves.

An aliquot of every purification step was collected and the Nycodenz gradient was fractionated in 11 aliquots. All the samples collected were analysed by SDS-PAGE and western blot.

The results obtained showed that even the use of this protocol did not allow to purify the CPMV eVLPs.BP100 that are not present in the expected gradient band as reported in Payret *et al.* (2015) (data not shown).

CONCLUDING REMARKS

The great advances in the last decade have turned the plant molecular farming from a theoretical science to an industrial and applicative biotechnological field.

The development and refinement of expression technologies and their application for the production in a wide range of crop species of target molecules, result in a flurry of patents and industrial applications.

As reported in Arntzen *et al.* (2015), pharmaceutical and agricultural biotechnology companies started to invest significantly in plant-based systems reflecting the realization of the potential of plant molecular farming.

In this context, the use of plant viruses as *in planta* expression tools is a particularly promising approach.

Plant viruses can be considered as innovative nanomaterials able to stabilize functional peptides on their surface; the resulting CVPs/eVLPs can be produced in plant without expensive production costs and may be implemented in a variety of industrial and biotechnological fields.

However, the expression of peptides with CVPs/eVLPs is a cutting-edge technology that up to now it is not always well standardized and it is strongly peptide and viral particle dependent. Indeed, in this project some problem with the expression (PVX CVPs.FADK₂) or purification (PVX CVPs.BANK₁, TuMV CVPs.LIP₁, CPMV eVLPs.BP100 and CPMV eVLPs.Tat) have been reported.

In the future, in order to overcome these drawbacks, viral expression particles could be optimized through a synthetic biology approach in order to increase the particles stability. The sequence of the viral CPs could be analysed and modified in order to improve the particles stability when the peptide of interest is fused on their surface. Moreover, through bioinformatics tools a new exposal site on the particles surface could be explored in order to achieve the best peptide exposition.

Nevertheless, in this project the therapeutic application of different viral expression system has been demonstrated.

In particular, CPMV eVLP.p524 results to be a potential pharmaceutical for the prevention of T1D; moreover, it has been demonstrated that TBSV CVPs.LIP₁ and TBSV CVPs.FADK₂ have a therapeutic potential in the treatment of RA.

The use of viral particles for peptide display allows to increase the effects of the peptide itself. Indeed, CPMV eVLPs.p524 results to have a regulative effect that has not been achieved using the synthetic peptide p524 with IFA.

The use of TBSV CVPs for peptide LIP₁ display confirms this evidence since the therapeutic effect of the particles results to be higher in comparison to the injection of LIP₁ peptide alone. On the other hand, although TBSV CVPs.FADK₂ showed regulative and therapeutic effects, the FADK₂ synthetic peptide injected with IFA results to be more effective.

These evidences are particularly interestingly considering that viral particles have been previously used before for the set up of vaccines (Jochmus *et al.*, 1999) and never for the therapy of autoimmune disease.

The role of a vaccine is to boost and stimulate the immune system in order to give the protection from a disease; on the contrary, in this project, it has been shown that CVPs/eVLPs displaying specific autoantigenic peptides can be used for the modulation of the immune system and for the induction of immunological tolerance against the autoantigenic peptide itself.

The restore of the immunological tolerance occurs through the activation of a subset of regulatory and antiinflammatory cytokines driven by the autoantigenic peptide displayed on viral particles surface.

RA and T1D are the two most widespread autoimmune diseases with a strong social impact, also in terms of public health costs.

Considering the increasing availability of diagnostic tools, that combine genetic marker with the presence of specific autoantibodies, that allows to estimate the probability that a person has to develop T1D, the use of CPMV eVLPs.p524 in T1D preventive campaigns could markedly reduce the cost associated to this disease. Currently, patients need daily insulin injection throughout their life, the prevention of this disorder would avoid the damage of the pancreatic cells and the use of insulin.

Regarding the prevention of RA, the current therapy available for patients consist in the use of immunosuppressant and non-steroidal anti-inflammatiry drugs (NSAID). These pharmaceutical relieve pain and steam symptoms without blocking the course of the disease.

However, the therapeutic effects of TBSV CVPs.LIP1 and TBSV CVPs.FADK₂ would allow to treat RA avoiding the sides effect of immunosuppressant and NSAID drugs.

Moreover, T1D and RA preclinical studies reported in this PhD thesis have demonstrated that viral particles displaying immunodominant peptides have showed a preventive and therapeutic effect without the use of any adjuvant. This could be due to the high density of peptide display on viral surface, that correspond to 6.1×10^{-3} and 6.4×10^{-2} peptide/nm² respectively for the CPMV and TBSV expression system. Although, the peptide superficial density reached with the TBSV expression system is ten-fold higher in comparison with the one reached with the CPMV based system, the latter results to be efficient as well.

Moreover, beside the stabilization and the exposition of the peptides, miming a viral structure, CVPs and eVLPs elicit the immune system without the need of any other molecules (Lico *et al.*, 2012). This evidence allows, not only to avoid the cost associated to the use of adjuvants but also, to avoid their side effects.

The comparison between plant viruses with the traditional nanomaterial gives rise several shared characteristics. Indeed, plants viruses are robust nanoparticles with a simple, repetitive and ordered structure. These features, common to nanomaterials, gives plant viruses excellent candidate for the development of reagents to be exploited also in diagnostic field. In this context, a kit for SjS diagnosis has been developed using PVX CVPs.lipo as coating reagent for the set-up of a diagnostic ELISA.

The comparison between the PVX CVPs.lipo-based ELISA and the same kit made using the synthetic peptide lipo have demonstrated that the use of PVX particles allows to increase the diagnostic sensitivity. Moreover, the use of the synthetic peptide did not provide reproducible results probably for its intrinsic peptide instability and its poorly absorption to the ELISA plate. This evidence is probably due to the flexibility and filamentous PVX structure that allows a high lipo peptide exposition. Furthermore, the filamentous viral particle shape results to be decisive for the diagnostic application; indeed,

the two icosahedral virus based system (CPMV and TBSV) are not be suitable for this application.

Moreover, the PVX CVPs.lipo based ELISA results to be remarkably stable up to 2 months at 4 °C.

The results obtained in the set-up of the Sjs diagnostic kit using the PVX CVPs.lipo could pave the way to the exploitation of plant viruses for the development of diagnostic tools able to improve the performance of current diagnostic procedures.

Beside the improvement that CVPs particles could provide in the diagnostic field, another strength of this application relies on the inexpensive production process because plants are used as natural bioreactor for the CVPs expression and amplification.

Finally, plant virus particles displaying biomarker peptides could be applied also to other diagnostic methods such as the immunofluorescence based one, chromatographic immunoassay or in a label-free immunoassay through the development of specific biosensor (Giavazzi *et al.*, 2013).

The last part of this project has explored other eVLPs application beside the therapeutic and diagnostic ones. In particular, the CPMV eVLPs expression system has been tested for the set-up of a biotechnological system for the internalization of peptide inside the cell and for the development of particles display an AMPs for the expression in plant of eco-pesticide.

Current pesticides are widely used in agricultural but serious concerns have been raise about the human health risks and the impact on environment. The development of eVLPs displaying AMP would lead to the development of a new form of biocontrol of plant pathogen. eVLPs are completely human and environmental safe because they are biodegradable molecule and, lacking the viral genome, not infective.

Although, the development of these two applications of eVLPs is at an early stage and it does not allow to obtain results because of some problems in the purification step of either CPMV eVLPs.Tat or CPMV eVLPs.BP100, other peptide and viral expression system are in process of evaluation to achieve the final goal.

REFERENCES

- Adorini L. Interleukin 12 and autoimmune diabetes. *Nature genetics* 2001.
- Akerblom H.K. Dietary manipulation of beta cell autoimmunity in infants at increased risk of type 1 diabetes: a pilot study. *Diabetologia* 2005; **48**: 829–837.
- Akihiko I., Nobuyoshi A., Takashi M. Regulation of autoimmune diabetes by interleukin 3-dependent bone marrow-derived cell in NOD mice. *Journal of Autoimmunity* 1997; **10**: 331–338.
- Alaa A.A. Alijabali, Shukla S., Lomonosoff G.P., Steinmatz N. F., Evans D. J. CPMV-DOX Delivers. *Mol Pharm* 2013; **10**: 3–10.
- Anderson M.S. and Bluestone J.A. The NOD mouse: a model of immune dysregulation. *Annual Rev Immunol.* 2005; **23**: 447–485.
- Arai T., Moriyama H., Shimizu M., Sasaki H., Kishi M., Okumachi Y., Yasuda H., Hara K., Yokono K. and Nagata M. Administration of a determinant of preproinsulin can induce regulatory T-cells and suppress anti-islet autoimmunity in NOD mice. *Clin Immunol* 2010; **136**: 74–82.
- Aramayo R., Merigoux C., Larquet E., Bron P., Perez J., Dumas C., Vachette P., Boisset N. Divalent ion-dependent swelling of Tomato bushy stunt virus: a multi-approach study. *Biochim. Biophys. Acta.* 2005; **1724**: 345–354.
- Arntzen C.J. Plant-made pharmaceuticals; from “edible vaccines” to Ebola therapeutics. *Plant Biotechnol J.* 2015; **13**: 1013–1016.
- Atabekov J., Dobrov E., Karpova O., Rodinova N. Potato Virus X: structure, disassembly and reconstitution. *Mol Plant Pathol* 2007; **8**: 667–675.
- Badosa E., Ferrè R., Frances J., Bardaji E., Feliu L., Planas M. Sporicidal activity of synthetic antifungal undecapeptides and control of *Penicillium* rot of apples. *Appl Environ Microbiol* 2009; **75**: 5563–5569.
- Barnett A.J., McNeilage L.J. Antinuclear antibodies in patients with scleroderma (systemic sclerosis) and in their blood relatives and spouses. *Annals of the rheumatic diseases* 1993; **52**: 365–368.

- Barrera M.J., Aguilera S., Veerman E. *et al.* Salivary mucins induce a Toll-like receptor 4-mediated pro-inflammatory response in human submandibular salivary cells: are mucins involved in Sjögren's syndrome? *Rheumatology* (Oxford) 2015; **54**: 1518-1527.
- Barta A., Sommergruber K., Thompson D., Hartmuth K., Matzke M.A., Matzke A.J. The expression of a nopaline synthase – human growth hormone chimaeric gene in transformed tobacco and sunflower callus tissue. *Plant. Mol. Biol.* 1986; **6**: 347-357.
- Baulcombe D.C., Chapman S., Santa Cruz S. Jellyfish green fluorescent protein as a reporter for virus infections. *Plant J.* 1995; **7**: 1045-1053.
- Betti C., Lico C., Maffi D., D'Angeli S., Altamura M. M., Benvenuto E., et al. Potato virus X movement in *Nicotiana benthamiana*: new details revealed by chimeric coat protein variants. *Mol. Plant Pathol* 2012; **13**: 198–203.
- Bluestone J.A., Herold K., Eisenbarth G. Genetics, pathogenesis and clinical interventions in type 1 diabetes. *Nature* 2010; **464**: 1293-1300.
- Boivin E.B., Lepage E., Matton D.P., De Crescenzo G., Jolicoeur M. Transient expression of antibodies in suspension plant cell suspension cultures is enhanced when co-transformed with the tomato bushy stunt virus p19 viral suppressor of gene silencing. *Biotechnol. Prog.* 2010; **26**: 1534-1543.
- Boyman O., Surh C.D., Sprent J. Potential use of IL-2/anti-IL-2 antibody immune complexes for the treatment of cancer and autoimmune disease. *Expert Opin Biol Ther* 2006; **6**: 1323–1331.
- Brand D.D., Latham K. A., Rosloniec E.F. Collagen-induced arthritis. *Nature Protocols* 2007; **2**: 1269-1275.
- Brennan F.R., Jones T.D., Gilleland L.B., Bellaby T, Xu F, North PC, Thompson A, Staczek J, Lin T, Johnson JE, Hamilton WD, Gilleland HE. *Pseudomonas aeruginosa* outer-membrane protein F epitopes are highly immunogenic in mice when expressed on a plant virus. *Microbiology* 1999; **145**: 211-220.
- Brennan F.R., Jones T.D., Longstaff M., Chapman S., Bellaby T., Smith H., Xu F., Hamilton W. D., Flock J. I. Immunogenicity of peptide derived from a fibronectin-binding protein of *S. aureus* expressed on two different plant viruses. *Vaccine* 1999; **17**: 1846-1857.
- Burton O.T., Logsdon S.L., Zhou J.S., Medina-Tamayo J., Abdel-Gadir A., Rivas M.N., Koleoglou K.J., Chatila T.A., Schneider L.C., Rachid R., Umetsu D.T., Oettgen H.C. Oral

immunotherapy induces IgG antibodies that act via Fc γ RIIb to suppress IgE-mediated hypersensitivity. *J Allergy Clin Immunol*. 2014; **134**:1310-1317.

Cameron M.J., Arreaza G.A., Zucker P., Chensue S.W., Strieter R.M., Chakrabarti S., Delovitch T.L. IL-4 prevents insulinitis and insulin-dependent diabetes mellitus in nonobese diabetic mice by potentiation of regulatory T helper-2 cell function. *J Immunol* 1997; **159**.

Cañizares M.C., Liu L., Perrin Y., Tsakiris E., Lomonossoff G.P. A bipartite system for the constitutive and inducible expression of high levels of foreign proteins in plants. *Plant Biotechnology Journal* 2006; **4**: 183-193.

Carter J.E., Yu J., Choi N.W., Hough J., Henderson D., He D. and Landgridge W.H.R. Bacterial and plant enterotoxin B subunit-autoantigen fusion proteins suppress diabetes insulinitis. *Mol Biotechnol* 2006; **32** (1): 1-15.

Cervera R., Font J., Ramos-Casals M., García-Carrasco M., Rosas J., Morlà R.M., Muñoz F.J., Artigues A., Pallarés L., Ingelmo M. Primary Sjögren's syndrome in men: clinical and immunological characteristics. *Lupus* 2000; **9**: 61-64.

Chapman S., Hills G., Watts J., Baulcombe D. Mutational analysis of the coat protein gene of Potato virus X: effects on virion morphology and viral pathogenicity. *Virology* 1992b; **191**: 223-230.

Chapman S., Kavanagh T., Baulcombe D. Potato virus X as a vector for gene expression in plants. *Plant J*. 1992a; **2**: 549-557.

Chen G., Han G., Feng J., Wang J., Wang R., Xu R., Shen B., Qian J. and Li Y. Glutamic acid decarboxylase-derived epitopes with specific domains expand CD4CD25 regulatory T-cells. *PLoS One* 2009; **4**: e7034.

Chilton M.D., Drummond M.H., Merlo D.J., Sciaky D., Montoya A. L., Gordon M.P., Nester E.W. Stable incorporation of plasmid DNA into higher plant cells: the molecular basis of crown gall tumorigenesis. *Cell* 1977; **11**: 263-271.

Ciccia F., Guccino G., Rizzo A. *et al.* Interleukin (IL)-22 receptor 1 is over-expressed in primary Sjögren's syndrome and Sjögren-associated non-Hodgkin lymphomas and is regulated by IL-18. *Clin Exp Immunol* 2015; **181**: 219-229.

- Circelli P., Donini M., Villani M.E., Benvenuto E., Marusic C. Efficient Agrobacterium-based transient expression system for the production of biopharmaceuticals in plants. *Bioeng. Bugs* 2010; **1**: 221-224.
- Cleveland J., Montville T.J., Nes I.F., Chikindas M.L. Bacteriocins: safe, natural antimicrobials for food preservation. *International Journal of Food Microbiology* 2001; 1-20.
- Collins M., Bartelt R.R., Houtman J.C. T cell receptor activation leads to two distinct phases of Pyk2 activation and actin cytoskeletal rearrangement in human T cells. *Mol. Immunol.* 2010; **47**: 1665-1674.
- Cooper G.S., Bynum M.L., Somers E.C. Recent insights in the epidemiology of autoimmune diseases: Improved prevalence estimates and understanding of clustering of diseases. *J Autoimmun* 2009; **33**:197–207.
- Cornec D., Jousse-Joulin S., Marhadour T., Pers J.O., Boisramé-Gastrin S., Renaudineau Y., Saraux A., Devauchelle-Pensec V. Salivary gland ultrasonography improves the diagnostic performance of the 2012 America College of Rheumatology classification criteria for Sjögren's Syndrome. *Rheumatology (Oxford)* 2014; **53**:1604-1607.
- Daniel D. and Wegmann D.R. Intranasal administration of insulin peptide B:9-23 protects NOD mice from diabetes. *Ann NY Acad Sci*, 1996 (b); **778**: 371-372.
- Daniel D. and Wegmann D.R. Protection of nonobese diabetic mice from diabetes by intranasal or subcutaneous administration of insulin peptide B-(9-23). *Proc Natl Acad Sci USA* 1996 (a); **93**: 956-960.
- De Winter L.M., Hansen W.L., van Steenberg H.W., Geusens P., Lenaerts J., Somers K., Stinissen P., van der Helm-van MII A.H., Somers V. Autoantibodies to two novel peptides in seronegative and early rheumatoid arthritis. *Rheumatology* 2016; **55**: 1431-1436.
- Depicker A., Stachel S., Dhaese P., Zambryski P., Goodman H. M. Nopaline synthase: transcript mapping and DNA sequence. *J. Mol. Appl. Genet.* 1982; **1**:561–573.
- Elias D. and Cohen I.R. Treatment of autoimmune diabetes and insulinitis in NOD mice with heat shock protein 60 peptide p277. *Diabetes* 1995; **44**: 1132-1138.

- Engvall E., and Perlmann P. Enzyme linked immunosorbent assay, ELISA. 3. Quantitation of specific antibodies by enzyme-labeled anti-immunoglobulin in antigen-coated tubes. *J. Immunol* 1972; **109**: 129–135.
- Erlich H., Valdes A.M., Noble J., Carlson J.A., Varney M., Concannon P., Mychaleckyj J.C., Todd J.A., Bonella P., Fear A.L., Lavant E., Louey A., Moonsamy P. HLA DR-DQ haplotypes and genotypes and type 1 diabetes risk: analysis of the type 1 diabetes genetics consortium families. *Diabetes* 2008; **57**: 1084-1092.
- Falkenburg W. J. J. IgG subclass specificity discriminates restricted IgM rheumatoid factor responses from more mature anti-citrullinated protein antibody-associated or isotype-switched IgA responses. *Arthritis & Rheumatology* 2015; **67**:12.
- Farnsworth N., Akerele O., Bingel A.S., Sojearto D.D., Guo Z. Medicinal plants in therapy. *Bulletin of the World Health Organization* 1985; **63**: 965-981.
- Fisher A., Feinberg M., Josephs S., Harper M., Marselle L., Reyes G., Gonda M., Aldovini A., Debouk R., Gallo R. C., Wong-staal F. The transactivator gene of HTLV-III is essential for virus replication. *Nature* 1986; **320**:367-371.
- Fonseca S. B., Pereira M. P., Kelley S. O. Recent advances in the use of cell-penetrating peptides for medical and biological applications. *Adv. Drug Delivery Rev.* 2009; **61**: 953 – 963.
- Fuller B.E., Okayasu I., Simon L.L., Giraldo A.A., Kong Y.M. Characterization of resistance to murine experimental autoimmune thyroiditis: duration and afferent action of thyroglobulin- and TSH-induced suppression. *Clin Immunol Immunopathol* 1993; **69**: 60-68.
- Gardner J.M., Fletcher A.L., Anderson M.S. and Turley S.J. AIRE in the thymus and beyond. *Current Opinion in Immunology* 2009; **21**: 582–589.
- Gaur A., Wiers B., Liu A., Rothbard J., Fathman C.G. Amelioration of autoimmune encephalomyelitis by myelin basic protein synthetic peptide-induced anergy. *Science* 1992; **258**: 1491-1494.
- Giavazzi F., Salina M., Ceccarello E., Ilacqua A., Damini F., Sola L., Chiari M., Chini B., Cerbino R., Bellini T., Buscaglia M. A fast and simple label-free immunoassay based on a smartphone. *Biosensor and Bioelectronics* 2014; **58**:395-402.

- Gleba Y., Klimyuk V., Marillonnet S. Magniffection – a new platform for expressing recombinant vaccines in plants. *Vaccine* 2005; **23**: 2042-2048.
- Gong Z., Pan L., Le Y., Liu Q., Zhou M., Xing W., Zhuo R., Wang S. and Guo J. Glutamic acid decarboxylase epitope protects against autoimmune diabetes through activation of Th2 immune response and induction of possible regulatory mechanism. *Vaccine* 2010; **28**: 4052-4058.
- Gonzalez A., Maradit Kremers H., Crowson C.S., Ballman K.V., Roger V.L., Jacobsen S.J., O’Fallon W.M., Gabriel S.E. Do cardiovascular risk factors confer the same risk for cardiovascular outcomes in rheumatoid arthritis as in non-rheumatoid arthritis patients? *Ann Rheum Dis* 2008; **67**: 64-69.
- Grasso S., Lico C., Imperatori F., Santi L. A plant derived multifunctional tool for nanobiotechnology based on *Tomato bushy stunt virus*. *Transgenic Res.* 2013; **22**: 519-535.
- Gregorius K., and Theisen M. In situ deprotection: a method for covalent immobilization of peptides with well-defined orientation for use in solid phase immunoassays such as enzyme-linked immunosorbent assay. *Anal. Biochem* 2001; **299**: 84–91.
- Gregorius K., Dalum I., Freisleben M., Mouritsen S. and Elsner, H. I. A novel microtiter plate based method for identification of B-cell epitopes. *J. Pept. Sci* 1999; **5**: 75–82.
- Griesmann G. E., McCormick D. J. and Lennon, V. A. An avidin- biotin-peroxidase assay to detect synthetic peptides bound to polystyrene plates. *J. Immunol Methods* 1991; **138**: 25–29.
- Hall J.C., Baer A.N., Shah A.A. *et al.* Molecular subsetting of interferon pathways in Sjögren’s syndrome. *Arthritis Rheumatol* 2015; **67**: 2437-2446.
- Haque M., Fino K., Lei F., Xiong X., Song J. Utilizing regulatory T cells against rheumatoid arthritis. *Frontiers in oncology* 2014; **4**.
- Harrison S. C., Olson A. J., Schutt C. E., Winkler F. K., Bricogne G. Tomato bushy stunt virus at 2.9 Å resolution. *Nature* 1978; **276**: 368–373.
- Hennegan K., Yang D., Nguyen D., Wu L., Goding J., Huang J. Improvement of human lysozyme expression in transgenic rice grain by combining wheat (*Triticum aestivum*) puroindoline b and rice (*Oryza sativa*) Gt1 promoter and signal peptides. *Transgenic Res* 2005; **14**: 583-592.

- Hernández-Molina G., Leal-Alegre G., Michel-Peregrina M. The meaning of anti-Ro and anti-La antibodies in primary Sjögren's syndrome. *Autoimmunity reviews* 2011; **10**: 123–125.
- Hesketh E.L., Meshcheriakova Y., Dent K.C., Saxena P., Thompson R.F., Cockburn J.J., Lomonosoff G.P., Ranson N.A. Mechanisms of assembly and genome packaging in an RNA virus revealed by high-resolution cryo-EM. *Nature communications* 2015; **6**.
- Hiatt A., Cafferkey R., Bowdish K. Production of antibodies in transgenic plants. *Nature* 1989; **342**: 76-78.
- Hood E. E., Woodard S.L., Horn M.E. Monoclonal antibody manufacturing in transgenic plant-myths and realities. *Curr. Opin. Biotechnol.* 2010; **8**: 564-587.
- Hsieh C.S., Macatonia S.E., Tripp C.S., Wolf S.F., O'Garra A., Murphy K.M. Development of Th1 CD4⁺ T cells through IL-12 produced by Listeria-induced macrophages. *Science* 1993; **260**: 547–549.
- Huang R., Yin J., Chen Y. et al. The amino acid variation within the binding pocket 7 and 9 of HLA-DRB1 molecules are associated with primary Sjögren's syndrome. *J Autoimmun* 2015; **57**: 53-59.
- Inoue H., Nojima H., Okayama H. High efficiency transformation of *Escherichia coli* with plasmids. *Gene* 1990; **96**:23-28.
- Isaacs J.D. The changing face of rheumatoid arthritis: sustained remission for all? *Nat Rev Immunol* 2010; **10**: 605-611.
- Jaekel E., Mpofo N., Saal N., and Manns M.P. Role of regulatory T cells for the treatment of type 1 diabetes mellitus. *Horm. Metab. Res* 2008; **40**: 126–136.
- Jegerlehner A., Tissot A., Lechner F., Sebbel P., Erdmann I., Kundig T., Bachi T., Storni T., Jennings G., Pumpens P., Renner W.A., Bachmann M.F. A molecular assembly system that renders antigens of choice highly repetitive for induction of protective B cell responses. *Vaccine* 2002; **20**: 3104-3112.
- Jochmus I., Schäfer K., Faath S., Müller M., Gissman L. Chimeric Virus-like Particles of the human papillomavirus type 16 (HPV 16) as a prophylactic and therapeutic vaccine. *Archives of Medical Research* 1999; **4**: 269-274.

- Jun H.S. and Yoon J.W. A new look at viruses in type 1 diabetes. *ILARJ* 2004; **45**: 349–374.
- Jung H.H., Ji Y.S., Sung M.S., Kim K.K., Yoon K.C. Long-term outcome of treatment with topical corticosteroids for severe dry eye associated with Sjögren's syndrome. *Chonnam Med J* 2015; **51**: 26-32;
- Kachapati K., Adams D., Bednar K., Ridgway W.M. The Non-Obese Diabetic (NOD) mouse as a model of Human Type 1 Diabetes. *Animal Models in Diabetes Research* 2012; **933**: 3-16.
- Kamenarova, K., Abumhadi, N., Gecheff, K. and Atanassov, A. Molecular farming in plants: an approach of agricultural biotechnology. *Journal of cell and molecular biology* 2005; **4**:77-86.
- Kaufman D.L., Clare-Salzler M., Tian J., Forsthuber T., Ting G.S., Robinson P., Atkinson M.A., Sercarz E.E., Tobin A.J., Lehmann P.V. Spontaneous loss of T cell tolerance to glutamic acid decarboxylase in murine insulin dependent diabetes. *Nature* **366**:69.
- Kavanaugh A., Tomar R., Reveille J., Solomon D.H., Homburger H.A. Guidelines for clinical use of the antinuclear antibody test and tests for specific autoantibodies to nuclear antigens. American College of Pathologists. *Archives of pathology & laboratory medicine* 2000; **124**: 71–81.
- Kendall A., McDonald M., Bian W., Bowles T., Baumgarten S. C., Shi J., Stewart P.L., Bullitt E., Gore D., Irving T.C., Havens W.M., Ghabrial S.A., Wall J.S., Stubbs G. Structure of flexible filamentous plant viruses. *J. Virol.* 2008; **82**: 9546-9554.
- Knäblein J. Plant-based expression of biopharmaceutical. *Encyclopedia of Molecular Cell Biology and Molecular Medicine* 2005; Ed R. A. Meyers, Wiley-VCH Verlag GmbH&Co: 385-410.
- Komorova T.V., Baschieri S., Donini M., Marusic C., Benvenuto E., Dorokhov Y.L. Transient expression systems for plant-derived biopharmaceutical. *Expert. Rev. Vaccines* 2010; **9**: 859-876.
- Konkel J.O., Jin W., Abbatiello B., Grainger J.R., Chen W.J. Thymocyte apoptosis drives the intrathymic generation of regulatory T cells. *PNAS* 2014; **111**: 465-473.
- Koreth J., Matsuoka K., Kim H.T., McDonough S.M., Bindra B., Alyea E.P., III, Armand P., Cutler C., Ho V.T., Treister N.S., Bienfang D.C., Prasad S., Tzachanis D., Joyce R.M.,

Avigan D.E., Antin J.H., Ritz J., Soiffer R.J. Interleukin-2 and regulatory T cells in graft-versus-host disease. *N Engl J Med* 2011; **365**: 2055–2066.

Kozyrev S.V., Abelson A.-K., Wojcik J., Zaghlool A., Linga Reddy M.V.P., Sanchez E., Gunnarsson I., Svengsson E., Sturfelt G., Joensen A., Truedsson L., Pons-Estel B.A., Witte T., D'Alfonso S., Barizzone N., Danieli M.G., Gutierrez C., Suarez A., Alarcon-Riquelme M.E. Functional variants in the B-cell gene BANK1 are associated with systemic lupus erythematosus. *Nat. Genet.* 2008; **40**: 211-216.

Kronenberg M., Rudensky A. Regulation of immunity by self-reactive T cells. *Nature* 2005; **435**: 598-604.

Kruse J., Kruse K.M., Witz J., Chauvin C., Jacrot B., Tardieu A. Divalent ion-dependent reversible swelling of Tomato bushy stunt virus and organization of the expanded virion. *J. Mol. Biol.* 1982; **162**:393–414.

Kumar Y., Bhatia A., Minz R.W. Antinuclear antibodies and their detection methods in diagnosis of connective tissue diseases: a journey revisited. *Diagnostic pathology* 2009; **4**: 1.

Kusnadi A.R., Nikolov Z.L., Howard J.A. Production of recombinant proteins in transgenic plants: practical considerations. *Biotechnol. Bioeng.* 1997; **56**: 473-484.

Langel Ü. Cell-penetrating peptides. Handbook Taylor & Francis (2006).

Lau K., Benitez P., Ardisson A., Wilson T.D., Collins E. L., Lorca G., Li N., Sankar D., Wasserfall C., Neu J., Atkinson M.A., Shatz D., Triplett E. W., Larkin J. Inhibition of Type 1 Diabetes correlated to a *Lactobacillus johnsonii* N6.2-mediated Th17 Bias. *Journal of Immunology* 2011.

Leiser & Richter. *Archiv für Phytopathologie und Pflanzenschutz* 1978; **14**: 337.

Lennon G.P., Bettini M., Burton A.R., Vincent E., Arnold P.Y., Santamaria P., Vignali D.A.A. T cell islet accumulation in type 1 diabetes is a tightly regulated, cell-autonomous event. *Immunity* 2009; **31**: 643–653.

Liang J., Aihua Z., Yu W., Yong L. and Jingjing L. H. HSP65 serves as an immunogenic carrier for a diabetogenic peptide P277 inducing anti-inflammatory immune response in NOD mice by nasal administration. *Vaccine* 2010; **28**: 3312-3317.

- Lico C., Capuano F., Renzone G., Donini M., Marusic C., Scaloni A., Benvenuto E. and Baschieri S. Peptide display on Potato *virus X*: molecular features of the coat protein-fused peptide affecting cell-to-cell and phloem movement of chimeric virus particles. *J. Gen. Virol.* 2006; **87**: 3103-3112.
- Lico C., Chen Q. and Santi L. Viral vectors for production of recombinant proteins in plants. *J. Cell Physiol.* 2008; **216**: 366-377.
- Lico C., Desiderio A, Banchieri S., Benvenuto E. Plants as biofactories: Production of pharmaceutical recombinant proteins. *International Congress "In the Wake of the Double Helix: From the Green Revolution to the Gene Revolution"*; 27-31 May 2003, Bologna, Italy; ©2005 Avenua media, Bologna, Italy.
- Lico C., Mancini C., Italiani P., Betti C., Boraschi D., Benvenuto E., Baschieri S. Plant-produced potato virus X chimeric particles displaying an influenza virus-derived peptide activate specific CD8+ T cells in mice. *Vaccine* 2009; **27**: 5069-5076.
- Lico C., Santi L., Twyman R.M., Pezzotti M. and Avesani L. The use of plants for the production of therapeutic human peptides. *Plan. Cell. Rep.* 2012; **31**: 439-451.
- Lie L., Wang B. and Tisch R. Suppression of ongoing T cell-mediated autoimmunity by peptide-MHC class II dimer vaccination. *J Immunol* 2009; **183**: 4809-4816.
- Liénard D., Sourrouille C., Gomord V., Faye L. Pharming and transgenic plants. *Biotechnology Annual Review* 2007; **13**: 115-147.
- Lin T., Johnson J.E. Structures of picorna-like plant viruses: implications and applications. *Adv. Virus. Res.* 2003; **62**: 167-237.
- Lin X., Rui K., Deng J. et al. Th17 cells play a critical role in the development of experimental Sjögren's syndrome. *Ann Rheum Dis* 2015; **74**: 1302-1310.
- Lipinski C.A., Loftus J.C. Targeting Pyk2 for therapeutic intervention. *Expert Opin.* 2010; **14**: 95-108.
- Liu L., Grainger J., Cañizares M.C., Angell S.M., Lomonossoff G.P. Cowpea Mosaic Virus RNA-1 acts as an amplicon whose effects can be counteracted by a RNA-2-encoded suppressor of silencing. *Virology* 2004; **323**: 37-48.
- Lomonossoff G.P., Johnson J.E. Eukariotic viral expression system for polypeptides. *Semin. Virol.* 1995; **6**: 257-267.

- Mackay F., Schneider P., Rennert P., Browning J. BAFF and APRIL: a tutorial on B cell survival. *Annual Rev Immunol* 2003; **21**: 231-264.
- Maedler, K. et al. Low concentration of interleukin-1 β induces FLICE-inhibitory protein-mediated β -cell proliferation in human pancreatic islets. *Diabetes* 2006; **55**: 2713–2722 .
- Maese P., Genovese M.C., Gladstein G., Kivitz A.J., Ritchlin C., Tak P.P., Wollenhaupt J., Bahary O., Becker J.C., Kelly S., Sigal L., Teng J., Gladman D. Abatacept in the treatment of patients with psoriatic arthritis: Results of six months, multicentre, randomized, double-blind, placebo controlled, phase II trials. *Arthritis Rheum* 2011; **63**: 939-948.
- Mallek, T. R., & Bayer, A. L. Tolerance, not immunity, crucially depends on IL-2. *Nature Reviews/Immunology* 2004; **4**: 665– 674.
- Mandrup-Poulsen, T. The role of interleukin-1 in the pathogenesis of IDDM. *Diabetologia* 1996; **39**:1005–1029.
- Marillonnet S., Giritch A., Gils M., Kandzia R., Klimyuk V., Gleba Y. *In planta* engineering of viral RNA replicons: Efficient assembly by recombinant of DNA modules delivered by *Agrobacterium*. *PNAS* 2004; **101**: 6852-6857.
- Markeljevic J., Sarac H., Bozina N., Henigsberg N., Simic M., Cicin Sain L. Serotonin transporter gene polymorphisms: Relation with platelet serotonin level in patients with primary Sjögren's syndrome. *J Neuroimmunol* 2015; **282**: 104-109.
- Martinez N.R., Augstein P., Moustakas A.K., Papadopoulos G.K., Gregori S., Adorini L., Jackson D.C. and Harrison L.C. Disabling an integral CTL epitope allows suppression of autoimmune diabetes by intranasal proinsulin peptide. *J Clin Invest* 2003; **111**: 1365-1371.
- Marusic C., Rizza P., Lattanzi L., Mancini C., Spada M., Belardelli F., Benvenuto E., Capone I. Chimeric plant virus particles as immunogens for inducing murine and human immune responses against human immunodeficiency virus type 1. *J. Virol.* 2001; **75**: 8434-8439.
- Maxwell L.J., Singh J.A., Abatacept for rheumatoid arthritis: a Cochrane systemic review. *J Rheumatol* 2010; **37**: 234-245.
- Mc Innes I. B., Schett G. The pathogenesis of rheumatoid arthritis. *N Engl J Med* 2011; **365**: 2205-2219.

- McGarvey P.B., Hammond J., Dienelt M.M., Hooper D.C., Fu Z.F., Dietzschold B, Koprowski H, Michaels F.H. Expression of the rabies virus glycoprotein in transgenic tomatoes. *Biotechnology (N Y)*; **13**: 1484-1487.
- Miceli-Richard C., Wang-Renault S.F., Boudaoud S. et al. Overlap between differentially methylated DNA regions in blood B lymphocytes and genetic at-risk loci in primary Sjögren's syndrome. *Ann Rheum Dis* 2016; **75**: 933-940.
- Montague N.P., Thuenemann E.C., Saxena P., Saunders K., Lenzi P. and Lomonosoff G.P. Recent advances of cowpea mosaic virus based particle technology. *Hum Vaccin* 2011; **7** (3): 383-390.
- Montesinos E., Bardaji E. Synthetic antimicrobial peptides as agricultural pesticides for plant-disease control. *Chem Biodiver* 2008; **5**: 1225-1237.
- Mortz E., Krogh T.N., Vorum H. and Görg A. Improved silver staining protocols for high sensitivity protein identification using matrix-assisted laser desorption/ionization-time of flight analysis. *Proteomics* 2001; **1**: 1359-1363.
- Mueller D.L., Mechanisms maintaining peripheral tolerance. *Nat Immunol* 2010; **11**: 21-27.
- Mukasa A., Itoh M., Tokunaga Y., Hiramane C., Hojo K. Inhibition of a novel model of murine experimental autoimmune orchitis by intravenous administration with a soluble testicular antigen: participation of CD8⁺ regulatory T cells. *Clin Immunol Immunopathol* 1992; **62**: 210-219.
- Myers L.K., Stuart J.M., Seyer J.M., Kang A.H. Identification of an immunosuppressive epitope of type II collagen that confers protection against collagen-induced arthritis. *J Exp Med* 1989; **170**: 1999-2010.
- Nakayama M., Abiru N., Moriyama H., Babaya N., Liu E., Miao D., Yu L., Wegmann D.R., Hutton J.C., Elliott J.F. and Eisenbarth G.S. Prime role for an insulin epitope in the development of type 1 diabetes in NOD mice. *Nature* 2005; **435**: 220-3.
- Nardi N., Brito-Zeron P., Ramos-Casals M., Aguilo S., Cervera R., Ingelmo M., et al. Circulating auto-antibodies against nuclear and non-nuclear antigens in primary Sjögren's syndrome: prevalence and clinical significance in 335 patients. *Clin. Rheumatol* 2006; **25**: 341-346.

- Natsumi T., Hiroshi K., Yoshikazu Y. Plant-based vaccines for animals and humans: recent advances in technology and clinical trials. *Therapeutic Advances in Vaccines* 2015; **3**: 139-154.
- Navone R., Lunardi C., Gerli R. Tinazzi E., Peterlana D., Bason C., Corrocher R, e Puccetti A. Identification of tear lipocalin as a novel autoantigen target in Sjogren's syndrome. *Journal of Autoimmunity* 2005. 25: 229-234.
- Nejentsev S., Walker N., Riches D., Egholm M., Todd J.A. Rare variants of IFIH1, a gene implicated in antiviral responses, protect against type 1 diabetes. *Science* 2009; **324**: 387-389.
- Nolasco G., De Blasc C., Torres V., Ponz F. A method combining immunocapture and PCR amplification in a microtiter plate for the detection of plant viruses and subviral pathogens. *J. Virol. Methods* 1993; **45**: 201-218.
- Nordberg L.B., Lillegraven S., Lie E., Aga A., Olsen I.C., Hammer H.B., Uhlig T., Jonsson M.K., van der Heijde, Kvien T.K., Haavardsholm E.A. Patients with seronegative RA have more inflammatory activity compared with patients ith seropositive RA in an inception cohort of DMARD-naïve patients classified according to the 2010 ACR/AULAR criteria. *Clinical and epidemiological research* 2016.
- Norris J.M., Yin X., Lamb M.M., Barriga K., Seifert J., Hoffman M., Orton H.D., Barón A.E., Salzler M.C., Chase H.P., Szabo N.J., Erlich H., Elsanbarth G.S., Rewers M. Omega-3 polyunsaturated fatty acid intake and islet autoimmunity in children at increased risk for type 1 diabetes. *J. Am. Med. Assoc.* 2007; **298**: 1420-1428.
- Obermayer-Straub P., Strassburg C.P., Manns M.P. Autoimmune hepatitis. *Journal of hepatology* 2000; **32**: 181-197.
- Odell J.T., Nagy F., Chua N.H. Identification of DNA sequences required for activity of the cauliflower mosaic virus 35S promoter. *Nature* 1985; **313**:810-812.
- Ogino T., Sato K., Miyokava N., Kimura S. and Katagiri M. Importance of GAD65 peptides and I-A^{g7} in the development of insulinitis in nonobese diabetic mice. *Immunogenetics* 2000; **51**: 538-545.
- Olson A. J., Bricogne G., Harrison S.C. Structure of tomato bushy stunt virus IV. The virus particle at 2.9 Å resolution. *J. Mol. Biol.*1983; **171**: 61-93.

- Orban T., Bundy B., Becker D.J., DiMeglio L.A., Gitelman S.E., Goland R., Gottlieb P.A., Greenbaum C.J., Marks J.B., Monzavi R., Moran A., Raskin P., Rodriguez H., Russell W.E., Schatz D., Wherrett D., Wilson D.M., Krischer J.P., Skyler J.S. Type 1 Diabetes TrialNet Abatacept Study Group, Co-stimulation modulation with abatacept in patients with recent-onset type 1 diabetes: A randomised, double-blind, placebo-controlled trial. *Lancet* 2011; **378**: 412–419.
- Palmer, J. P. et al. Interaction of β -cell activity and IL-1 concentration and exposure time in isolated rat islets of Langerhans. *Diabetes* 1989; **38**: 1211–1216.
- Papaccio G., Pisanti F.A., Montefiano R.D., Graziano A., Latronico M.V. Th1 and Th2 cytokines exert regulatory effects upon islet microvascular areas in the NOD mouse. *J Cell Biochem* 2002; **86**:651-64.
- Parker L., Kendall A., Stubbs G. Surface features of Potato virus X from fiber diffraction. *Virology* 2002. 291-295.
- Patel R. and Shahane A. The epidemiology of Sjögren’s syndrome. *Clin. Epidemiol* 2014; **6**: 247–255.
- Peakman M. and von Herrath M. Antigen-specific immunotherapy for type 1 diabetes: maximizing the potential. *Diabetes* 2010; **59**: 2087-2093.
- Pennline K.J., Roque-Gaffney E., Monahan M. Recombinant human IL-10 prevents the onset of diabetes in the nonobese diabetic mouse. *Clin Immunol Immunopathol* 1994; **71**:169-75.
- Pertovaara M., Silvernooinen O., Isoma K.I. STAT-5 is activated constitutively in T cells, B cells and monocytes from patients with primary Sjögren’s syndrome. *Clin Exp Immunol* 2015; **181**: 29-38.
- Peterlin B. M., Luciw P. A., P. J. Barr P. J., and Walker M. D. Elevated levels of mRNA can account for the trans-activation of human immunodeficiency virus. *Proc. Natl. Acad. Sci.* 1986; **83**: 9734-9738.
- Peyret H. A protocol for the gentle purification of virus-like particles produced in plants. *J Virol Methods* 2015; **225**: 59-63.
- Peyret H., Gehin A., Theunemann E.C., Blond D., Turabi A.E., Beales L., Clarke D., Gilbert R.J.C., Fry E.E., Stuard D.I., Holmes K., Stonehouse N.J., Whelan M., Rosenberg W., Lomonosoff G.P., Rowlands D.J. Tandem fusion of hepatitis B antigen allows

assembly of virus-like particles in bacteria and plants with enhanced capacity to accommodate foreign peptide. *Plos One* 2015. .

Peyret H., Lomonossoff G. The pEAQ vector series: the easy and quick way to produce recombinant proteins in plants. *Plant Mol Bio* 2013; **83**: 51-58.

Pniewski T. The twenty-year story of plant-based vaccine against hepatitis B: stagnation or promising prospects? *Int. J. Mol. Sci.* 2013; **14**: 1978-1998.

Porta C., Lomonossoff G.P. Viruses as vectors for the expression of foreign sequences in plants. *Biotechnol. Genet. Eng. Rev.* 2002; **19**: 245-291.

Porta C., Spall V.E., Findlay K.C., Gergerich R.C., Farrance C.E., Lomonossoff G.P. Cowpea mosaic virus-based chimaeras – Effects of inserted peptide on the phenotype, host range, and transmissibility of the modified viruses. *Virology* 2003; **310**: 50-63.

Porta C., Spall V.E., Loveland J., Johnson J.E., Barker P.J., Lomonossoff G.P. Development of cowpea mosaic virus as a high-yielding system for the presentation of foreign peptide. *Virology* 1994; **202**:949-955.

Qiang C., Keith R.D. The potential of plants as a system for the development and production of human biologics. *F1000 Faculty Reviews* 2016.

Qin B., Wang J., Yang Z. et al.: Epidemiology of primary Sjögren's syndrome: a systematic review and meta-analysis. *Ann Rheum Dis* 2015; **74**: 1983-1989.

Qin H. Y. and Singh B. BCG vaccination prevents insulin-dependent diabetes mellitus (IDDM) in NOD mice after disease acceleration with cyclophosphamide. *J. Autoimmun* 1997; **10**: 271–278.

Quinn A., McInerney B., Reich E.P., Kim O., Jensen K.P. and Sercarz E.E. Regulatory and effector CD4 T cells in nonobese diabetic mice recognize overlapping determinants on glutamic acid decarboxylase and use distinct $v\beta$ genes. *J Immunol* 2001; **166**: 2982-2991.

Rabinovich G.A., Gabrilovich D., Sotomayor E.M. Immunosuppressive strategies that are mediated are mediated by tumor cells. *Ann Rev Immunol* 2007; **25**: 267-296.

Raefaeliy, Y., Parijs, L. V., Alexander, S. I., & Abbas, A. K. Interferon γ is required for activation-induced death of T lymphocytes. *Journal of Experimental Medicine* 2002; **196**: 999–1005.

- Rai M., Padh H. Expression systems for production of heterologous proteins. *Current science* 2001; **80**: 1121-1128.
- Rapoport M.J., Jaramillo A., Zipris D., Lazarus A.H., Serreze D.V., Leiter E.H., Cyopick P., Danska J.S., Delovitch T.L. Interleukin 4 reverses T cell proliferative unresponsiveness and prevents the onset of diabetes in nonobese diabetic mice. *J Exp Med* 1993; **178**:87-99.
- Rasheed Z. Hydroxyl radical damaged immunoglobulin G in patients with rheumatoid arthritis: biochemical and immunological studies. *Clinical Biochemistry* 2008; **41**: 663-669.
- Rates S. M. K. Plant as source of drugs. *Toxicon* 2001; **39**: 603-613.
- Rhee D.K., Marcelino J., Baker M. The secreted glycoprotein lubricin protects cartilages surfaces and inhibits synovial cell overgrowth. *J Clin Invest* 2005; **115**: 622-631.
- Richardson S.J. *et al.* The prevalence of entero viral capsid protein vp1 immunostaining in pancreatic islets in human type 1 diabetes. *Diabetologia* 2009; **52**: 1143–1151.
- Riechmann J. L., Lain S., García J. A. Highlights and prospects of potyvirus molecular biology. *J. Gen. Virol.* 1992; **73**: 1-16.
- Rohll J.B., Holness C.L., Lomonosoff G.P., Maule A.J. 3'-terminal nucleotide sequence important for the accumulation of Cowpea Mosaic Virus M-RNA. *Virology* 1993; **193**: 672-679.
- Romagnani S. Immunological tolerance and autoimmunity. *Intern Emerg Med* 2006; **1**: 187-196.
- Roncarolo M.G., Gregori S., Battaglia M., Bacchetta R., Fleischhauer K., Levings M.K. Interleukin-10-secreting type 1 regulatory T cells in rodents and humans. *Immunol Rev.* 2006; **212**: 28–50.
- Russell M.A., Morgan N.G. The impact of anti-inflammatory cytokines on the pancreatic β -cell. *Islets* 2014.
- Ruusala A., Aspenstrom P. The atypical Rho GTPase Wrch1 collaborates with the nonreceptor tyrosine kinases Pyk2 and Src in regulating cytoskeletal dynamics. *Mol. Cell. Biol.* 2008; **28**: 1802-1814.

- Sai P., Rivereau A.S., Granier C., Haertlé TH. and Martignat L. Immunization of non-obese diabetic (NOD) mice with glutamic acid decarboxylase-derived peptide 524-543 reduces cyclophosphamide-accelerated diabetes. *Clin Exp Immunol* 1996; **105**: 330-337.
- Sainsbury F. and Lomonosoff G.P. Extremely high-level and rapid transient protein production in plants without the use of viral replication. *Plant Physiol* 2008; **148**: 1212-1218.
- Sainsbury F., Cañizares C.C., Lomonosoff G.P. Cowpea mosaic virus: the plant virus-based biotechnology workhorse. *Annu. Rev. of Phytopathol* 2010; **48**: 437-455.
- Sainsbury F., Thuenemann E.C., Lomonosoff G.P. pEAQ: versatile expression vectors for easy and quick transient expression for heterologous proteins in plants. *Plant Biotechnology Journal* 2009; **7**: 682-693.
- Sakaguchi S., Miyara M., Costantino C.M., Hafler D.A. FOXP3⁺ regulatory T cells in the human immune system. *Nat Rev Immunol* 2010; **10**: 490–500.
- Sallberg M., Blixt M., Zhang Z. X. and Ekstrand J. Passive adsorption of immunologically active and inactive synthetic peptides to polystyrene is influenced by the proportion of non-polar residues in the peptide. *Immunol. Lett.* 1995; **46**: 25–30.
- Sánchez F., Martínez-Herrera D., Aguilar I., Ponz F. Infectivity of Turnip Mosaic potyvirus cDNA clones and transcripts on the systemic host *Arabidopsis thaliana* and local lesion host. *Virus Research* 1998; **55**: 207-219.
- Sánchez F., Sáez M., Lunello P., Ponz F. Plant viral elongated nanoparticles modified for log-increases of foreign peptide immunogenicity and specific antibody detection. *Journal of Biotechnology* 2013; **168**:409-415.
- Sanjabi S., Zanewicz L.A., Kamanaka M., Flavell R.A. Anti- and Pro-inflammatory roles of TGF- β , IL-10, and IL-22 in immunity and autoimmunity. *Curr Opin Pharmacol* 2009; **9**:447-453.
- Santi L., Huang Z., Mason H. Virus like particles production in green plants. *Methods* 2006; **40**: 66-76.
- Sasamoto Y., Kawano Y.I., Bouligny R., Wiggert B., Chader G.J., Gery I. Immunomodulation of experimental autoimmune uveo-retinitis by intravenous injection of uveitogenic peptides. *Invest Ophthalmol Vis Sci* 1992; **33**: 2641-2649.

- Saunders K., Sainsbury F. And Lomonosoff G.P. Efficient generation of *cowpea mosaic virus* empty virus-like particles by the proteolytic processing of precursors in insect cells and plants. *Virology* 2009; **393**: 329-337.
- Scholthof H.B., Scholthof K.B.G. Plant virus gene vectors for transient expression of foreign proteins in plants. *Annu. Rev. of Phytopathol* 1996; **34**: 299-323.
- Seebach D., Namoto K., Mahajan Y.R., Bindschädler P., Sustmann R., Kirsch M., Ryder N. S., Weiss M., Sauer M., Roth C., Werner S., Beer H. D., Munding C., Walde P., Voser P. Chemical and biological investigations of β -Oligoarginines. *Chem. Biodiversity* 2004; **1**: 65–97.
- Serra-Pages C., Kedersha N.L., Fazikas L., Medley Q.G., Debant A., Streuli M. The LAR transmembrane protein tyrosine phosphatase and a coiled-coil LAR-interacting protein co-localize at focal adhesions. *EMBO* 1995; **12**: 2827-2838.
- Sgouroudis E. and Ciriaco A.P. Control of type 1 diabetes by CD4⁺Foxp3⁺ regulatory T cells: lessons from mouse models and implications for human disease. *Diabetes Metab Res Rev* 2009; **25**: 208-218.
- Shoseyov O., Posen Y., Grynspan F. Human collagen produced in plants, More than just another molecule. *Bioengineered* 2014. **5**: 49-52.
- Sijmons P.C., Dekker B. M., Schrammeijer B., Verwoerd T.C., van den Elzen P.J., Hoekema A. Production of correctly processed human serum albumin in transgenic plants. *Biotechnology (N Y)* 1990; **8**: 217-221.
- Sivakumar G. Bioreactor technology: a novel industrial tool for high-tech production of bioactive molecule and biopharmaceuticals from plant root. *Biotechnology Journal* 2006; **1**: 1419-1427.
- Smith A.A. and Germolec D.R. Introduction to immunology and autoimmunity. *Environmental Health Perspectives* 1999; **107**:661-665.
- Soltész G., Patterson C.C. and Dahlquist G. (on behalf of EURODIAB Study Group). Worldwide childhood type 1 diabetes incidence - what can we learn from epidemiology? *Pediatric Diabetes* 2007; **8**: 6-14.
- Sonenberg N., Shatkin A. J., Ricciardi R. P., Rubin M., Goodman R. M. Analysis of terminal structures of RNA from potato virus X. *Nucleic Acids Res.* 1978; **5**: 2501-2512.

- Sudzius G., Mieliauskaite D., Siaurys A., Viliene R., Butrimiene I., Characiejus D., Dumalakiene I. Distribution of peripheral lymphocyte populations in primary Sjögren's Syndrome patients. *Journal of Immunology Research* 2015; **2015**.
- Sun C.K., Man K., Ng K.T., Ho J.W., Lim Z.X., Cheng Q., Lo C.M., Poon R.T., Fan S.T. Proline-rich tyrosine kinase 2 (Pyk2) promotes proliferation and invasiveness of hepatocellular carcinoma cells through c-Src/ERK activation. *Carcinogenesis* 2008; **29**: 2096-2105.
- Symmons D.P., Bankhead C.R., Harrison B.J. Blood transfusion, smoking and obesity as risk factors for the development of rheumatoid arthritis: results from a primary care-based incident case-control study in Norfolk, England. *Arthritis Rheum* 1997; **40**: 1955-1961.
- Szittyá G., Salamon P., Burgyan J. The complete nucleotide sequence and synthesis of infectious RNA of genomic and defective interfering RNAs of TBSV-P. *Virus. Res.* 2000; **69**:131–136.
- Tacket C.O., Mason H.S., Losonsky G., Clements J.D., Levine M.M., Arntzen C.J. Immunogenicity in humans of a recombinant bacterial antigen delivered in a transgenic potato. *Nat. Med.* 1998; **4**: 607-609.
- Taylor K.M., Lin T., Porta C., Mosser A.G., Giesing H.A., Lomonosoff G.P., Johnson J.E. Influence of three dimensional structure on the immunogenicity of a peptide expressed on the surface of plant virus. *J. Mol. Recognit.* 2000; **13**: 71-82.
- Thanavala Y., Mahoney M., Pal S., Scott A., Richter L., Natarajan N., Goodwin P., Arntzen C.J., Mason H.S. Immunogenicity in humans of an edible vaccine of hepatitis B. *Proc. Natl. Acad. Sci. U S A* 2005; **102**: 3378-3382.
- Tian J., Atkinson M.A., Clare-Salzler M., Herschenfeld A., Forsthuber T., Lehmann P.V. and Kaufman D.L. Nasal administration of glutamate decarboxylase (GAD65) peptides induces Th2 responses and prevents murine insulin-dependent diabetes. *J Exp Med* 1996; **183**: 1561-1567.
- Tinazzi E., Merlin M., Bason C., Beri R., Zampieri R., Lico C., Bartoloni E., Puccetti A., Lunardi C., Pezzotti M., Avesani L. Plant-derived chimeric virus particles for diagnosis of primary Sjögren Syndrome. *Frontiers in Plant Science* 2015; **6**: 1080.
- Tisch R., Wang B. and Serreze D.V. Induction of glutamic acid decarboxylase 65-specific Th2 cells and suppression of autoimmune diabetes at late stages of disease is epitope dependent. *J Immunol* 1999; **163**: 1178-1187.

- Touriño A., Sánchez F., Fereres A., Ponz F. High expression of foreign proteins from a biosafe viral vector derived from Turnip mosaic virus. *Spanish Journal of Agricultural Research* 2008; **6**: 48-58.
- Tschofen M., Knopp D., Hood E., Stöger E. Plant molecular farming: much more than medicines. *Annual Review of Analytical Chemistry* 2016. **9**: 271-294.
- Turley S., Poirot L., Hattori M., Benoist C., Mathias D. Physiological beta cell death triggers priming of self-reactive T cells by dendritic cells in a type-1 diabetes model. *J. Exp. Med.* 2003; **198**: 1527–1537.
- Ü. Langel in Handbook of Cell Penetrating Peptides, 2nd ed. (Ed.: Ü. Langel), CRC, Boca Raton, 2006.
- Udzius G., Mieliauskaite D., Siautys A. *et al.* Distribution of Peripheral Lymphocyte populations in primary Sjögren's syndrome Patients. *J Immunol Res* 2015; **2015**: 854706.
- Uhde K., Fischer R. and Commandeur U. Expression of multiple foreign epitopes presented as synthetic antigens on the surface of *Potato virus X* particles. *Arch Virol* 2005; **150**: 327-340.
- Van de Sande M.G., de Hair M.J., van der Leij C., Klarenbeek P.L., Bos W.H., Smith M.D., Maas M., de Vries N., van Schaardenburg D., Dijkmans B.A., Gerlag D.M., Tak P.P. Different stages of rheumatoid arthritis: features of the synovium in the preclinical phase. *Ann Rheum Dis* 2011; **70**: 772-777.
- Van der Heijde D.M. Joint erosions and patients with early rheumatoid arthritis. *Br J Rheumatol* 1995; **34**: 74-78.
- Van der Kooji S.M., de Vries-Bouwstra J.K., Goekoop-Ruiterman Y.P., van Zeben D., Kerstens P.J., Gerars A.H., Limited efficacy of conventional DMARDs after initial methotrexate failure in patients with recent onset rheumatoid arthritis treated according to the disease activity score. *Ann Rheum Dis* 2007; **66**: 1356-1362.
- van Engelen F.A., Molthoff J.W., Conner A.J., Nap J.P., Pereira A., and Stiekema W.J. pBINPLUS – an improved plant transformation vector based on pBIN19. *Transgenic Res.* 1995; **4**: 288-290.
- Verchot J., Herndon K. L., Carrington J. C. Mutational analysis of the tobacco etch potyviral 35-kDa proteinase: identification of essential residues and requirements for autoproteolysis. *Virology* 1992; **190**: 298-306.

- Virtanen S.M., Kenward M.G., Erkkola M., Kautiainen S., Kronberg-Kippila C., Hakulinen T., et al. Age at introduction of new foods and advanced beta cell autoimmunity in young children with HLA-conferred susceptibility to type 1 diabetes. *Diabetologia* 2006; **49**: 1512-1521.
- Wang B. and Tisch R. Parameters influencing antigen-specific immunotherapy for type 1 diabetes. *Immunol Res* 2008; **41**: 175-187.
- Weintrob N., Sprecher E., Israel S., Pinhas-Hamiel O., Kwon O.J., Bloch K., Abramov N., Arbel A., Josefsberg Z., Brautbar C., Vardi P. Type 1 diabetes environmental factors and correspondence analysis of HLA class II genes in the Yemenite Jewish community in Israel. *Diabetes Care* 2001; **24**: 650-653.
- Wen L., Ley R.E., Volchkov P.Y., Stranges P.B., Avanesyan L., Stonebraker A.C., Hu C., Wong F.S., Szot G.L., Bluestone J.A., Gordon J.I., Chervonsky A.V. Innate immunity and intestinal microbiota in the development of type 1 diabetes. *Nature* 2008; **455**: 1109-1113.
- Wenzel J., Gerdson R., Uerlich M., Bauer R., Bieber T., Boehm I. Antibodies targeting extractable nuclear antigens: historical development and current knowledge. *The British journal of dermatology* 2001; **145**: 859-867.
- Yaciuk J.C., Pan Y., Schwarz K. *et al.* Defective selection of thymic regulatory T cells accompanies autoimmunity and pulmonary inltrates in T cra-deficient mice double transgenic for human La/Sjögren's syndrome- B and human La-specific TCR. *J Immunol* 2015; **194**: 1514-1522
- Yang D., Guo F., Liu B., Huang N., Watkins S. Expression and localization of human lysozyme in the endosperm of transgenic rice. *Planta* 2002; **216**: 597-603.
- Yao J., Weng Y., Dickey A., Wang K.Y. Plants as factories for human pharmaceuticals: applications and challenges. *International Journal of Molecular Sciences* 2015; **16**: 28549-28565.
- Yokoyama K., Su I., Tezuka T., Yasuda T., Mikoshiba K., Tarakhowsky A., Yamamoto T. BANK regulates BCR-induced calcium mobilization by promoting tyrosine phosphorylation of IP3 receptor. *EMBO J* 2002; **21**: 83-92.
- Zaccane P., Phillips J., Conget I., Gomis R., Haskins K., Minty A., Bendtzen K., Cooke A., Nicoletti F. Inter- leukin-13 prevents autoimmune diabetes in NOD mice. *Diabetes* 1999; **48**: 1522-8.